MECHANISMS OF COORDINATION BETWEEN ONE- AND TWO-JOINT SYNERGIST MUSCLES

A Dissertation
Presented to
The Academic Faculty

by

Ricky Mehta

In Partial Fulfillment
of the Requirements for the Degree
Doctor of Philosophy in the
School of Applied Physiology

Georgia Institute of Technology
May 2016

MECHANISMS OF COORDINATION BETWEEN ONE- AND TWO-JOINT SYNERGIST MUSCLES

Approved by:

Dr. Boris I. Prilutsky, Advisor
School of Applied Physiology
Georgia Institute of Technology

Dr. T. Richard Nichols
School of Applied Physiology
Georgia Institute of Technology

Dr. Minoru Shinohara
School of Applied Physiology
Georgia Institute of Technology

Dr. Young-Hui Chang
School of Applied Physiology
Georgia Institute of Technology

Dr. Samit Chakrabarty
School of Biomedical Sciences
University of Leeds

Date Approved: March 9, 2016

Dedicated to my loving wife Dhara, my incredible parents, family and friends, and to Selene and Iris

ACKNOWLEDGEMENTS

I would especially like to thank my wife, Dhara, without whose love and support I would not be where I am now. I would also like to thank my mother, father, and brother for all their love and support over the years. I wish to also thank my advisor, Boris, for his invaluable mentorship. Finally, thank you to all of my committee and colleagues in Applied Physiology for their valuable input.

TABLE OF CONTENTS

LIST OF TABLES

Page

LIST OF FIGURES

Page

SUMMARY

Major muscle groups (e.g. triceps surae, quadriceps, hamstrings, triceps brachii) contain synergist muscles that cross either one or two joints; they are called one- and two-joint muscles. The functional significance of this musculoskeletal design, extensively studied in the past, has been suggested to increase the economy and efficiency of movement. Much less attention has been paid to the mechanisms responsible for the differential activation, or coordination, between one- and two-joint synergists. The understanding of these mechanisms will not only add to the basic knowledge of neural control of movement but also contribute to prevention and therapeutic interventions of muscle injuries that often occur in two-joint muscles. Previous work has suggested that mechanical intermuscular interactions, resultant muscle moment requirements at the adjacent joints, movement speed, and muscle length-velocity related sensory feedback can affect this coordination. Additionally, the comparison of motoneuronal and muscle activity patterns between fictive and real locomotion in cats suggests a greater influence of motion related sensory feedback on activity of proximal two-joint muscles (i.e., rectus femoris and hamstrings) compared to one-joint muscles and distal two-joint muscles (medial and lateral gastrocnemius). Therefore, the first goal of this work was to test the possible contribution of mechanical intermuscular interactions between one- and two-joint ankle extensors in the cat. The second goal was to examine the role of joint moment requirements, movement speed and length-velocity related feedback in distinct activation of distal one- and two-joint muscles (soleus and gastrocnemius). The third goal was to investigate the effect of removal of length-velocity sensory feedback from proximal one-

and two-joint muscles (vastii and rectus femoris) on coordination of these muscles. To address the above goals, an array of motor tasks with different speeds and combinations of joint moments were studied in cats and humans. The tasks included level, downslope and upslope walking and paw shake response in cats, as well as back and leg load lifting and jumping in humans. Motion capture and force plate data were recorded to analyze kinematics and joint moments, sonomicrometry was used to measure muscle fascicle length in cats, and electromyography (EMG) was used to quantify muscle activity. Length-velocity related sensory feedback was removed in cats by muscle self-reinnervation. Results show that mechanical intermuscular interactions via myofascial force transmission should be considered in the coordination between adjacent one- and two-joint synergist muscles in certain pathological conditions leading to increased muscle lengths. Coordination between distal and proximal one- and two-joint synergists depends on joint moment requirements, and the differential inhibition of soleus and excitation of gastrocnemius does not depend on movement speed or length-velocity related sensory feedback. Removal of length-velocity related sensory feedback has a strong effect on coordination between the studied proximal synergist pair (vastii and rectus femoris) but not on coordination of the distal synergist pair (soleus and gastrocnemius). Findings presented here expand on understanding the role of mechanical interactions, sensory feedback and feedforward control in the coordination between one- and two-joint muscles. These findings have potential implications for developing targeted rehabilitation strategies/treatment and implementation of new control strategies for robotics and prosthetics to improve movement efficiency.

CHAPTER I

INTRODUCTION

Imagine if one had to consciously think about controlling every muscle in the leg in order to perform a simple task such as walking. It would be an almost impossible task due to muscle redundancy and the presence of multi-joint muscles. We, however, are able to control all of our muscles without thinking about them. This is because our neural control system is hierarchically organized (Bernstein, 1967) – the upper control levels give simple commands to initiate or stop walking, and lower control levels (brainstem and spinal cord) organize activity of individual muscles. It appears that the organization of neural pathways linking multiple muscles within and between synergist groups match well with the musculoskeletal anatomy and muscle mechanical actions (Nichols, 1994). For example, the same action of a pair of one-joint muscles crossing neighboring joints is often accomplished by a single two-joint muscle crossing the same joints (Wells and Evans, 1987, Sergio and Ostry, 1994); as a result activity of two-joint muscles is much higher than that of their one-joint synergists when the two-joint muscles can contribute to the desired moments at the joints they cross (Prilutsky, 2000a). Despite muscle redundancy and presence of multi-joint muscles, this type of stereotypical coordination pattern between synergist muscles are selected by the nervous system in many automatic or skilled motor behaviors. Muscle coordination will be defined here as the distinct activation of synergists in terms of their magnitude and timing of activity (Prilutsky, 2000a, Wakeling et al., 2010). Previous research has provided insight into the functional

implications of these muscle coordination strategies, however, the mechanisms which underlie the coordination between one-joint and two-joint synergists remain unclear. For example, recent evidence suggests different contributions of the central pattern generator (CPG) and motion-dependent feedback to activity patterns of specific one- and two-joint distal and proximal leg muscles (Daley et al., 2007, Markin et al., 2012b). It is important to investigate these questions since the detailed mechanisms underlying coordination between synergist muscles are not well understood, and the gained knowledge will aid prevention and rehabilitation of neuromuscular injuries and could contribute to the development of new efficient designs and control strategies of robotic systems and powered prostheses.

1.1 Perspectives on the Coordination of One- and Two-Joint Muscles and their Functional Implications

For many centuries, the unique anatomical characteristics of two-joint muscles have caught the attention of many scientists, dating back to the time of the Greek physician, Galen (131-201 AD). It was Galen who was likely the first to report on the unique function of two-joint muscles, and specifically rectus femoris, when he stated, "…when it is tensed, it naturally not only draws up the tibia towards itself, but also flexes the femur…" (Schenau, 1989, originally from 'De usu patium II p. 373, translation: May, 1968'). This was an important observation since it naturally led to the question of why two-joint muscles exist when two one-joint muscles could be used instead.

In order to answer this question, many researchers turned to mathematical optimization techniques to try and discover the functional significance underlying control

strategy of one- and two-joint muscles. Due to the large amount of muscles exceeding the number of kinematic degrees of freedom at joints, it is extremely difficult to make predictions of muscle activity without making gross assumptions (Seireg and Arvikar, 1975). In both linear and non-linear optimization, the operator must assume that the nervous system has been tuned to optimize a specific objective or cost function. Early work found varying degrees of agreement between predicted and experimental muscle activity patterns, however, that work was criticized for the use of non-physiological objective functions. The introduction of physiological objective functions within optimization techniques allowed researchers to link well-matched predictions of muscle activity or force to concepts of a neural control strategy. There is fairly considerable consensus from multiple studies that suggest a control strategy which minimizes muscle fatigue, energy expenditure, perceived effort or muscle force dependent neural noise (Crowninshield and Brand, 1981, Harris and Wolpert, 1998, Prilutsky et al., 1998b, Prilutsky, 2000a, Anderson and Pandy, 2001, Prilutsky and Zatsiorsky, 2002, Haruno and Wolpert, 2005, Bottasso et al., 2006). Computed muscle forces or activation matched reasonably well with the measured ones for many automatic behaviors, including walking. Specifically, the predicted and recorded activity of two-joint muscles was the highest when these muscles contributed to the resultant muscle moments at the two joints they cross, and the activity of two-joint muscles was the lowest when they had the antagonistic action at both joints. Thus, it appears from those studies that the functional significance of specific activity of two-joint muscles in many automatic well practiced tasks may be to reduce muscle effort, fatigue and/or neural noise. Although there is

general agreement for why the nervous system has been tuned to operate this way, the neural mechanisms are not yet clear.

1.2 Potential Mechanisms Underlying Coordination between One- and Two-Joint Muscles

One possible mechanism that could contribute to the coordination (relative force produced by) between one- and two-joint synergist muscles is epimuscular myofascial force transmission. This is a mechanism by which forces developed by one muscle may be transmitted, via myofascial linkages, to other adjacent muscles (for review see Huijing, 2009). It has been found that for normal physiologic muscle lengths of intact soleus and gastrocnemius during typical ranges of motion in the cat and rat, no significant effects of epimuscular myofascial force transmission were apparent (Maas and Sandercock, 2008, Tijs et al., 2015), suggesting that in this situation differences in activity of these muscles are determined by neural constraints in the form of afferent pathways and central commands. On the other hand, there is evidence for mechanical interactions between synergists within the human triceps surae during passive movement and in hamstrings following tendon rupture and muscle retraction (Clark et al., 2011, Huijing et al., 2011, Tian et al., 2012). Additionally, at abnormally increased relative lengths between adjacent muscles, mechanical interactions between them through myofascial linkages may be substantial (Huijing and Baan, 2003, Maas and Sandercock, 2010).

Another possible mechanism underlying coordination between one- and two-joint muscles involves the dependence of the activity magnitude of two-joint muscles on the

task requirements to produce specific resultant muscle moments at the joints the muscles cross. As mentioned previously, two-joint muscles exhibit their highest activity when they can contribute to the resultant muscle moments at both joints they cross as biomechanical agonists (Andrews and Hay, 1983). It has been shown that recruitment of the two-joint MG muscle is highly dependent on the moment at the knee and the ankle (Ballantyne et al., 1993). Many other studies have shown a greater activity in two-joint muscles for tasks in which they can contribute agonistically to the resultant muscle moments at both joints (Wells and Evans, 1987, Jacobs and van Ingen Schenau, 1992, Jacobs and Macpherson, 1996, Prilutsky and Gregor, 1997, Prilutsky et al., 1998a, Prilutsky et al., 1998b, Prilutsky and Gregor, 2000). It is likely that this increased activation is a result of inputs from both populations of flexor and extensor interneurons possibly comprising half-centers of a central pattern generator (CPG) (Perret and Cabelguen, 1980, Prilutsky, 2000a, Shevtsova et al., 2016). On the other hand, one-joint muscles appear to only receive input from one interneuronal population.

Lastly, proprioceptive feedback can modulate patterns of muscle activity and its role in locomotion, balance, and other motor tasks has been extensively explored previously (Pearson, 1995, Abelew et al., 2000, Lam and Pearson, 2002, Donelan and Pearson, 2004, Maas et al., 2007, Windhorst, 2007, Livingston and Nichols, 2014, Roden-Reynolds et al., 2015). Despite this large wealth of information, the extent to which feedback can contribute to coordination between one- and two-joint synergist muscles during motor tasks has not been explored. Synergist muscles share many heterogenic feedback pathways including both length-dependent (Ia/II) and force-dependent (Ib) afferent pathways, which could influence coordination of synergist

muscles (Eccles et al., 1957a, Eccles et al., 1957b, Eccles and Lundberg, 1958, Nichols, 1994, Nichols, 1999, Wilmink and Nichols, 2003, Ross and Nichols, 2009).

1.3 Specific Aims

Stereotypical muscle coordination patterns (relative muscle activity or forces of redundant synergist muscles) are selected by the nervous system in many automatic or skilled motor behaviors. Previous research has provided insight into the functional implications of these muscle coordination strategies, however, the mechanisms which underlie the coordination between one-joint and two-joint synergists remain unclear. Previous evidence also suggests differential roles of biomechanical task requirements (i.e., joint moment and movement speed) and motion dependent feedback in coordination between specific distal and proximal one- and two-joint leg muscles. Therefore, the overall goal of this work is to investigate the contribution of joint moment requirements, movement speed and length-velocity related sensory feedback to the coordination between one- and two-joint synergist muscles and determine whether these mechanisms differ in select distal versus proximal leg muscles. In addition, possible intermuscular mechanical interactions between paralyzed and intact one- and two-joint muscles that may affect muscular coordination will be studied. Results of this work will add to our fundamental understanding of motor control and have implications for rehabilitation, injury prevention and novel design of robotic systems and powered prostheses.

1.3.1 Specific aim 1

Aim 1 investigated mechanical interactions between denervated one-joint soleus (SO) and intact two-joint medial gastrocnemius (MG) muscles in the cat by measuring

the extent of muscle fascicle length changes in denervated SO during the stance phase of walking. There is evidence suggesting mechanical interactions between cat SO and MG muscles are limited (Maas and Sandercock, 2008). Although at unnaturally long muscle lengths myofascial force transmission between synergists can increase (Maas and Sandercock, 2010), and partial denervation of cat ankle extensors results in abnormally long lengths of the SO and MG during stance of walking (Maas et al., 2010), strong passive mechanical interactions between SO and MG are not expected in this case.

Hypotheses: Fascicles of the denervated SO (1) would mirror lengthening of the SO MTU during ankle yield and (2) would not significantly shorten during push-off in the stance phase of walking.

1.3.2 Specific aim 2

Aim 2 investigated the coordination between distal one-joint SO and two-joint MG muscles by examining effects of length-velocity related sensory feedback from these muscles, movement speed and joint moment requirements. Two explanations have been proposed for the differential activity of one-joint SO and two-joint MG muscles in some tasks. The first explanation suggests that during high-speed movements, length-velocity related afferent feedback inhibits slow-twitch SO, while fast-twitch GA is highly active (Smith et al., 1980, Smith and Zernicke, 1987, Prochazka et al., 1989). Another explanation is that joint moment requirements (related to central inputs to motoneurons) modulate activity of two-joint MG, and SO activity is inhibited at high MG forces (Prilutsky, 2000a). In this scenario, coordination between SO and MG depends more on central inputs to motoneurons of MG and force-dependent inhibition of SO from MG (Perret and Cabelguen, 1980, Nichols, 1994, Prilutsky, 2000a).

Hypothesis. The hypothesis will test two possible explanations for the differential activity of SO and GA: (1) SO activity would be low compared to GA activity at high movement velocities and be mediated by length-velocity related sensory feedback and (2) SO activity would be low compared to GA activity for tasks requiring an ankle extension–knee flexion joint moment combination and would not require high movement velocities or length-velocity related sensory feedback.

1.3.3 Specific aim 3

Aim 3 investigated the mechanisms of coordination between proximal one- and two-joint muscles (vastii/rectus femoris, VA/RF) by examining the effects of joint moment requirements at the knee and hip joints and the removal of muscle length-velocity related afferent feedback from these muscles. It has been shown that normalized patterns of motoneuronal and muscle activity of one-joint muscles and distal two-joint gastrocnemius were similar in fictive (no motion dependent feedback) and real locomotion in cats, whereas this was not the case for proximal two-joint muscles, hamstrings and RF (Markin et al., 2012b), suggesting a greater role of motion-dependent feedback in regulating activity of these two-joint muscles during real locomotion.

Hypotheses: I tested the following hypotheses: (1) coordination between VA and RF would depend on combination of joint moment requirements at the hip and knee and would be altered by removal of length-velocity related afferent feedback and (2) removal of length-velocity related afferent feedback from VA and RF would have a greater effect on activity of RF than VA.

1.3.4 Innovation and significance

When attempting to understand any physiological system, there is substantial scientific value in investigating mechanisms which are generalizable across the entire system. This task can be difficult, however, if there are differences in mechanisms depending on factors such as applicability across tasks or segment of the body. Attempting to apply a single generalized neuromechanical model to an entire system may therefore lead to error and inconsistent results. The knowledge of specific physiological mechanisms can be crucial in a clinical setting where a rehabilitation strategy needs to be prescribed to a patient with a very specific injury. Although it is important to apply general rehabilitation techniques based on a general model, an understanding of specific mechanisms involved in the area which have been affected would help provide even better targeted treatment. Within the field of robotics, in order to create the most human-like movement, a similar argument can be made about the organization of control for specific limb segments. Addressing the aims outlined above will start the creation of a framework for understanding the mechanical and neural mechanisms which underlie the coordination between one- and two-joint muscles throughout the entire neuromuscular system. This framework can then be applied in a clinical and robotics setting to provide strategies for rehabilitation, injury prevention, and better control algorithms.

CHAPTER II

SPECIFIC AIM 1

UNEXPECTED FASCICLE LENGTH CHANGES IN DENERVATED FELINE SOLEUS MUSCLE DURING STANCE PHASE OF WALKING

(Mehta et al. Sci Rep 5: 17619, 2015)

2.1 Introduction

In normal physiological ranges of motion at the ankle and knee joints, no significant effects of epimuscular myofascial force transmission between SO and MG muscle in cats and rats have been reported (Maas and Sandercock, 2008, Tijs et al., 2015). At abnormally increased lengths between adjacent muscles, which may occur after partial denervation of ankle extensors (Maas et al., 2007, Maas et al., 2010), mechanical interactions between them through myofascial linkages may be substantial (Huijing and Baan, 2003, Maas and Sandercock, 2010). Although there are indications of mechanical interactions between passive muscle heads of the human triceps surae in vivo (Huijing et al., 2011, Tian et al., 2012) and between muscles in the injured human hamstrings group after rupture of synergist tendon and muscle retraction (Clark et al., 2011), detailed information about the *in vivo* mechanical conditions of muscle fascicles in a denervated muscle surrounded by intact synergists is currently unavailable. The extent to which fascicles of a denervated muscle passively lengthen and shorten, while its intact synergists undergo active lengthening and shortening, during normal motor behaviors is

unknown. Information about muscle fascicle mechanical behavior in the injured muscle, specifically in denervated muscle, would improve our understanding of the mechanical behavior of paralyzed muscles and their possible interactions with intact synergists.

The aim of these experiments was to investigate to what extent muscle fascicles of the denervated feline SO change length during the stance phase of walking. In a denervated muscle, there is no active force generation while passive force production by cat SO muscle-tendon unit (MTU) stretched by ankle dorsiflexion up to ~90^{o}-120^{o} is negligible (Tabary et al., 1972, Herzog et al., 1992). Fascicles of the cat SO would also have a greater compliance compared to the tendon in this situation (Rack and Westbury, 1984). Finally, a negligible myofascial force transmission has been reported between cat SO and its synergists (Maas and Sandercock, 2008, Tijs et al., 2015).

2.2 Hypothesis

Based on the above rationale, it would be expected that SO fascicles would mirror lengthening of the MTU during ankle yield in the stance phase of walking. During passive ankle extension (plantarflexion) caused by external forces applied to the foot while all ankle muscles are relaxed, the fascicles and tendon of denervated SO would be expected to buckle as shown to be the case at short lengths of passive muscles in vivo (Muraoka et al., 2002, Herbert et al., 2015). On the other hand, I expected no buckling or decreased shortening of denervated SO fascicles during ankle extension in stance of walking. Buckling of passive SO fascicles during SO MTU shortening would be prevented by high pressure inside the superficial posterior crural compartment (Garfin et al., 1981, Ward et al., 2007) developed by bulging fascicles of active muscles (Otten,

1988) surrounding SO. Decreased shortening of the denervated SO fascicles would also be expected because of limited myofascial force transmission from contracting synergists (Maas and Sandercock, 2008, Tijs et al., 2015).

2.3 Methods

2.3.1 Ethical approval and animal training

The surgical and experimental procedures employed corresponded to the "Principles of Laboratory Animal Care" (NIH Publication No. 86-23, Revised 1985) and were approved by the Institutional Animal Care and Use Committee of the Georgia Institute of Technology. Seven adult female cats (*Felis domesticus*, mass 3.7 ± 0.8 kg; mean ± SD) were studied. Cats were trained using operant conditioning methods to walk within a custom-made, Plexiglas-enclosed walkway (3.0 m x 0.4 m) with up to three embedded force platforms (16 cm x 11 cm and 11 cm x 7 cm; Bertec Corporation, Columbus, OH, USA) and covered with nonslip rubberized matting. Cats were trained to walk at three walkway slopes – level surface (0%, i.e. 0^o), upslope (50%, i.e. 27^o) and downslope (-50%, i.e. -27^o) – for several hours a day, 5 days a week for 3-4 weeks; for more details see Prilutsky et al. (2005) and Gregor et al. (2006).

2.3.2 Surgical procedures

The surgical procedures have been described in detail previously (Gregor et al., 2006, Maas et al., 2009, Prilutsky et al., 2011), therefore only a brief account of the procedures is provided below. Following locomotor training and initial locomotor recordings, each cat underwent two survival surgeries under aseptic conditions and general isoflurane anesthesia.

Implantation surgery. The animal was anesthetized using ketamine (10 mg/kg, S.C.), atropine (0.05 mg/kg, S.C.), and isoflurane (inhalation, 5%), and anesthesia was maintained with isoflurane (1-3%). The animal's vital physiological parameters (temperature, respiration, heart rate, blood pressure) were monitored throughout the surgery. After shaving and cleaning with surgical disinfectant the skin overlying the skull, the lower back, and dorsal aspects of the right shank, skin incisions were made. Teflon-insulated multi-stranded stainless steel fine wires (CW5402; Cooner Wire, Chatsworth, CA, USA) and leads with piezoelectric sonomicrometry crystals (2 mm in diameter; Sonometrics, London, ON, Canada) were passed subcutaneously along the back from the skull to an incision in the hindlimb. Four of the seven cats were implanted with the sonomicrometry crystals. All wire leads were attached to two multi-pin Amphenol connectors that were secured to the skull with four stainless steel or titanium screws and dental cement. A thin strip of insulation (~1 mm) was removed near the distal end of each pair of the fine wires and secured inside the muscle belly of SO, LG and MG muscles. Mild electrical stimulation of the muscles through the head connectors was used to verify wire placements. The implanted fine wires were used to record electromyographic (EMG) activity. To measure SO fascicle length, one pair of the piezoelectric crystals was implanted near the origin and insertion (i.e., proximal and distal aponeurosis) of SO muscle fascicles along the muscle belly midline. The superficial surface of the muscle belly at the location of the crystal implantation was reached through a small cut of the fascia surrounding the muscle. A small pocket inside the muscle was created between the muscle fibers. The crystal was inserted in the pocket

beneath the muscle surface, and the pocket was closed by a 4-0 silk suture, which also anchored the crystal lead wire.

After implantation of EMG electrodes and sonomicrometry crystals, the skin incisions were closed using Vicryl 4-0 suture for the deep fascia and Vicryl 5-0 subcuticular suture for dermal closure. The animal recovered after surgery for 14 days with pain medication administered for at least 3 days and antibiotics for 10 days.

After animal recovery, hindlimb mechanics, EMG activity of SO, LG, and MG muscles, and SO muscle fascicle lengths were collected during level, downslope and upslope walking (see below) to obtain baseline values.

Nerve transection and repair surgery. These surgical procedures were similar to those described previously (Maas et al., 2007, Maas et al., 2010, Prilutsky et al., 2011). Animal preparation, anesthesia, monitoring during surgery and pain medication after surgery were the same as described for the implantation surgery. The branch of the tibial nerve supplying SO and LG muscles was reached through a longitudinal incision in the popliteal region of the right hindlimb. A small portion of the LG-SO nerve branch (~2-4 mm) was carefully separated from surrounding tissues, leaving the fat pad in the popliteal region intact, and then transected with sharp scissors. The SO and LG nerves were not separated. Muscle denervation was verified by mild electrical stimulation of the proximal nerve stump. The transected nerve stumps were approximately aligned with each other and secured in place by fibrin glue (equal parts of thrombin and a 1:1 mixture of fibrin and fibronectin; Sigma-Aldrich, St. Louis, MO, USA). After the surgery, the animal recovered for 3-5 days before the locomotion experiments resumed.

2.3.3 Locomotion experiments

Each cat was tested in two series of locomotion experiments before and after SO-LG nerve transection and repair to measure hindlimb mechanics, EMG of SO and MG, as well as SO fascicle length. Locomotor data collection before nerve injury was performed approximately 2 hours a day, 3-5 days a week for about a month. Post nerve injury locomotor data reported here were collected during the first 3-14 days (1-2 weeks) after SO-LG nerve transection and repair using the same recording schedule as for pre-nerve injury data collection.

In order to record hindlimb kinematics, light reflective markers were placed using double-sided adhesive tape on the following right hindlimb anatomical landmarks: iliac spine, greater trochanter, lateral femoral epicondyle, lateral malleolus, 5^{th} metatarsophalangeal (MTP) joint and the distal end of the 5^{th} digit. Marker positions were recorded using a 3D, 6-camera motion capture system (Vicon Motion Systems Ltd, Oxford, UK) at a sampling rate of 120 Hz. The three components of the ground reaction force vector and coordinates of its application point to the paw were recorded at a sampling rate of 360 Hz by 1 of the 3 small force plates (Bertec Corporation, Columbus, OH, USA) embedded into the walkway surface and actually contacted during any specific trial. SO fascicle length was recorded by the sonomicrometry system (Sonometrics Corporation, London, ON, Canada) at a sampling rate of 1059 Hz. EMG signals were collected at a sampling rate of 3000 Hz, band-pass filtered (30-1000 Hz, 3 dB), amplified (100x), and saved on a PC for further analysis. The EMG and sonomicrometry signals were collected via a 16-conductor shielded flexible cable attached to the Amphenol connectors on the animal's head. The simultaneous data

collection onset was triggered by the electronic pulse of the Vicon system to synchronize recordings of the walking mechanics, EMG and SO fascicle length.

2.3.4 Data analysis

Hindlimb kinematics. Recorded coordinates of markers on the right hindlimb were low-pass filtered using a Butterworth low-pass, zero-lag filter (cut-off frequency 6 Hz). To reduce knee marker errors due to excessive skin movement, the estimated knee joint center position at each video frame was recalculated using the recorded position of the ankle and hip joints and length of the shank and thigh segments (Goslow et al., 1973); the segment lengths were measured by a caliper during the surgery. Individual walking cycles and their stance and swing phases were identified as the periods between the right hind paw contact (PC) and paw off (PO) time instances determined from the force plate recordings. The computed hindlimb joint angles, as defined in Gregor et al. (2006), and a geometric musculoskeletal model of the hindlimb (Goslow et al., 1973) were used to calculate SO muscle-tendon unit (MTU) length. MTU length was normalized to a reference length (L_{ref}), defined as the mean between the maximum and minimum of the averaged MTU lengths during the swing phase in baseline level walking (Maas et al., 2009).

EMG. Recorded EMG signals were band-pass filtered (see above) and full-wave rectified. Within each walking cycle an EMG burst of SO, LG or MG was considered on when the EMG signal was above a threshold signal level for at least 50 ms, and off when the signal was below the threshold for at least 50 ms. The threshold level was defined as 2 standard deviations (SD) above the mean EMG signal during a muscle silent period (during most of the swing phase of walking) (Gregor et al., 2006). Mean EMG burst

activity for each of the three muscles was determined as the ratio of the time integral of the rectified EMG burst and the burst duration. The mean EMG burst magnitudes of each muscle within an animal were normalized by the maximum mean burst magnitude found across all walking cycles and conditions recorded before denervation.

SO fascicle length. Fascicle length was computed from the measured propagation time of ultrasound between the implanted piezoelectric crystals and the known speed of ultrasound propagation in muscle tissue (1540 m/s) (Biewener et al., 1998). Fascicle length calculations and low-pass filtering was done using the SonoView software (Sonometrics Corporation, London, ON, Canada). The SO fascicle length was normalized to a reference length, defined as the mean of the maximum and minimum fascicle lengths during the swing phase of level walking (Maas et al., 2009).

2.3.5 Fascicle length measurements in a sedated cat

To assess the minimum SO fascicle length in relaxed muscle, fascicle length measurements were made in one cat (CO) before SO-LG denervation while the cat was sedated (dexmedetomidine, 40-60 μg/kg, S.C.). The ankle joint angle was fully plantar flexed at 180^{o} and the knee joint flexed at 35^{o}. SO fascicle length was also measured at the same ankle and knee joint angles while the SO was electrically stimulated through the implanted EMG electrodes. A single pulse (100 ms) was used with the current selected to cause maximum fascicle shortening.

2.3.6 Treatment of data and statistics

Walking cycles with a steady-state speed and without paw slippage were selected and used for further analysis. For MTU and muscle fascicle length analysis, a total of 186 walking cycles were processed across 4 cats with implanted sonomicrometry crystals, pre

and post SO-LG denervation, and three walking slope conditions (Table 2.1). For EMG analysis, 289 walking cycles across 7 cats with implanted EMG electrodes (including 4 cats with sonomicrometry crystals) and all experimental conditions were processed. In some cats, I was unable to analyze EMG data due to the low signal-to-noise ratio, specifically for MG in downslope and level walking before denervation. This could have resulted from implantation of electrodes in the mid-belly compartment of MG with a low percentage of slow-twitch fibers (English, personal communication). As a result, very low EMG activity could be detected during downslope and level walking at self-selected speeds, as opposed to upslope walking that requires recruitment of additional faster motor unit populations (Gregor et al., 2006, Hodson-Tole et al., 2012). EMG activity of MG also increases following denervation of its synergists (Pearson and Misiaszek, 2000, Maas et al., 2010, Prilutsky et al., 2011). For detailed information about the number of trials included in the analysis, see Table 2.1. For the purpose of this study, the following stance phase related characteristics of SO length were determined and analyzed for each cycle across 4 cats, for whom SO fascicle length was measured (Table 2.1), and experimental conditions: the MTU and fascicle lengthening in stance defined as the difference in normalized length between the initial length at PC and peak length in stance; and the MTU and fascicle shortening in stance defined as the difference in normalized length between the peak length in stance and the minimum length in terminal stance (illustrated in Fig. 2.1).

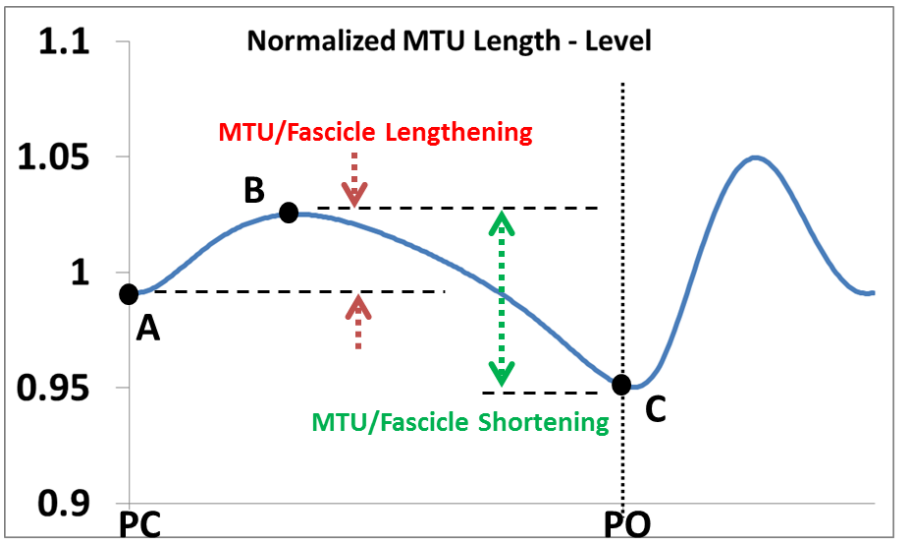

Figure 2.1. Illustration of calculated variables on exemplary normalized SO MTU length trace during level walking. (A) Initial length. (B) Max length during stance. (C) Length at end of stance. PC, paw contact; PO, paw off

First, a single sample t-test was performed for each cat with implanted sonomicrometry crystals (Table 2.1) and slope to determine if SO fascicle shortening was present following denervation, i.e. was greater than zero (SPSS 20.0, SPSS Inc. Chicago, IL, USA). To determine effects of SO paralysis and walking slope condition on SO length characteristics, the linear mixed model analysis (SPSS 20.0, SPSS Inc. Chicago, IL, USA) was used to account for varying number of trials between the factors. For the linear mixed model analysis of individual cats, SO pre-post paralysis condition and walking slope were considered fixed factors, while the walking cycle was considered a random factor. When the mixed model analysis was applied to data from all cats pooled together, an additional random factor, "cat", was introduced. The linear mixed model analysis was performed on each SO muscle length characteristic described above. The same analysis was also performed for separate sets of EMG data of SO, LG and MG muscles in 7 cats to test effects of denervation and walking slope on mean EMG burst

activity. For one cat (CO), a single sample t-test was used to compare the absolute SO fascicle length at the end of stance against the minimum SO fascicle length during passive movement of the ankle joint. Finally, two-sample, unpaired t-tests were performed to compare the magnitude of change in SO fascicle shortening/lengthening post-denervation versus baseline between all walking conditions (for downslope (n = 25/27), level (n = 39/32) and upslope (n = 38/25), respectively; see Table 2.1). Statistical significance level was set at $P<0.05$.

2.4 Results

Table 2.1. Number of walking cycles from each cat and slope condition analyzed before and after denervation. SO length variables include fascicle lengthening/shortening and MTU lengthening/shortening.

		SO Length		SO EMG		LG EMG		MG EMG	
Slope	Cat	Pre	Post	Pre	Post	Pre	Post	Pre	Post
Level	GE	11	10	10	13	10	13	10	13
	CO	8	7	8	10	4	10	8	10
	NA	8	10	–	–	–	–	–	–
	RI	5	12	–	–	–	–	–	–
	IN	–	–	10	10	14	10	–	–
	KO	–	–	6	10	–	10	–	10
	BL	–	–	12	8	–	8	–	8
	Total	32	39	46	51	38	51	18	41
Up	GE	4	16	10	10	5	10	10	6
	CO	5	5	5	9	10	9	5	9
	NA	8	12	2	6	–	6	–	6
	RI	8	5	–	–	–	–	–	–
	IN	–	–	10	10	11	10	–	–
	KO	–	–	10	10	10	10	10	10
	BL	–	–	10	6	–	6	10	6
	Total	25	38	47	51	36	51	35	37
Down	GE	5	10	13	12	11	12	10	10
	CO	12	4	1	4	1	4	–	–
	NA	3	7	4	5	4	5	–	–
	RI	7	4	–	–	–	–	–	–
	IN	–	–	10	8	10	8	–	–
	KO	–	–	9	11	2	11	3	11
	BL	–	–	11	6	–	6	–	3
	Total	27	25	48	46	28	46	13	24

During days 3 to 14 after SO-LG nerve transection and repair, SO and LG muscles were paralyzed, which was evident from the lack of EMG bursts during walking (Fig. 2.2). During the same period, the mean EMG burst magnitude in the intact MG muscle increased significantly ($P<0.05$; Fig. 2.2). Although the general patterns of SO MTU length (Fig. 2.3) or fascicle length (Fig. 2.4) during level and slope walking were surprisingly similar pre- and post-nerve transection and repair, there were substantial differences in the magnitude of SO muscle shortening and lengthening during the stance phase of walking (Figs. 2.5 and 2.6).

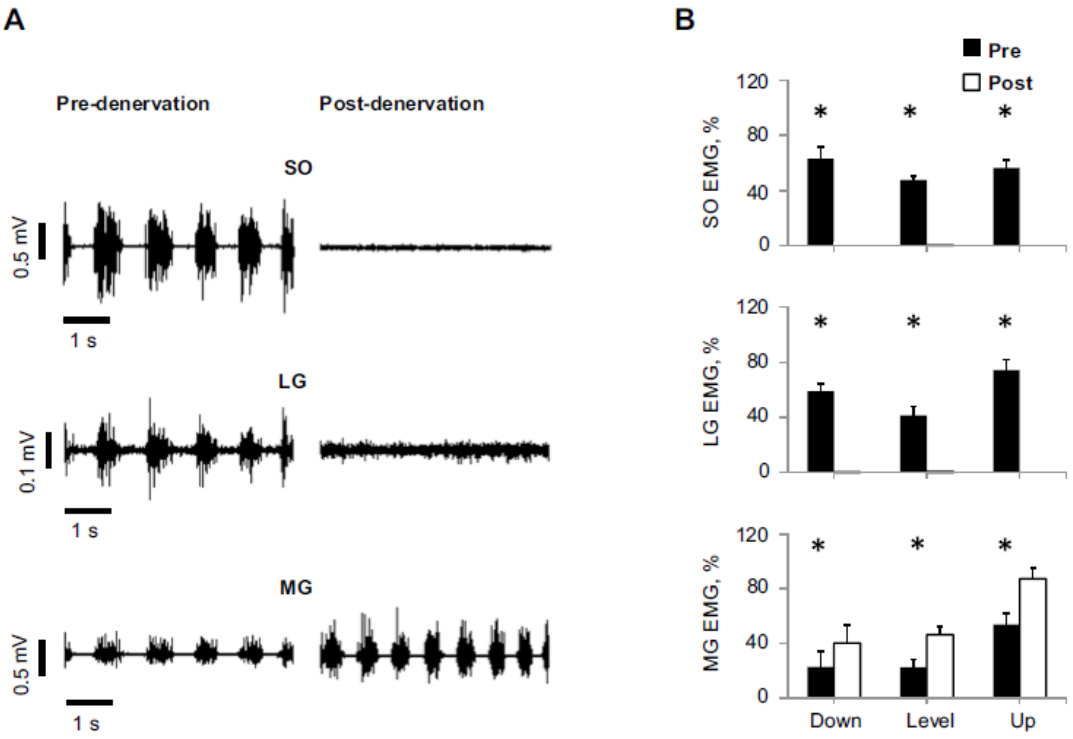

Figure 2.2. EMG activity of soleus (SO), lateral gastrocnemius (LG) and medial gastrocnemius (MG) muscles during level and slope walking before and after SO-LG denervation. (A) Representative raw EMG activity of SO, LG and MG before and after denervation for level walking; Cat CO. (B) Averaged normalized EMG activity (mean±SD) of SO, LG and MG during downslope, level, and upslope walking before and after denervation; 7 cats (Table 2.1). *Significant differences between pre- and post-denervation ($P<0.001$).

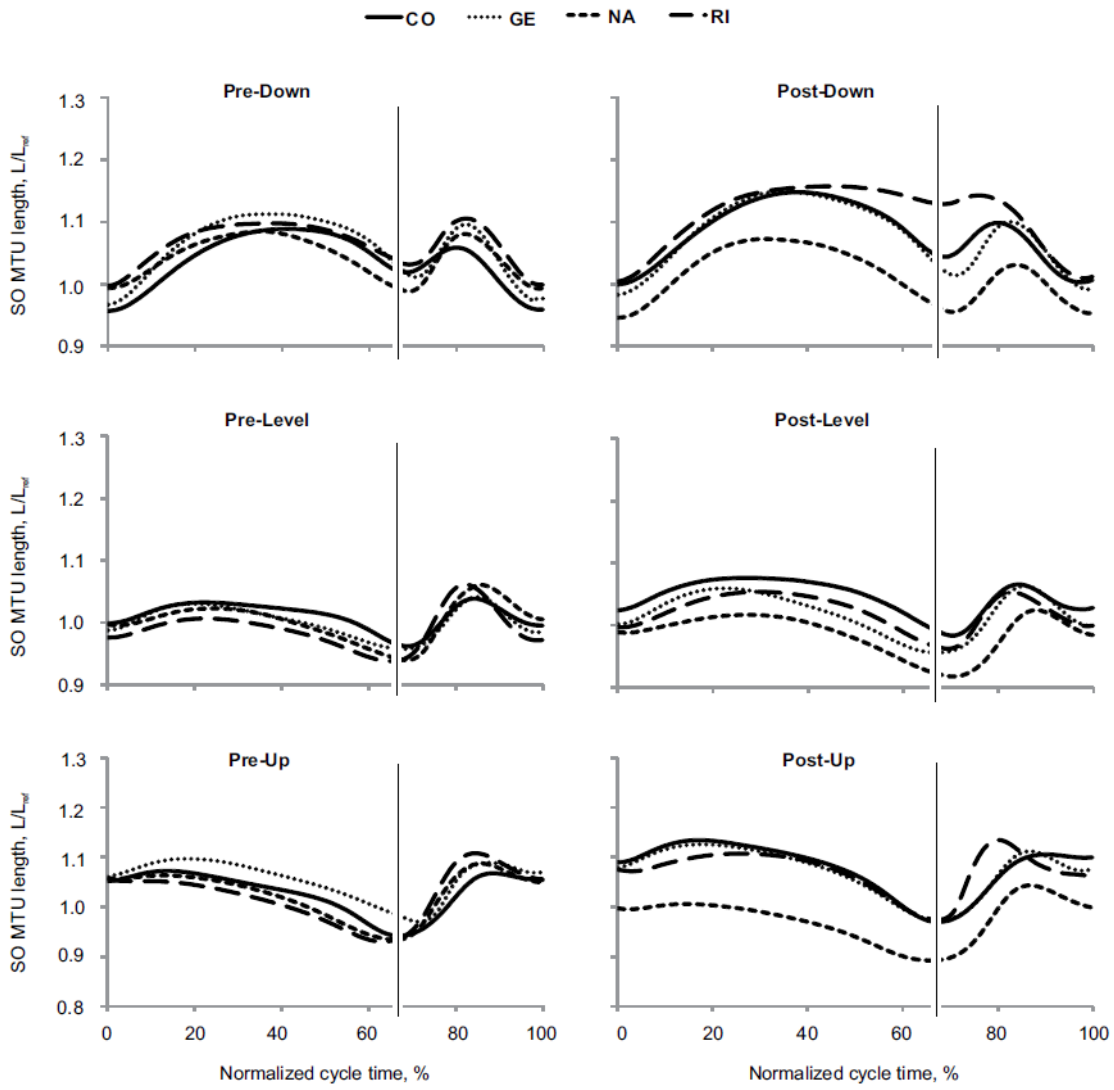

Figure 2.3. Normalized SO MTU length of each cat during three walking slope conditions, pre and post SO-LG denervation. Values are a fraction of the MTU reference length (L_{ref}), which is the mean of the maximum and minimum MTU lengths during the swing phase of level walking before denervation. Time is normalized to the duration of stance phase and swing phase separately. The thin vertical line represents the end of stance phase and the beginning of swing phase. 4 cats: CO, GE, NA, RI (Table 2.1).

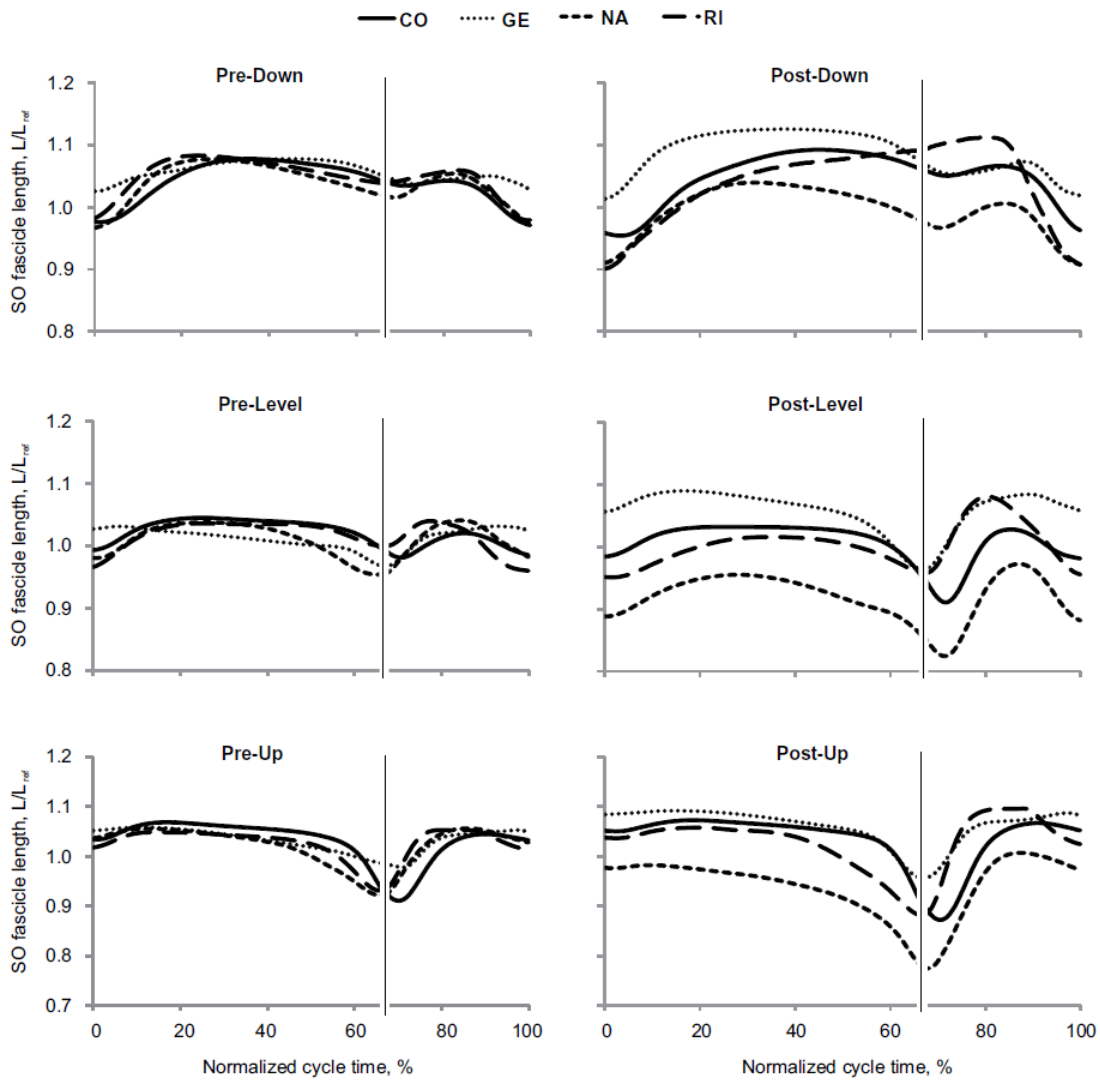

Figure 2.4. Normalized SO fascicle length of each cat during three walking slope conditions, pre and post SO-LG denervation. Values are a fraction of the fascicle reference length (L_{ref}), which is the mean of the maximum and minimum fascicle lengths during the swing phase of level walking before denervation. Time is normalized to the duration of stance phase and swing phase separately. The thin vertical line represents the end of stance phase and the beginning of swing phase. 4 cats: CO, GE, NA, RI (Table 2.1).

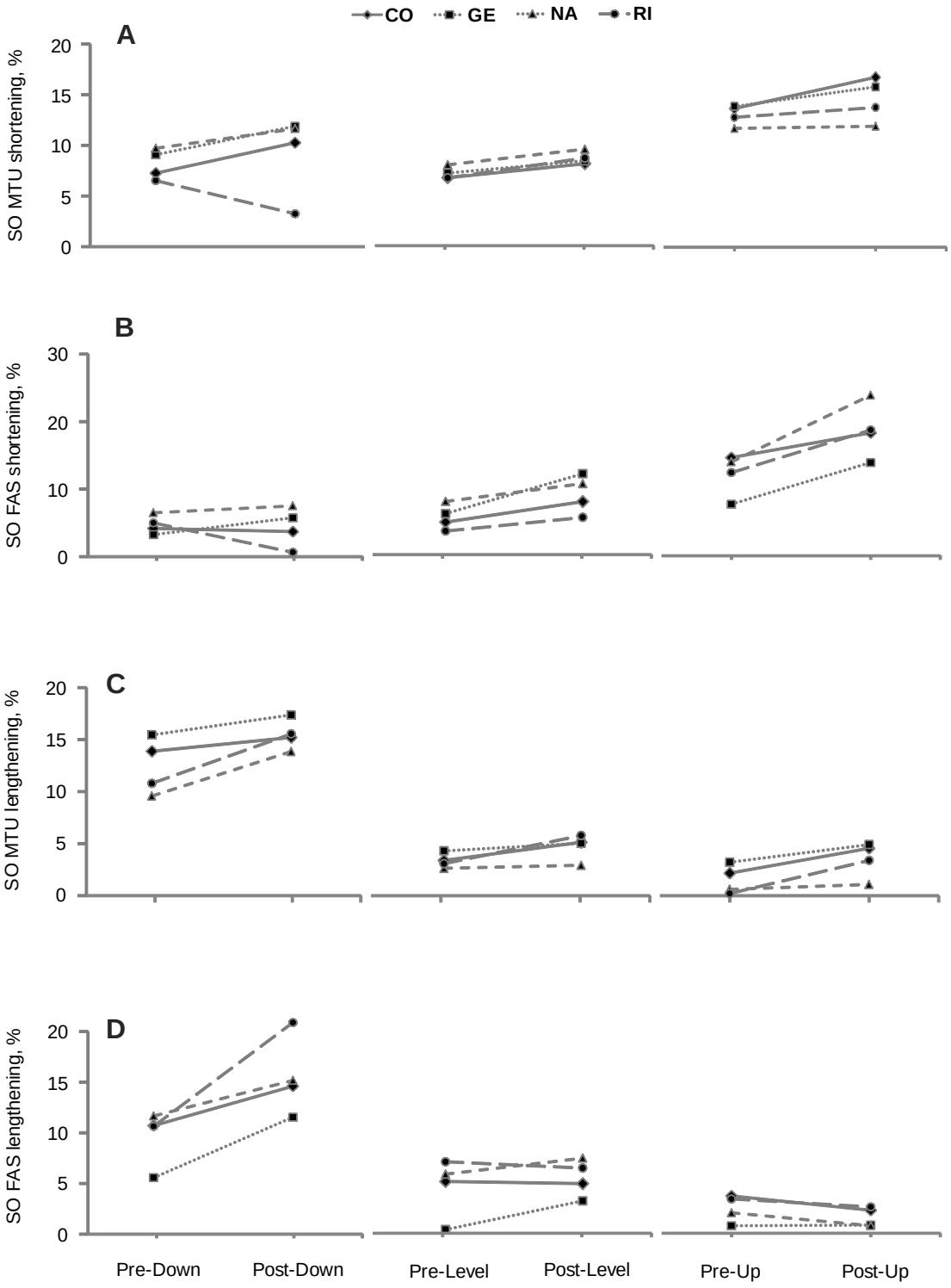

Figure 2.5. Normalized mean magnitude of shortening and lengthening of SO fascicles (FAS) and MTU during stance phase for each cat (CO, GE, NA, RI, Table 2.1) and walking slope condition pre and post SO-LG denervation. All values are a percentage of reference length L_{ref} (see text for further explanations). (A) SO MTU shortening before and after denervation. (B) SO fascicle shortening pre and post denervation. (C) SO MTU lengthening before and after denervation. (D) SO fascicle lengthening pre and post denervation.

2.4.1 Soleus MTU and fascicle shortening

SO MTU shortening during the stance phase increased significantly following denervation in all slope conditions (Fig. 2.6; mean±SD: 7.7±2.2 vs 8.9±2.1 $\%L_{ref}$, $F_{1,47}$ = 4.45, P≤0.001 for downslope walking; 7.2±0.9 vs 8.8±0.7 $\%L_{ref}$, $F_{1,64}$ = 15.23, P≤0.001 for level; 13.0±1.3 vs 13.9±1.2 $\%L_{ref}$, $F_{1,59}$ = 4.74, P=0.033 for upslope). Analysis of SO MTU shortening after SO denervation in individual animals revealed a significant increase in 2 out of 4 animals in each of the slope walking conditions (P≤0.01), while one cat showed a decrease during downslope walking (P=0.001, Fig. 2.5A). The change in SO MTU shortening in response to denervation differed only between level and upslope walking (1.6±0.5 vs. 0.9±1.5 $\%L_{ref}$, respectively, P=0.011). There were no significant differences between level and downslope (P=0.393), and downslope and upslope (P=0.595) conditions.

SO fascicle shortening persisted following denervation in all walking conditions. The majority of SO fascicle shortening occurred during the end of stance (approximately between 45% and 65% of cycle time, Fig. 2.4) before and after denervation. The magnitude of SO fascicle shortening during stance following denervation was significantly greater than zero in all cats and slope conditions (P≤0.004; see Table 2.1 for number of samples) except for one cat in downslope condition (RI, P=0.138, Fig. 2.5B). After denervation, SO fascicle shortening in stance increased on average by 65% and 56% in level and upslope walking, respectively. The corresponding mean normalized shortening magnitudes were 9.1±1.7 and 17.3±2.2 $\%L_{ref}$, respectively, which were significantly greater than those before denervation (5.5±0.2 and 11.1±2.7 $\%L_{ref}$; $F_{1,62}$ = 50.04, P≤0.001 and $F_{1,59}$ = 61.33, P≤0.001, respectively; Fig. 2.6B). The change in SO

fascicle shortening in response to denervation was significantly greater for the upslope condition compared to the level condition (5.8±3.0 vs. 3.6±2.3 $\%L_{ref}$, $P \leq 0.001$, Fig. 2.7). Post-denervation changes in fascicle shortening during upslope and level conditions were both greater than that during downslope condition (-0.3±1.7 $\%L_{ref}$; $P \leq 0.001$; Fig. 2.7). The pre- versus post-denervated change in SO fascicle shortening for each walking condition was correlated to the corresponding mean MG EMG activity, with greater changes in fascicle shortening corresponding to higher EMG (Fig. 2.7, closed symbols).

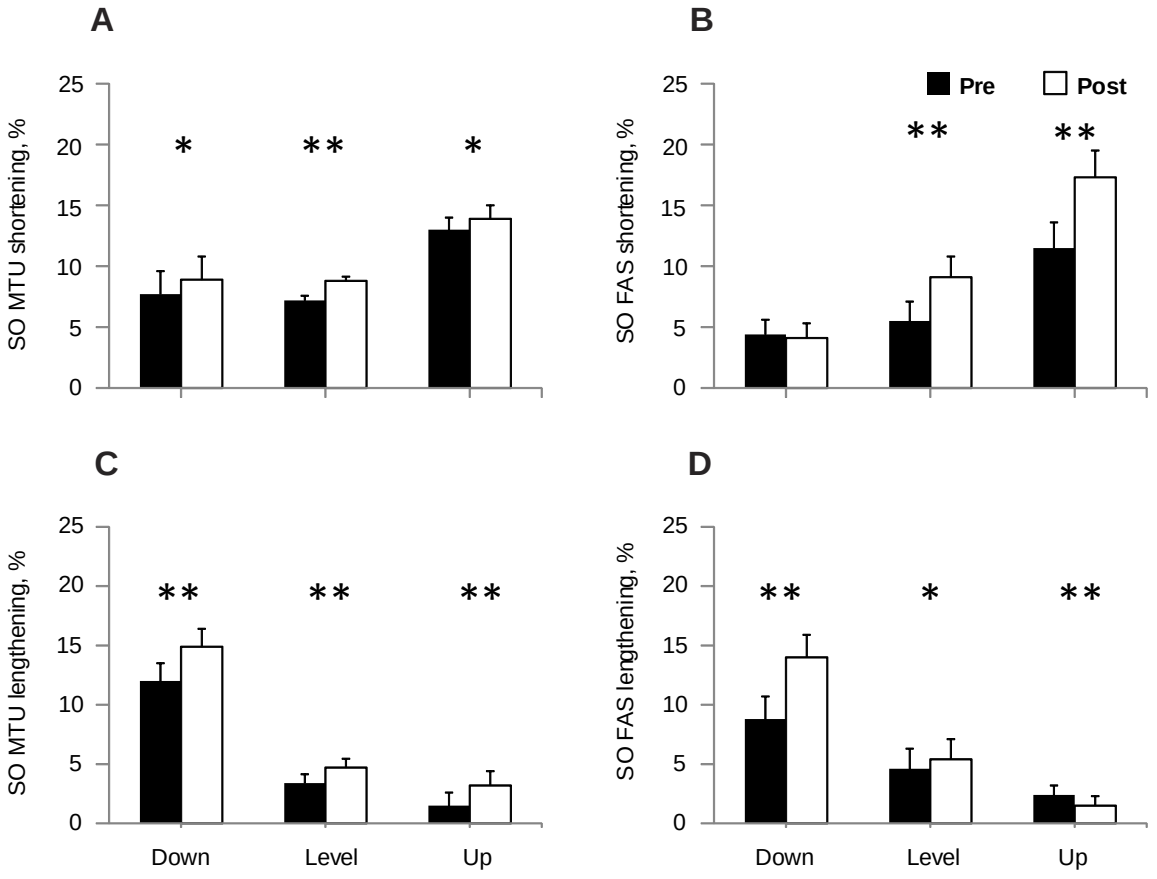

Figure 2.6. Normalized mean magnitude of shortening and lengthening of SO MTU and fascicles during stance of level and slope walking pre- and post-denervation averaged across 4 animals (CO, GE, NA, RI, Table 2.1). (A) Mean SO MTU shortening. (B) Mean SO fascicle (FAS) shortening. (C) Mean SO MTU lengthening. (D) Mean SO FAS lengthening. Values are a percentage of L_{ref} (mean±SD). Significant differences between pre- and post-denervation values were found in all walking conditions except for SO FAS shortening during downslope walking. *p<0.05, **p<0.001

2.4.2 Soleus MTU and fascicle lengthening

There was a significant increase in SO MTU lengthening following denervation in all walking conditions (Fig. 2.6C). It increased by 22% for downslope walking (12.4±2.5 vs. 15.1±1.8 $\%L_{ref}$, $F_{1,47} = 34.648$, $P \leq 0.001$), 34% for level walking (3.5±1.0 vs. 4.7±1.9 $\%L_{ref}$, $F_{1,62} = 15.475$, $P \leq 0.001$), and by 200% for upslope walking (1.1±1.2 vs. 3.3±2.0 $\%L_{ref}$, $F_{1,58} = 35.739$, $P \leq 0.001$). SO MTU lengthening following denervation in individual cats increased in most walking conditions and cats ($P \leq 0.001$-0.010; Fig. 2.5C); the exceptions were no changes in cat CO during downslope, GE during level and NA during level and upslope walking (P=0.052-0.540). For the change in MTU lengthening in response to denervation, there was a significant difference between downslope and level walking (2.9±2.1 vs. 1.3±1.1 $\%L_{ref}$, respectively, $P \leq 0.001$), and downslope and upslope walking (2.9±2.1 vs. 1.7±1.6 $\%L_{ref}$, P=0.019). There was no difference between level and upslope walking (P=0.234).

SO fascicle lengthening in stance increased after denervation in level and downslope walking by 17% and 59%, respectively (from 4.6±2.9 to 5.4±1.9 $\%L_{ref}$, $F_{1,62} = 7.845$, P=0.007 and from 8.8±2.2 to 14.0±2.9 $\%L_{ref}$, $F_{1,46} = 106.330$, $P \leq 0.001$, respectively); but decreased in upslope condition by 38% (from 2.4±0.9 to 1.5±0.8 $\%L_{ref}$, $F_{1,58} = 21.661$, $P \leq 0.001$; Fig. 2.6D). During downslope walking, fascicle lengthening increased after SO-LG denervation in three cats ($P \leq 0.001$), but did not change in one cat (NA: $F_{1,7} = 3.198$, P=0.117). During level walking, SO fascicle lengthening increased after denervation in only one cat from 0.5±0.3 to 3.4±1.3 $\%L_{ref}$ (GE: $F_{1,19} = 50.14$, $P \leq 0.001$, Fig. 2.5D). For the upslope condition, SO fascicle lengthening decreased significantly in two cats after denervation (NA: $F_{1,18} = 42.34$, $P \leq 0.001$; CO: $F_{1,8} = 79.04$,

P≤0.001, respectively), whereas two cats showed no significant changes (RI: $F_{1,11}$ = 0.946, P=0.352, and GE: $F_{1,18}$ = 0.305, P=0.588). There were significant differences in the magnitude of change of SO fascicle lengthening in response to denervation between downslope, level and upslope conditions (5.2±2.7, 0.8±2.4, and -0.9±1.1 $\%L_{ref}$, respectively; P≤0.001; Fig. 2.7). There also appeared to be a close relationship between the change in SO fascicle lengthening and MG EMG activity after denervation (Fig. 2.7, open symbols).

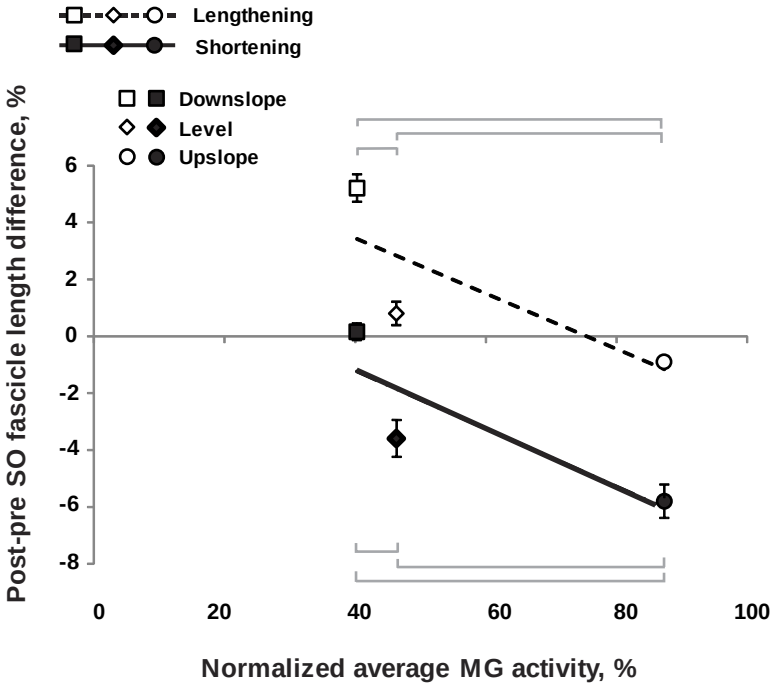

Figure 2.7. Mean post-pre difference in SO fascicle lengthening/shortening during stance as a function of mean MG activity post-denervation. The post-pre difference in fascicle shortening was computed as the difference in SO fascicle shortening between pre- and post-denervation values (see Fig. 2.6B); a negative value indicates the increase in shortening post-denervation. The post-pre difference in fascicle lengthening was computed as the difference in SO fascicle lengthening between post- and pre-denervation values (Fig. 2.6D); a positive value means the increase in lengthening post-denervation. Values are a percentage of L_{ref} (mean±SD). Lines of best linear fit are shown for changes in SO fascicle shortening (solid line, black symbols) and SO fascicle lengthening (dashed line, open symbols). Squares, diamonds and circles correspond to downslope, level and upslope walking conditions, respectively. Significant differences between pairs of walking conditions are shown by horizontal brackets (P≤0.001).

2.4.3 Fascicle lengths in passive and electrically stimulated SO muscle in a sedated cat

SO fascicle length measured in one cat (CO) under sedation at a fully extended ankle (180^{o}), corresponding to its shortest MTU length, was 35.7 mm. When the SO muscle was electrically stimulated via implanted EMG electrodes to cause maximum fascicle shortening at the same joint angle, SO fascicle length decreased to 32.7 mm. Following denervation, SO fascicle lengths of the same cat at the end of stance during downslope, level and upslope walking were 38.7±0.3 mm (ankle joint angle of 103.9 ± 4.3^{o}), 34.8±0.6 mm (130.9 ± 2.6^{o}), and 33.0±0.5 mm (135.4 ± 4.8^{o}), respectively. The fascicle lengths in the denervated SO during level and upslope walking were significantly shorter than the minimum fascicle length of passive SO in the sedated condition ($P=0.005$ and $P<0.001$, respectively). When compared to fascicle length of electrically stimulated SO in the sedated condition, fascicle lengths of the denervated SO at paw lift-off during level and downslope walking were longer ($P<0.001$ and $P<0.001$, respectively), whereas SO fascicle length during upslope walking was not different (one sample t-test, $P=0.308$).

2.5 Discussion

Previous studies have documented differential changes in MTU length and EMG of SO and MG in intact cats (Gregor et al., 2006, Maas et al., 2009, Hodson-Tole et al., 2012), as well as muscle fascicle length changes in intact MG after denervation of SO and LG (Maas et al., 2010) during level and slope walking. MTU length and EMG activity of SO and MG before denervation obtained in this study are in good agreement with the previous studies. This report is the first to describe fascicle length changes in a

denervated muscle during locomotion. It was hypothesized (see Introduction) that given no myofascial force transmission between denervated SO and its intact synergists, SO fascicles would mirror lengthening of SO MTU during the stance phase of walking (Fig. 2.8 A1), whereas during SO MTU shortening in the stance phase, denervated SO fascicles would not shorten substantially. The obtained results contradicted the hypothesis. They indicate that after denervation of SO and LG (i) there are differential changes in MTU and fascicle lengthening of SO in the yield phase of stance, i.e. during upslope walking, SO fascicle lengthening decreased while SO MTU lengthening increased (Figs. 2.6 C,D); (ii) there is indeed SO fascicle shortening during the stance phase of walking; and (iii) the magnitude of the changes in shortening and lengthening appears to be related to the EMG magnitude of the intact synergist (MG, Figs. 2.2B and 2.7) rather than to the SO MTU length changes (Fig. 2.6 A,B), i.e. the increase in SO fascicle shortening and MG EMG activity change in parallel from downslope to level and to upslope walking conditions (Figs. 2.2B, 2.6B, and 2.7). Finally, (iv) the fascicle length of the denervated SO at the end of fascicle shortening in stance during level and upslope walking was shorter than the passive SO fascicle length measured at a much more extended ankle angle and, thus, at a lower SO MTU length in one sedated animal.

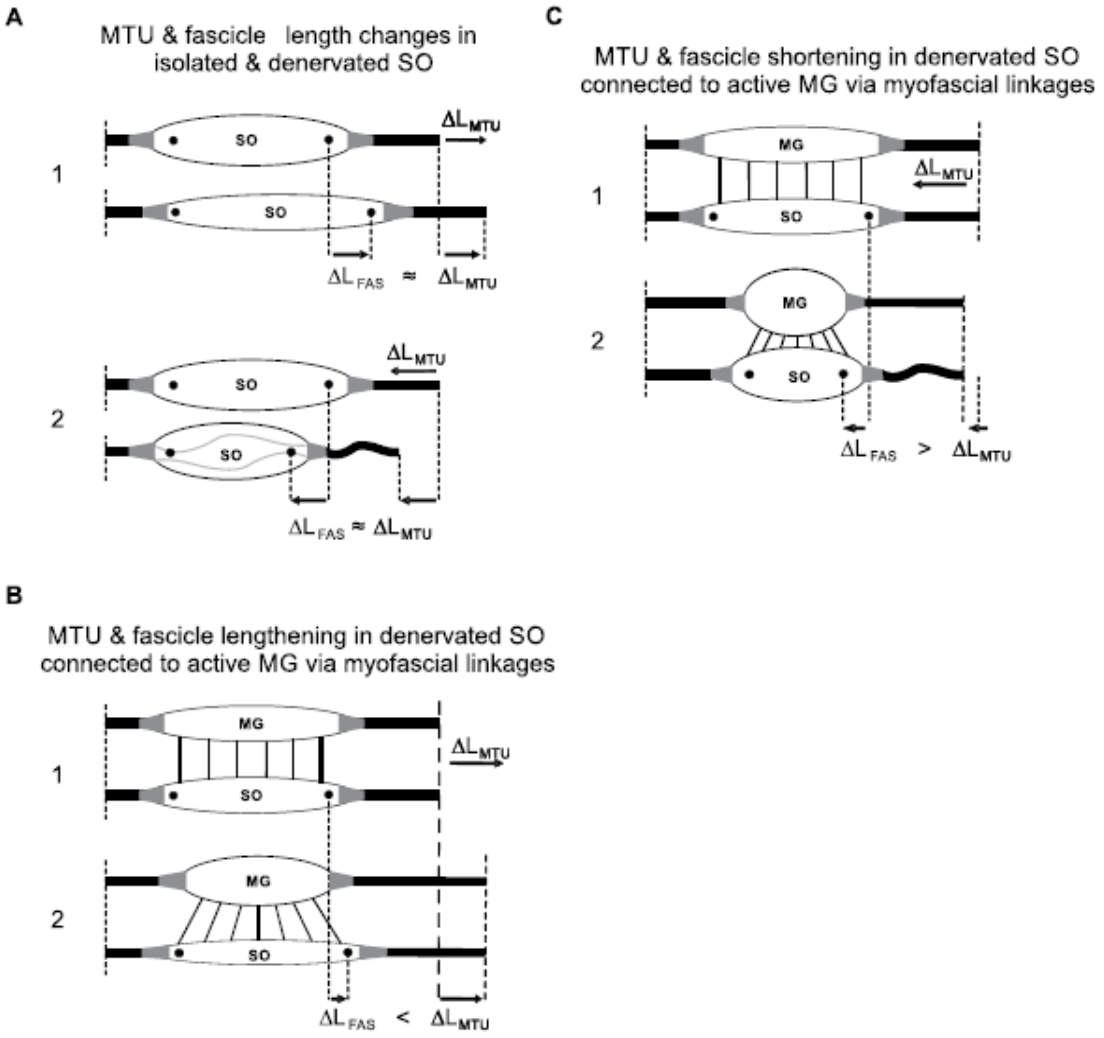

Figure 2.8. Schematic illustrating changes in SO fascicle length (ΔL_{FAS}) during SO MTU length changes in different conditions. Black circles in SO indicate implanted sonomicrometry crystals to measure muscle fascicle length as distance between the crystals. (A) MTU and fascicle lengthening (1) and shortening (2) in passive SO muscle with no myofascial force transmission between SO and its synergists. During MTU lengthening, SO fascicles are expected to take up most of the MTU stretch. During MTU shortening at lengths below the SO MTU resting length (at which SO MTU produces no passive force), both the fascicles and tendon are expected to buckle (see text for further explanations). (B) MTU and fascicle lengthening in passive denervated SO while MG MTU is elongating starting from a passive condition (1) to a final elongation in which MG is active and its fascicles are shortened (2). In this situation, myofascial links between MG and SO fascicles might pull on SO muscle belly and reduce its elongation. (C) MTU and fascicle shortening in passive denervated SO while MG MTU is shortening starting from a passive condition (1) to a final shortening in which MG is active and its fascicles are shortened (2). In this situation, myofascial links between MG and SO fascicles might pull on SO fascicles and increase its shortening.

2.5.1 Passive muscle fascicle elasticity and fascicle buckling

Any explanation for the observed behavior of SO fascicles would depend on assumptions about relative compliance of the tendon and muscle fascicles of the denervated (passive) SO MTU in the studied conditions. First, if the muscle fascicles were more compliant than the tendon, as shown to be the case in the cat SO at very small muscle forces, i.e. low EMG levels (Rack and Westbury, 1984, Scott and Loeb, 1995), then lengthening of SO MTU would be mirrored in the muscle fascicles (Fig. 2.8 A1). An increase in SO MTU lengthening in the yield phase of stance during all three slope conditions after denervation of the LG and SO muscles (Fig. 2.6C; see also Pearson et al. (1999), Maas et al. (2007), and Maas et al, (2010)) would result in an increase in SO fascicle lengthening. In contrast, SO fascicle lengthening decreased during upslope walking following SO-LG denervation (Figs. 2.6D and 2.7). This result, however, is consistent with the idea of increased external forces acting on the SO muscle belly and resisting its lengthening (see Fig. 2.8 B2).

Second, shortening of the denervated SO MTU and muscle fascicles during the propulsion phase in stance occurs in most walking slope conditions (Figs. 2.3-2.5 and 2.6 A,B). The fascicle lengths of the denervated SO at the end of the shortening phase during level and upslope walking were significantly shorter than the minimal possible fascicle length of passive SO measured in the same sedated animal at a much more extended ankle and thus at shorter SO MTU length (the latter condition is shown schematically in Fig. 2.8 A2). Therefore, simple joint kinematics cannot explain the behavior observed in the denervated SO fascicles during walking. Also, shortening of muscle fascicles of denervated SO by its passive forces in this situation does not seem likely. This is because

passive forces of cat SO within the in vivo range of motion at the ankle joint (above 90^{o}-120^{o}, see Introduction) are very small (peak passive forces do not exceed 0-10% of SO maximum isometric force or peak SO tendon force during walking (Rack and Westbury, 1969, Tabary et al., 1972, Herzog et al., 1992, Scott et al., 1996)). In addition, buckling of passive SO fascicles (Muraoka et al., 2002, Herbert et al., 2015) (see Fig. 2.8 A2) during SO MTU shortening in the stance phase of walking (Figs. 2.3, 2.6A) appears unlikely due to high pressure inside the superficial posterior crural compartment (Garfin et al., 1981, Sjogaard et al., 2004, Ward et al., 2007) caused by actively contracting intact ankle extensor synergists, such as MG (Fig. 2.2) (Maas et al., 2010) and plantaris (Prilutsky et al., 2011). The above arguments suggest that length changes of SO fascicles during stance cannot be explained solely by SO intrinsic passive forces or fascicle buckling. Therefore, a mechanism such as myofascial force transmission likely contributes to the observed behavior.

2.5.2 Epimuscular myofascial force transmission

These results support the presence of epimuscular myofascial force transmission between the denervated SO and intact ankle extensors based on three key findings; (1) lengthening of denervated SO fascicles during the yield phase in stance does not correspond to SO MTU lengthening (compare upslope walking in Fig. 2.6 C and D) and appears to decrease with increasing synergist muscle activity (Figs. 2.2B, 2.6D and 2.7; see also Fig. 2.8 A1 and B2); (2) passive SO fascicles shorten during the push-off phase in late stance (Figs. 2.4 and 2.6B), despite the expected high pressure inside the superficial posterior crural compartment preventing buckling of passive SO fascicles (see discussion above and Fig. 2.8 A2 and C2); and (3) SO fascicle shortening following

denervation appears to increase with levels of synergist muscle activity (MG, Figs. 2.2B and 2.7; plantaris (Prilutsky et al., 2011)) during level and slope walking conditions (compare Figs. 2.2B and 2.6B).

Epimuscular myofascial force transmission is mediated by connective tissue structures at the muscle belly boundaries. In normal physiological conditions, myofascial force transmission between SO and synergistic ankle extensor muscles in cats and rats was found to be limited (Maas and Sandercock, 2008, Tijs et al., 2015). Denervation of SO results in an increased activity of an intact synergist MG during walking (Fig. 2.2; (Maas et al., 2010, Prilutsky et al., 2011)). In addition, SO-LG denervation leads to a greater yield at the ankle and less knee flexion during the stance phase of walking (Maas et al., 2007, Chang et al., 2009). As a consequence, the MTU length of the denervated SO and intact MG muscles increases following SO-LG denervation and this increase is larger for MG than SO. This in turn might result in a higher than normal relative displacement between SO and MG muscle bellies. It has been shown that the extent of myofascial force transmission is dependent on this relative position (Huijing and Baan, 2003, Maas et al., 2004, Huijing et al., 2011, Tian et al., 2012), as this affects the length and stiffness of the epimuscular linkages. It is reasonable to propose that following SO-LG denervation, forces exerted by these linkages on the denervated SO may cause reduced lengthening (during the yield phase) or increased shortening (during push-off phase) of SO muscle fascicles. An illustration of this proposed mechanism is presented in Fig. 2.8 B and C, respectively. Such an effect of epimuscular connective tissues is in agreement with its previously hypothesized function as a safety net for traumatic events in muscles and tendons (Maas and Sandercock, 2010).

2.5.3 Potential functional implications of increased fascicle length changes in denervated muscles

The above findings may have several functional implications. The presence of unexpectedly large length changes in the paralyzed muscle as a result of peripheral nerve injury could result in decreased muscle atrophy (Edgerton et al., 2002, Bodine, 2013). Several studies have reported that repetitive lengthening of paralyzed muscles reduces the effect of disuse on muscle atrophy through stretch- and/or stress-induced activation of signaling pathways responsible for muscle growth (Roy et al., 1998, Martineau and Gardiner, 2001, Sakakima and Yoshida, 2003, Bassel-Duby and Olson, 2006, Agata et al., 2009). Therefore, passive lengthening and shortening of muscle fascicles in denervated muscles, as observed in this study, may provide a mechanism by which atrophy of paralyzed muscles may be reduced. Additional studies would be required in order to test the effect on muscle atrophy.

Paralysis or reduction in force output (e.g., due to atrophy) of a single muscle in a muscle group may lead to asymmetric loading of the joint and subsequent development of joint tissue degeneration, osteoarthritis, and possible other secondary joint conditions (Roos et al., 2011, Vincent et al., 2012, Bennell et al., 2013). Fascicle shortening and tendon lengthening within a paralyzed muscle may contribute to maintaining a more symmetric loading pattern in the joint by redistributing forces to tendons of all synergists in the group, including those of injured muscles. A reduction in muscle atrophy, as mentioned in the paragraph above, would also help to reduce any asymmetry after muscle function is restored. Future studies are needed to test this potential effect.

2.5.4 Future work

This study was designed to document fascicle length changes in denervated SO and its possible interactions with intact MG during locomotion. Although the suggested mechanism of myofascial force transmission between denervated SO and its intact synergists (i.e. MG) appears to be the most likely explanation (see Discussion above), direct testing is required. One approach could be to sever the myofascial linkages between SO and MG. This approach, however, will not likely result in the desired condition. Due to plasticity of connective tissues, which tend to quickly (within a few days) reestablish connections (Loeb, 1999, Maas et al., 2015, Bernabei et al., 2016), it would be very difficult to obtain measurements in which full isolation of these muscles can be assured. Another approach could be to attenuate effects of myofascial linkages by injecting type A botulinum toxin into the muscle (Yucesoy et al., 2015), but such an intervention will affect the force-producing capacity in both the target and adjacent muscles (Yaraskavitch et al., 2008). The most adequate approach would probably be to sequentially denervate the synergists.

2.6 Conclusion

This chapter presents the first report of increased muscle fascicle length changes in denervated SO fascicles during the stance phase of walking that could affect the extent of muscle atrophy and joint loading. Evidence from SO fascicle and MTU length, as well as from MG EMG activity recordings, suggests that this behavior might result from the action of epimuscular myofascial linkages between intact and paralyzed ankle extensors. Additional studies are needed to confirm the importance of this mechanism.

CHAPTER III

SPECIFIC AIM 2

TASK-DEPENDENT INHIBITION OF SLOW-TWITCH SOLEUS AND EXCITATION OF FAST-TWITCH GASTROCNEMIUS DO NOT REQUIRE HIGH MOVEMENT SPEED AND VELOCITY DEPENDENT SENSORY FEEDBACK

(Mehta, Prilutsky. Front Physiol 5: 410, 2014)

3.1 Introduction

Skeletal muscles have diverse morphological properties and can differ substantially in muscle fiber type composition, fascicle length, physiological cross-sectional area, pennation, tendon length and thickness, etc. (Ariano et al., 1973, Johnson et al., 1973, Sacks and Roy, 1982, Wood et al., 1989, Cutts et al., 1991, Ward et al., 2009). Distinct morphological properties of muscle fascicle groups within a muscle, i.e. muscle compartments, are also well documented. Single muscle compartments are separated by a sheath of connective tissue and often differ in muscle fiber architecture, fiber histochemical properties, mechanical action at the joint and innervation (English and Letbetter, 1982, Loeb et al., 1987, Segal et al., 1991, Nichols, 1994, Richmond et al., 1999). As a result, activity patterns and mechanical actions of individual muscles within a synergistic muscle group or those of individual muscle compartments within a muscle are distinct and task-dependent (English, 1984, Chanaud and Macpherson, 1991, Lawrence et

al., 1993, Carrasco and English, 1999, Brown et al., 2007). The diversity of morphological properties and mechanical actions of individual muscles and muscle compartments has been explained by a wide range of functional requirements on the animal during everyday motor behaviors (Loeb, 1985, Otten, 1988, Gans and Gaunt, 1991, Benjamin et al., 2008).

Some large skeletal muscles, e.g. triceps surae, quadriceps, hamstrings and triceps brachii, consist of individual muscle heads that not only differ from each other in their morphological properties, but also in the number of joints they cross. For example, one-joint ankle extensor soleus (SO) and two-joint ankle extensor and knee flexor gastrocnemius (GA) are individual muscle heads of triceps surae. The fact that GA can contribute to both ankle extension and knee flexion moments gives this muscle head a mechanical advantage over SO in tasks that require this combination of joint moments; this is also true for two-joint heads of the quadriceps, hamstrings and triceps brachii muscles mentioned above (Wells and Evans, 1987, Prilutsky, 2000a).

Although GA and SO, being separate muscle heads of triceps surae, are often considered close anatomical and functional synergists and show similar activity patterns in many motor tasks (e.g., during level walking, running (Prilutsky and Gregor, 2001, Cappellini et al., 2006, Markin et al., 2012a) and jumping (Bobbert and van Ingen Schenau, 1988, Pandy and Zajac, 1991)), studies have also shown distinct activity or force patterns between SO and GA across different speeds or slopes of walking and running (Walmsley et al., 1978, Prilutsky et al., 1996a, Kaya et al., 2003, Neptune and Sasaki, 2005), cycling (Ryan and Gregor, 1992), cat paw shake response (Smith et al., 1980, Fowler et al., 1988), and external force control in humans (Wells and Evans, 1987,

Jacobs and van Ingen Schenau, 1992). The reasons and mechanisms explaining differential activity of the individual one-joint and two-joint heads of the large limb muscles, and specifically triceps surae, in some tasks but not others are still debated.

Several researchers have suggested that the differential inhibition of the slow-twitch SO but not the fast-twitch GA during fast movements such as cat paw shaking (Smith et al., 1980), cat upslope walking (Kaya et al., 2003) and human fast walking (Neptune and Sasaki, 2005) is advantageous because the contracting SO might not be able to contribute much force to and slow down the ongoing fast movement. It seems reasonable to suggest that the differential inhibition of slow-twitch SO and excitation of fast-twitch GA muscle heads during fast movements could be mediated via the velocity-sensitive spindle Ia afferents (Smith and Zernicke, 1987, LaBella et al., 1989). For example, during fast cat paw shake responses accompanied by inhibition of SO and high EMG activity of GA, extremely high firing rates of the primary spindle afferents from triceps surae have been reported to occur in phase with stretches and EMG bursts of triceps surae (Prochazka et al., 1977, Prochazka et al., 1989). On the other hand, removal of proprioceptive inputs from muscle afferents by cutting the muscle nerve does not affect the recruitment order of motor units in the cat mixed medial gastrocnemius (MG) muscle from slow-twitch to fast-twitch during evoked stretch and cutaneous reflexes in the decerebrate cat (Haftel et al., 2001). Thus, the neural mechanisms by which slow-twitch motor units during fast movements are inhibited are still unclear.

Another explanation of the functional significance of the differential activation of SO and GA seen in some motor behaviors might not be directly related to the difference in muscle fiber type composition of these triceps surae heads, but potentially depend on

the number of joints they cross. It has been shown that during tasks in which GA, a two-joint muscle, has agonistic actions at both joints it crosses, i.e. contributes to resultant ankle extension and knee flexion moments, its EMG activity is much higher than at other combinations of ankle and knee joint moments. This GA behavior has been documented in back (straight-leg) load lifting (Prilutsky et al., 1998b, Mehta and Prilutsky, 2012), cycling (Prilutsky and Gregor, 2000) and exertion of leg force on the external environment in humans (Wells and Evans, 1987, Jacobs and van Ingen Schenau, 1992). This activation strategy of GA, and other two-joint muscles, has been shown to be mechanically advantageous: it allows for minimization of the total muscle stress and fatigue in musculoskeletal models of the human leg performing a variety of motor tasks (Prilutsky and Gregor, 1997, Prilutsky et al., 1998a, Prilutsky et al., 1998b, Prilutsky, 2000a, Raikova and Prilutsky, 2001, Prilutsky and Zatsiorsky, 2002). The total muscle force requirement for producing the ankle extension and knee flexion joint moments would be substantially reduced if these moments are primarily produced by two-joint ankle extensors and knee flexors, such as GA, compared to one-joint ankle extensors (SO) and knee flexors (short head of biceps femoris). A neural mechanism that might be responsible for such behavior has been suggested to originate from two independent inputs to motoneuronal pools of two-joint muscles from spinal interneuron circuitry comprising flexor and extensor half-centers of spinal pattern generator networks (Perret and Cabelguen, 1980, Prilutsky, 2000a, Shevtsova et al., 2016). A neural mechanism to satisfy the required moments at adjacent joints while ensuring a greater contribution of the two-joint muscles spanning these joints has been postulated – a force-dependent inhibition from a two-joint muscle to its one-joint synergists (Prilutsky, 2000a). Such

force-dependent inhibition from GA to SO has in fact been reported for muscle stretch evoked responses in the decerebrate cat (Nichols, 1994, Nichols, 1999).

The goal of these experiments was to test the two possible explanations emerged from the literature for the differential activation of SO and GA – (1) SO activity is low compared to GA activity at high movement velocities and is mediated by length-velocity related sensory feedback and (2) SO activity would be low compared to GA activity for tasks requiring an ankle extension–knee flexion joint moment combination and does not require high movement velocities or length-velocity related sensory feedback. The hypotheses were tested by comparing the SO EMG / MG EMG ratio during fast and slow motor behaviors – cat paw shake responses vs. back, straight leg load lifting in humans, which had the same ankle extension–knee flexion moment combination (de Looze et al., 1993, Prilutsky et al., 1998b, Prilutsky et al., 2004, Klishko et al., 2011); and during fast and slow behaviors with the ankle extension–knee extension moment combination – human vertical jumping (Bobbert and van Ingen Schenau, 1988) and stance phase of walking in cats (Gregor et al., 2006) and leg load lifting in humans (de Looze et al., 1993).

If the ratio SO EMG / GA EMG was found to be lower in fast tasks (paw shaking and jumping) than in slow tasks (load lifting and walking) irrespective of joint moment combinations, hypothesis 1 would be supported and hypothesis 2 rejected. To test if low SO activity is mediated by length-velocity dependent sensory feedback from SO and GA, EMG activities of SO and MG were recorded during cat paw shake responses and level walking in the cat before and after length-velocity dependent sensory feedback from SO and lateral gastrocnemius (LG) or MG and LG was removed by self-reinnervation of

these muscles (Cope and Clark, 1993, Cope et al., 1994). After self-reinnervation of ankle extensors (transecting and repairing the nerves innervating the muscles), locomotor muscle activity recovers in several months (O'Donovan et al., 1985, Gregor et al., 2003), however self-reinnervated muscles permanently lose stretch reflex (Cope and Clark, 1993, Cope et al., 1994) due to retraction of excitatory synapses with motoneurons by primary spindle afferents (Alvarez et al., 2011, Bullinger et al., 2011). If relatively low SO activity, judged by the ratio SO EMG / GA EMG, during paw shake responses was reduced (the ratio increased) after SO and/or GA self-reinnervation, then hypothesis 1 would be rejected and hypothesis 2 would be supported.

Preliminary results have been published in abstract form (Prilutsky et al., 2004, Klishko et al., 2011, Mehta and Prilutsky, 2012).

3.2 Methods

3.2.1 Cat ethical approval, surgical procedures and experiments

The surgical and experimental procedures employed in this study corresponded to the "Principles of Laboratory Animal Care" (NIH Publication No. 86-23, Revised 1985) and were approved by the Institutional Animal Care and Use Committee of the Georgia Institute of Technology. Six female, adult cats (*felis domesticus*, mass = 2.5±0.8 kg) were used in this study. Animal training and surgical procedures utilized were the same as in Chapter 2.

3.2.1.1 Data collection

Animal kinematics and electromyographic (EMG) activity were recorded during upslope (27^{o}) and level walking and paw shake responses before and at least 12 weeks

after nerve transection and repair. The period of 12 weeks was sufficient for the injured muscles to be reinnervated and regain the pre-nerve transection EMG activity level (O'Donovan et al., 1985, Gregor et al., 2003, Pantall et al., 2016).

To record kinematics of walking and paw shake responses, light reflective markers were attached by double-sided adhesive tape to shaved skin, as described in Chapter 2. Marker displacements were recorded using a 3D, 6-camera motion capture system (Vicon Motion Systems Ltd, Oxford, UK) at a sampling rate of 120 Hz. Ground reaction forces were collected during walking using embedded force plates (Bertec Corporation, Columbus, OH, USA) at 360 Hz. A 16-conductor, shielded flexible cable was connected to the Amphenol connector on the cat's head to record EMG activity. EMG and mechanics data collection was synchronized by an electronic trigger pulse from the Vicon system. EMG signals were recorded at 3000 Hz, band-pass filtered (30-1000 Hz, 3 dB), amplified (1000x), and saved on a computer for further analysis.

Two motor behaviors were studied – level walking, a slow task, in which ankle extension and knee extension moments are developed during the stance phase (Gregor et al., 2006, Prilutsky et al., 2011); and paw shake responses, a fast task, in which ankle extension and knee flexion moments are produced simultaneously during one half of the paw shake cycle (Hoy et al., 1985, Prilutsky et al., 2004). Paw shake responses (PSRs) were elicited by placement of a small piece of adhesive tape on paw pad of the right hindlimb. The animal was then placed in the recording area and was free to walk along a Plexiglas enclosed walkway. This allowed for the collection of several unconstrained PSRs which occur during swing phases of walking while the cat stopped and shook the hindlimb before continuing walking. In some cases, PSRs occurred spontaneously during

recordings of level walking. PSR and locomotion experiments were performed both before and at least 12 weeks after LG-MG and SO-LG nerve transection and repair.

3.2.1.2 Cat data analysis and statistics

EMG activity and hindlimb mechanics during PSR episodes (Fig. 3.1) and walking cycles (Fig. 3.2) were analyzed using custom software (Prilutsky et al., 2005, Gregor et al., 2006). Walking and PSR cycles were identified using vertical ground reaction forces produced by the right hindlimb or recorded kinematics, respectively. Joint angles were calculated after filtering recorded marker coordinates using a fourth order, zero lag Butterworth filter (10 and 15 Hz cut-off frequencies for walking and paw shakes, respectively; and muscle-tendon unit (MTU) lengths of SO and MG were calculated using a scaled geometric model of the cat hindlimb assuming a straight muscle path between muscle origin and insertion (Goslow et al., 1973, Gregor et al., 2006)). Muscle velocity was calculated as the time-derivative of MTU length using the method of finite differences. The resultant muscle moments at the hindlimb joints in the sagittal plane were computed using a standard inverse dynamics analysis, described in detail previously (Prilutsky et al., 2005, Gregor et al., 2006, Prilutsky et al., 2011). Inertial properties of cat hindlimb segments necessary for calculations were obtained using the regression equations from Hoy and Zernicke (1985). The computed moments were normalized by cat mass.

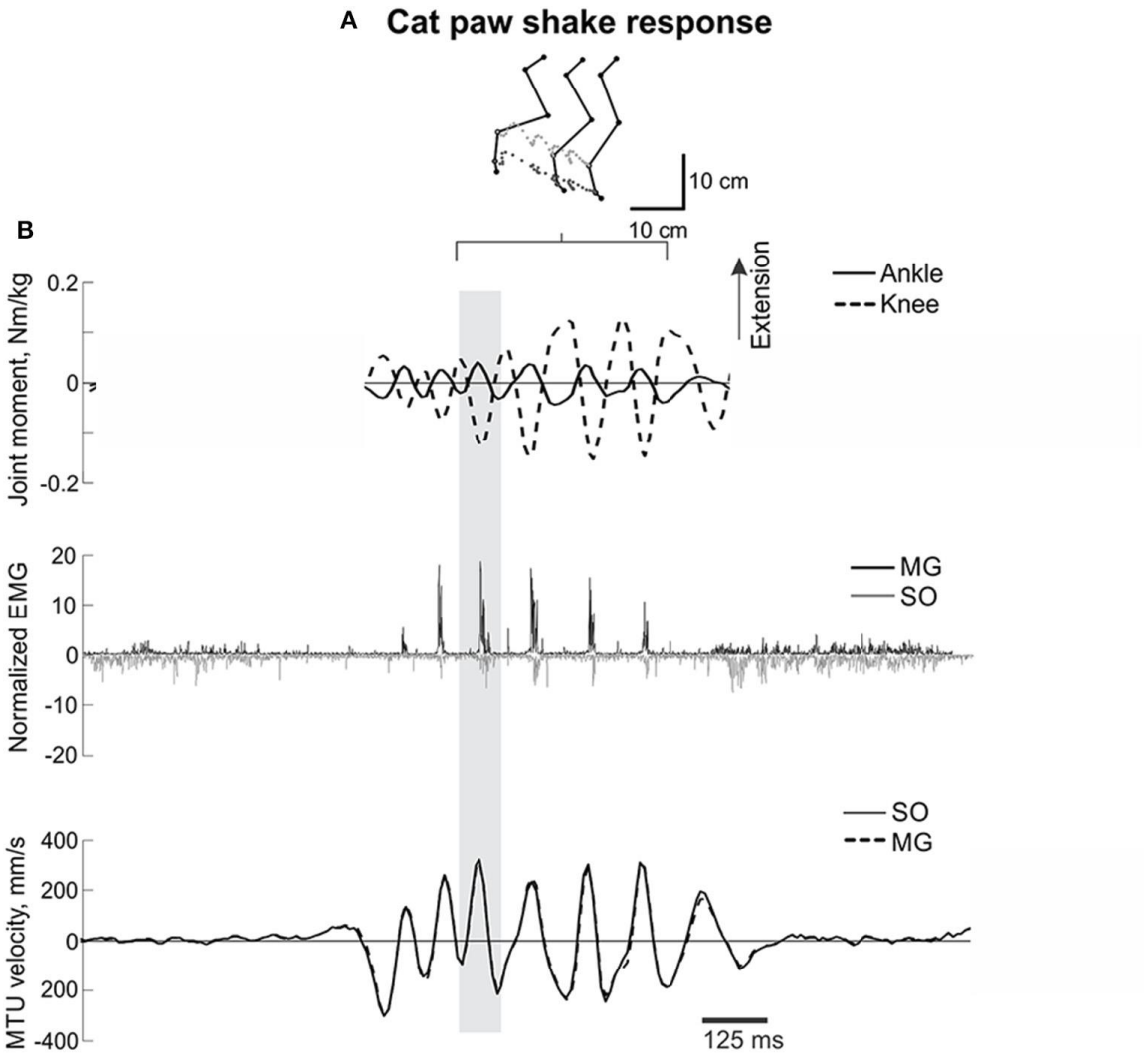

Figure 3.1. A representative episode of a cat paw shake response. (A) Stick figures and trajectories of the right metatarsophalangeal and ankle joints during several cycles of paw shake. (B) Normalized resultant muscle moments at the ankle and knee (top, positive values designate extension); normalized raw, full-wave rectified EMG activity (middle traces) of MG (positive values) and SO (negative values); and MTU velocity (bottom traces) of MG and SO, where positive MTU velocity corresponds to lengthening. The grey rectangle indicates a single paw shake cycle.

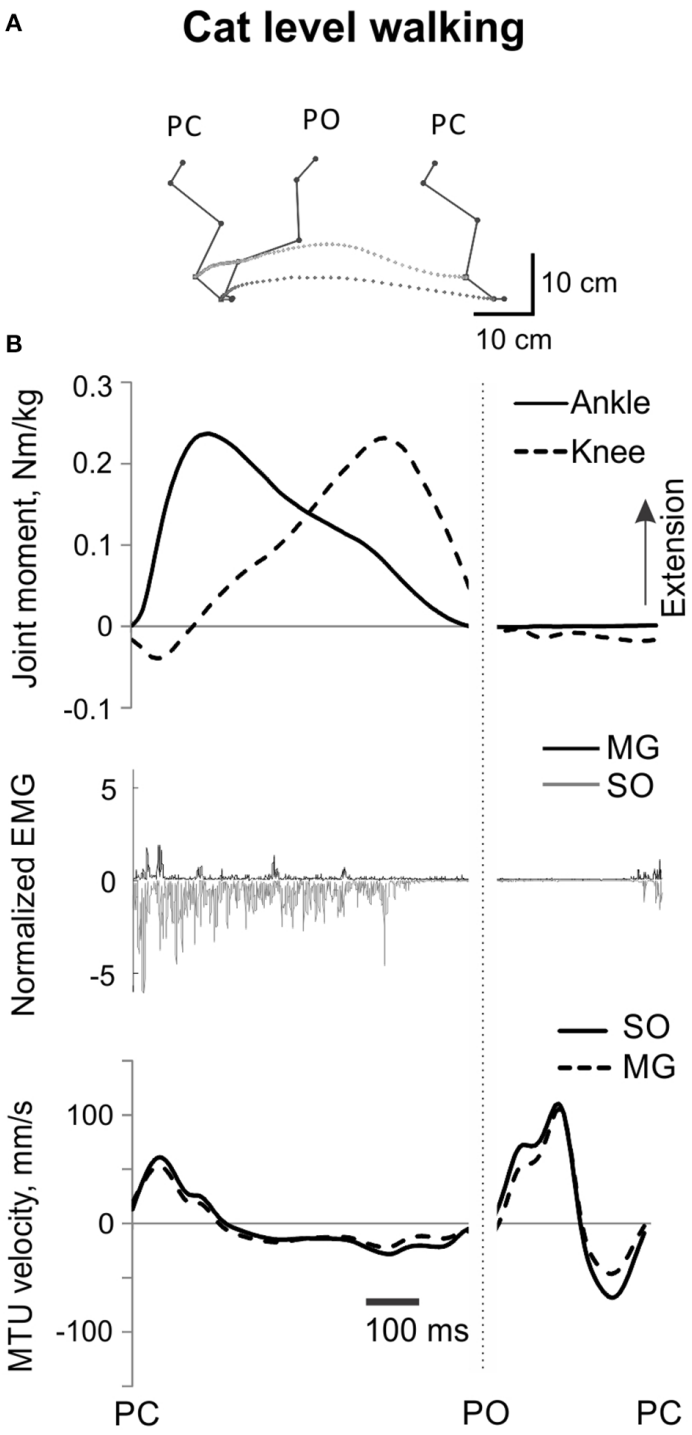

Figure 3.2. A representative cycle of cat level walking. (A) Stick figures and trajectories of the right metatarsophalangeal and ankle joints during a walking cycle. (B) Normalized resultant muscle moments at the ankle and knee (top, positive values designate extension); normalized raw, full-wave rectified EMG activity (middle traces) of MG (positive values) and SO (negative values); and MTU velocity (bottom traces) of MG and SO, positive MTU velocity corresponds to lengthening. Dotted vertical line separates stance and swing phase. PC, paw contact; PO, paw off

Recorded and band-passed EMG signals (see above) were full-wave rectified and the EMG burst onset and offset times were determined either by observing the signal on the computer screen or by a computer program using a 2-SD threshold above the EMG baseline, observed during the swing phase of walking (Gregor et al., 2006). The mean burst EMG activity was computed for each cycle of level walking or paw shake response. Full-wave rectified signals were also low-pass filtered (fourth order, zero lag Butterworth filter, cut-off frequency of 30 and 75 Hz for walking and paw shake, respectively) to obtain EMG linear envelopes. The mean EMG burst and linear EMG envelope values were normalized to the maximum mean burst EMG magnitude found across all walking conditions (level and upslope) before nerve cut and repair for each cat and muscle.

For further PSR analysis, individual steady-state cycles in the middle of paw shake episodes were visually identified using consecutive peaks of the ankle flexion moment considered as the start and end of the paw shake cycle (grey rectangle in Fig. 3.1). In total, 124 individual PSR cycles were identified across all cats and PSR episodes. For each PSR cycle, the mean ankle extension and knee extension moments were calculated during the phase of the cycle in which this combination of joint moments and EMG bursts of SO and MG occurred (Fig. 3.1). The SO and MG EMG bursts identified, as described above, were also averaged using the full-wave rectified signals and then normalized by the corresponding maximum mean EMG values for SO and MG muscles found across all recorded walking cycles for a given cat.

All analyzed mechanical and EMG variables obtained for 45 cycles of level walking across all cats before and after self-reinnervation were time-normalized to the duration of the stance and swing phase separately. The mean ankle and knee joint

moments and mean SO and MG EMG activity were calculated for the stance phase of walking (from paw contact, PC to paw off, PO), during which the ankle and knee joint moments were mostly extension and most of SO and MG EMG bursts occurred (Fig. 3.2). The mean SO and MG EMG values were normalized to the maximum mean EMG burst of each muscle, as described above. For each stance phase of level walking and each PSR cycle, the ratio (normalized mean SO EMG / normalized mean MG EMG) was calculated.

All statistical tests were performed using IBM SPSS Statistics v20 software (IBM SPSS, Chicago, IL, USA). A linear mixed model analysis was used to test several hypotheses: (1) the ratio SO EMG / MG EMG would be smaller (or SO inhibition would be greater) at ankle extension–knee flexion combinations of joint moments (during fast PSRs) than at ankle extension–knee extension combinations of joint moments (during a slow task of walking, Table 3.1); and (2) removal of length-velocity dependent feedback from SO and/or GA muscles (by self-reinnervation) would increase the ratio SO EMG / MG EMG during PSRs (would reduce SO inhibition with respect to GA).

Table 3.1. Subjects and experimental tasks with different velocity requirements and combinations of ankle and knee joint moments.

Movement speed / Joint moment combination	Slow	Fast
Ankle extension–knee extension	Stance of walking (pre/post-reinnervation: 5/4 cats, 20/25 cycles, $V_{MG} = 0.115 \pm 0.039$, $V_{SO} = 0.203 \pm 0.067$) Leg load lifting (5% BW) (5 humans, 29 trials, $V_{MG} = 0.020 \pm 0.003$, $V_{SO} = 0.081 \pm 0.031$)	Vertical jump (5 humans, 40 trials, $V_{MG} = 0.241 \pm 0.034$, $V_{SO} = 1.559 \pm 0.136$)
Ankle extension–knee flexion	Back load lifting (5/15% BW: 5/5 humans, 25/28 trials, $V_{MG} = 0.020 \pm 0.009$, $V_{SO} = 0.063 \pm 0.021$)	Paw shake response (pre/post-reinnervation: 5/4 cats, 62/62 cycles, $V_{MG} = 0.473 \pm 0.353$, $V_{SO} = 0.814 \pm 0.482$)

BW is body weight, V_{MG} and V_{SO} are the peaks of MTU shortening velocities of MG and SO, respectively, normalized to the maximum shortening velocity of the corresponding muscle. Maximum shortening velocities of cat SO = 176 mm/s and MG = 259 mm/s were taken from measurements of Spector et al. (1980); maximum shortening velocities of human SO = 172 mm/s and MG = 683 mm/s were taken from estimates of Prilutsky (2000b). Although the peak of human SO MTU shortening velocity during jumping exceeds its SO maximum velocity, SO fascicles shorten at a much lower velocity during jumping (Kurokawa et al., 2001).

In the linear mixed model analysis, the dependent variables were the SO EMG / MG EMG ratio and the mean normalized SO and MG EMG burst magnitude. The fixed factors were the joint moment combination (ankle extension–knee flexion, in PSR, and ankle extension–knee extension, in stance of walking) and muscle proprioception status (pre and post self-reinnervation). Individual cats and PSR or walking cycles were considered random factors. The Bonferroni post-hoc test was used for pairwise comparisons. One-sample t-tests were also performed to determine whether the SO EMG / MG EMG ratio for each task was significantly different from a test value of 1; the latter value indicates an equal normalized activity of SO and MG. Descriptive statistics values are reported as mean±SD. Significance level for all tests was set at an alpha level of 0.05.

3.2.2 Human experiments

3.2.2.1 Participants and preparation

Five healthy adults (4 males, 1 female; age = 31±12 years, mass = 78±9.0 kg, height = 1.7±0.1 m) participated in this study. All participants reviewed and signed an informed consent form approved by the Institutional Review Board of the Georgia Institute of Technology prior to the study. Participants were recruited if they were over the age of 18 and had no history of known musculoskeletal or neurological disorders.

Participants were first prepared for placing EMG surface electrodes (Noraxon Inc., Scottsdale, AZ, USA; 1 cm diameter, 2 cm inter-electrode distance), which included shaving and lightly rubbing the skin with an alcohol pad. Locations of the muscles were found by palpation of the triceps surae while the participant was performing active contractions. After finding appropriate locations for electrode placement in the mid-belly of SO and MG muscles, the electrodes with the pre-amplifiers and cables were secured in

place with adhesive tape and elastic bandage to reduce motion artifacts. As was also the case in cats, only the MG muscle was tested since MG and LG have similar architecture and fiber type composition in humans (Johnson et al., 1973, Ward et al., 2009). The cables were connected to a belt-worn wireless transmitter. To record kinematics, light reflective markers were placed on anatomical landmarks (calcaneus, 2nd metatarsal head, lateral malleolus, lateral aspect of shank, lateral epicondyle, lateral aspect of thigh, greater trochanter, anterior/posterior superior iliac spine, acromion process, and head) of both lower limbs and upper body using double-sided adhesive tape.

3.2.2.2 Data collection

Marker positions were recorded using a 3D, 6-camera motion capture system (Vicon Motion Systems Ltd, Oxford, UK) at a sampling rate of 120 Hz. EMG signals from two of the three heads of triceps surae (MG and SO) were band-pass filtered (10-500 Hz) by the pre-amplifiers, transmitted by the belt worn transmitter to a wireless receiver (MyoSystem 1400A, Noraxon Inc., Scottsdale, AZ, USA), amplified by 500x, sampled at 1080 Hz and stored on a computer via Vicon data station for further analysis. The EMG recording system had a constant time delay of 100 ms. Ground reaction forces were collected from one force plate (Bertec Corporation, Columbus, OH, USA) via the Vicon data station at a sampling rate of 1080 Hz.

3.2.2.3 Maximal voluntary contraction

Participants first performed maximum voluntary contractions (MVC) by ankle extensors using an isokinetic dynamometer (Kin-Com, Isokinetic International, East Ridge, TN, USA) in order to determine the maximum EMG activity of MG and SO. Participants were seated in the Kin-Com chair and the ankle frontal joint axis was placed

in line with the dynamometer arm's axis of rotation. The participant's trunk, thigh, shank, and foot were secured using straps such that flexion angles at the ankle, knee and hip joints were 90^{o}, 0^{o}, and 90^{o}, respectively. The participant was instructed to exert maximum ankle plantar flexion against resistance provided by the dynamometer using only the foot in order to target MG and SO muscles. Only EMG activity was recorded during this task. The MVC task was performed under isometric conditions, in which leg joint angles remained unchanged. The subject performed 3 MVC tests with sufficient rest between each contraction. Participants also performed 5 maximum height, counter-movement vertical jumps while EMG activity of SO and MG was recorded; subjects were free to swing their arms.

3.2.2.4 Load lifting tasks

Participants completed two types of load lifting, slow tasks (Table 3.1) – back (straight leg) and leg load lifting – with two loads (5% and 15% of body weight). For the back lift conditions, participants were instructed to reach a plastic box (40 x 32 x 15 cm^3) filled with sand on the floor in front of the subject from an upright body position and lift the box by extending the back while minimally flexing/extending the knees (Fig. 3.3, stick figures). This task requires production of ankle extension and knee flexion joint moments known to cause high activity of GA (Prilutsky et al., 1998b); see also Fig. 3.3. For the leg lifting conditions, participants were instructed to reach the same load from an upright body position by flexing the ankle and knee joints, and then lift the load by extending the leg joints. In contrast to back lifting, this task requires extension joint moments at the ankle and knee (de Looze et al., 1993); see also Fig. 3.4.

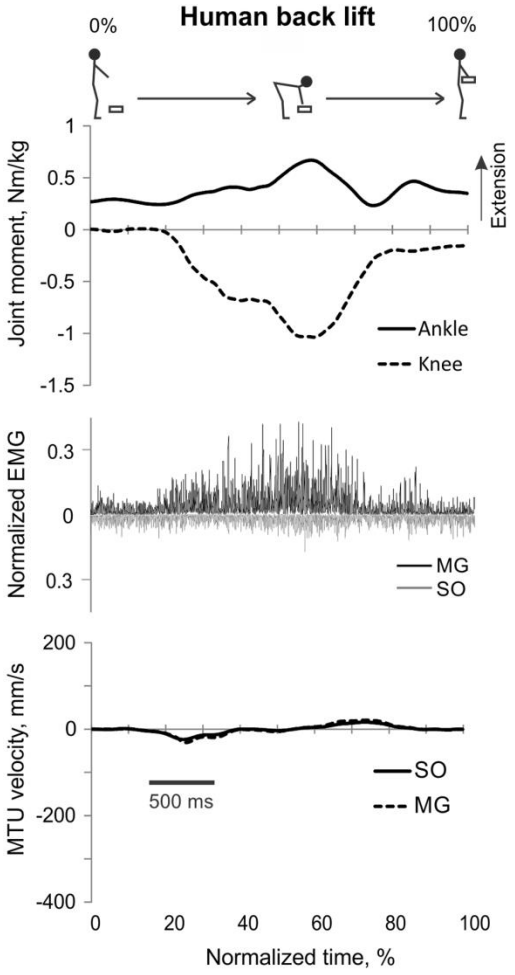

Figure 3.3. A representative trial of human back load lifting. From top to bottom: Stick figures illustrating the task; normalized resultant muscle moments at the ankle and knee joints (positive values correspond to extension); normalized raw, full-wave rectified EMG activity of MG (positive values) and SO (negative values); and MTU velocity of GA and SO (positive values correspond to lengthening).

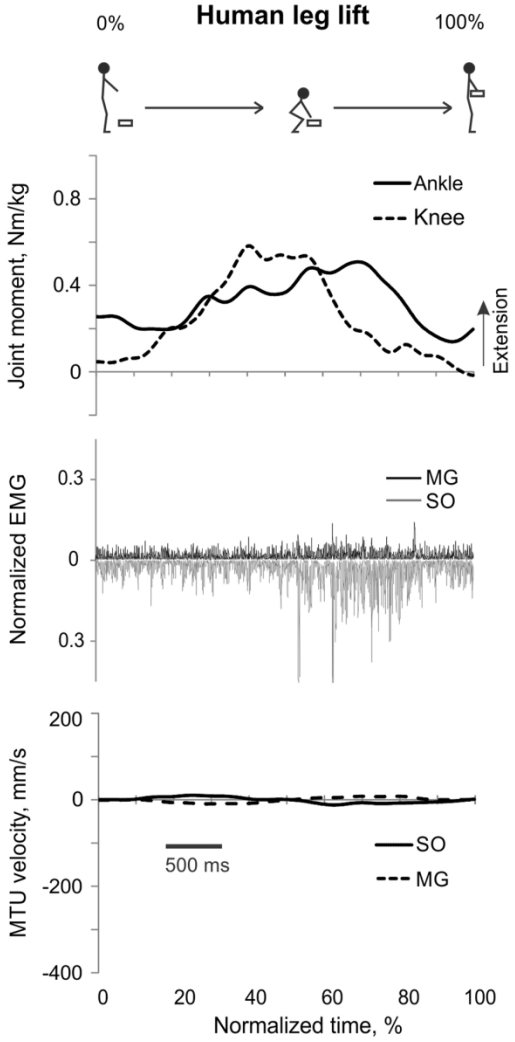

Figure 3.4. A representative trial of human leg load lifting. From top to bottom: Stick figures illustrating the task; normalized resultant muscle moments at the ankle and knee joints (positive values correspond to extension); normalized raw, full-wave rectified EMG activity of MG (positive values) and SO (negative values); and MTU velocity of MG and SO (positive values correspond to lengthening).

In both tasks the load was placed directly in front of the participant at a distance 20% of body height away from the toes and 10% of body height above the ground. One trial consisted of reaching the load on the floor and lifting it up until reaching an upright standing position. Participants performed at least 5 trials for each condition. Before any data were collected, participants were instructed to lift the load at a comfortable, self-selected speed and asked to practice the task for about one minute before each condition.

Participants rested between conditions to minimize fatigue. The order of lifting conditions was randomized.

3.2.2.5 Counter-movement vertical jumping

Participants performed at least 5 trials of a fast task (Table 3.1), i.e. a maximum-height counter-movement vertical jump with swinging the arms (Fig. 3.5, stick figures). Participants were instructed to jump as high as they could while starting and landing with only their right foot on the force plate. They were given as much rest as needed between jumps.

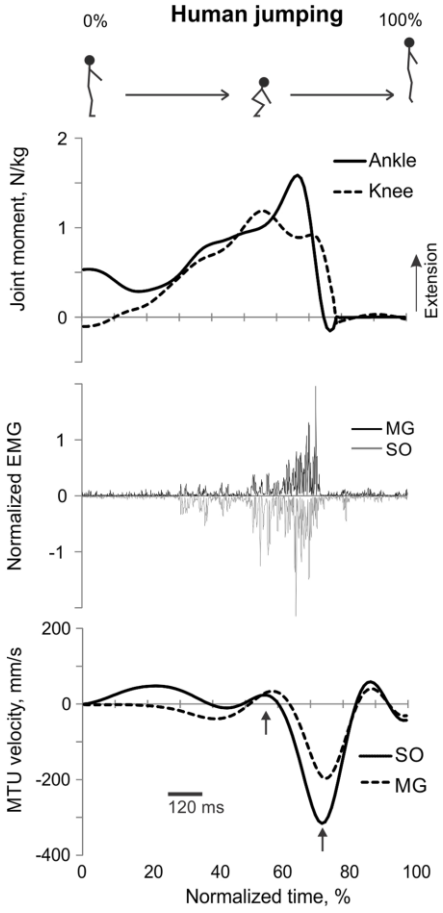

Figure 3.5. A representative trial of human jumping. From top to bottom: Stick figures illustrating the task; normalized resultant muscle moments at the ankle and knee joints (positive values correspond to extension); normalized raw, full-wave rectified EMG activity of MG (positive values) and SO (negative values); and MTU velocity of MG and SO (positive values correspond to lengthening). Arrows in the bottom panel indicate the time period, for which the mean ankle and knee moments and SO and MG EMG activity were computed.

3.2.2.6 Data analysis and statistics

Recorded leg kinematics and ground reaction forces were used to compute the resultant muscle moments at the right ankle and knee joints using a standard inverse dynamics analysis (Prilutsky et al., 1998b) and a custom computer program written in Matlab (MathWorks, Natick, MA, USA). The kinematic and force data were low-pass filtered at 10 Hz (fourth order, zero-lag Butterworth filter). Body segment inertia parameters were computed for each subject using the regression equations and subject's height and mass (Zatsiorsky, 2002). Smoothed marker coordinates were used to compute joint angles, from which MTU length changes of SO and MG muscles were calculated using the regression equations (Prilutsky and Gregor, 1997). MTU muscle velocities were computed using the method of finite differences.

The load lifting trial time was identified based on the vertical velocity of the head marker. The start of the trial was defined as 0.5 s before reaching the peak of head marker downward vertical velocity; the end of the trial was defined as 0.5 s after reaching the peak of head marker upward vertical velocity. All time-dependent mechanical and EMG variables were time-normalized to the duration of each lifting trial. The jumping trial onset was defined as 0.25 s before initiation of a downward movement of the shoulder marker; the jumping offset corresponded to 0.25 s after the shoulder marker reached its vertical position at jump onset.

Band-pass filtered EMG signals were full-wave rectified and low-pass filtered (cut-off frequency 10 Hz) to obtain a linear EMG envelope, which was used to compute the mean EMG burst activity of SO and MG during each load lifting and jumping trial, as described above (see also Figs. 3.3-3.5). Inspection of the low-pass EMG signals

recorded during MVC contractions and vertical jumping revealed that EMG activity for ankle extensor muscles was always greater during jumping than during the MVC task. Therefore, the mean of EMG linear envelope peaks across 5 maximum jumps was used to normalize the EMG activity magnitude of each muscle during all human motor tasks. The ratio (mean SO EMG / mean GA EMG) was computed using normalized EMG values of each load lifting and jumping trial.

EMG low-pass filtered activity, joint moments and MTU velocities were averaged for each percent of the load lifting and jumping time across 5 trials of each condition and participant and then across participants since all subjects showed similar trends. In addition, the mean ankle and knee joint moments, mean SO and MG EMG and the SO EMG / MG EMG ratio were computed for the time periods of each load lifting corresponding to the ankle extension–knee flexion joint moment combination (during back lifting, Fig. 3.3, Table 3.1) and to the ankle extension–knee extension joint moment combination (during leg lifting, Fig. 3.4, Table 3.1). The same analysis was performed for jumping, however the period for determining the mean moments and EMG corresponded to the time between the two peaks of SO MTU velocity corresponding approximately to 55% and 75% of the jump trial (Fig. 3.5, arrows).

A linear mixed model analysis (IBM SPSS Statistics v20 software, Chicago, IL, USA) was used to test the hypothesis that the SO EMG / MG EMG ratio would be lower during a slow task of back load lifting (at the ankle extension–knee flexion joint moment combination) than during a slow task of leg load lifting or a fast task of vertical jumping (at the ankle extension–knee extension joint moment combination). One-sample t-tests were performed to determine whether the SO EMG / MG EMG ratio for each task was

significantly different from 1. The linear mixed model analysis was also used to examine effects of joint moment combination in all studied tasks on the mean SO and MG EMG. Significance for all tests was set at an alpha level of 0.05.

3.3 Results

3.3.1 Cat experiments

3.3.1.1 Paw shake response

Typical paw shake episodes in intact cats consisted of 4-7 cycles of fast hindlimb oscillations with frequencies between 8 and 12 Hz (Fig. 3.1). During steady-state paw oscillations, which occurred typically in the middle of paw shake episodes, the ankle extension and knee flexion joint moments, MG and SO EMG bursts and MTU positive velocity (lengthening) occurred at approximately the same time period in the cycle (Figs. 3.1 and 3.6). In the other half of the paw shake cycle, the ankle flexion and knee extension moments were produced simultaneously; during this period SO and MG muscles had no or low activity and were mostly shortening (Figs. 3.1 and 3.6). MTU lengthening and shortening velocity peaks were reaching values of about ±300 mm/s, which exceeded peak lengthening and shortening MTU velocities during cat level walking by approximately 2 and 6 times, respectively (Figs. 3.1, 3.2; Table 3.1 (Cronin et al., 2013)). Before reinnervation, SO EMG bursts were very short and their mean magnitude was higher than that during level walking ($F_{1,77}$ = 14.08, P<0.001; Figs. 3.1, 3.2 and 3.12B); the mean MG EMG was over 10 times higher during paw shake than during level walking ($F_{1,77}$ = 135.38, P<0.001; Fig. 3.1, 3.2 and 3.12A). As a result, the SO EMG / MG EMG ratio was much smaller during paw shake response (0.26±0.18), at

the ankle extension–knee flexion moment combination, than during stance of level walking, at the ankle extension–knee extension moment combination (3.23±1.34, $F_{1,79}$ = 334.75, P<0.001; Fig. 3.7A and 3.11 A,B). The ratio was also statistically smaller than 1 (one-sample t-test; n = 62, P<0.001).

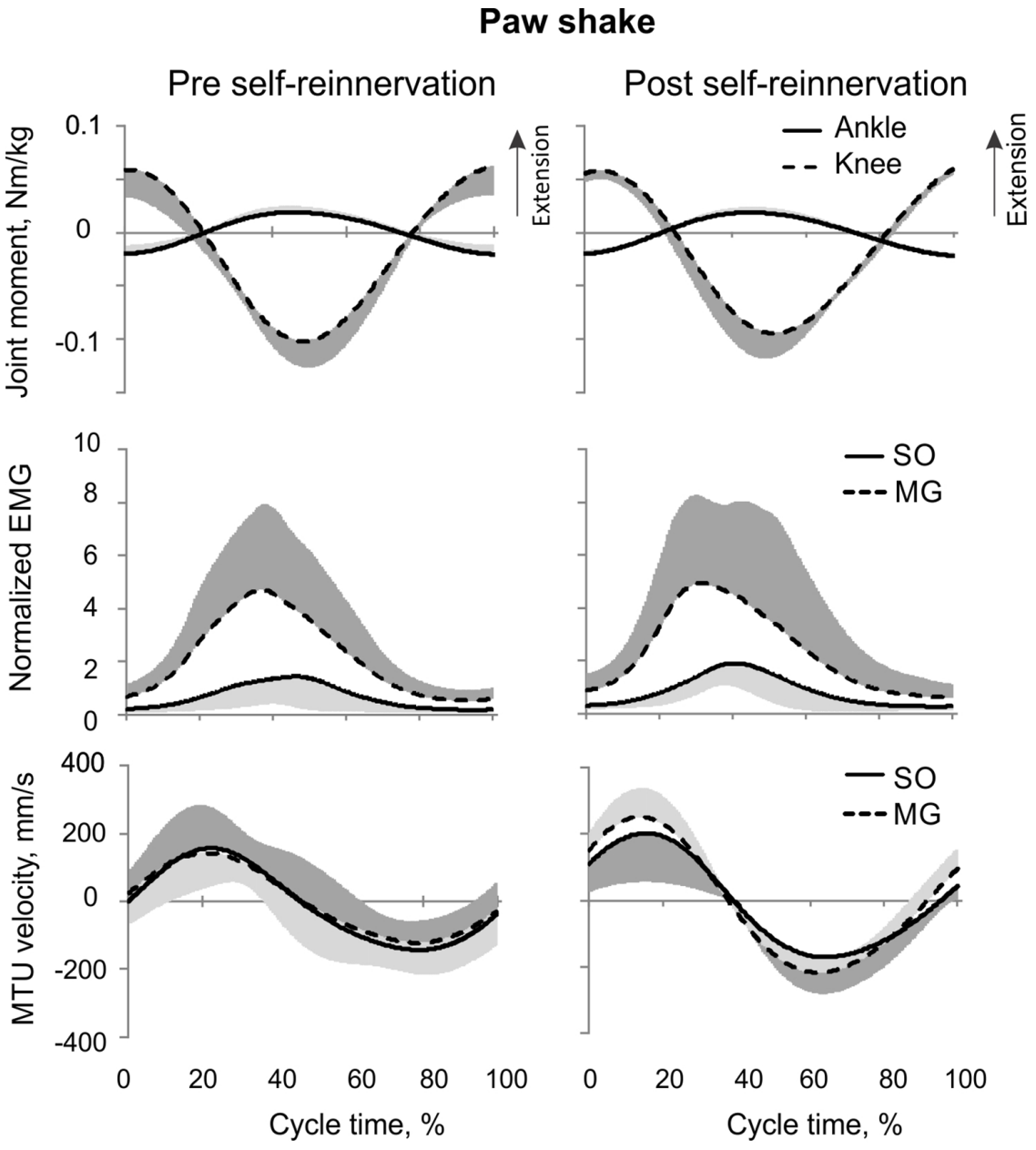

Figure 3.6. Mean (+/- SD) of normalized muscle moments at the ankle and knee joints (top), low-pass filtered normalized EMG of MG and SO (middle), and MTU velocity of MG and SO (bottom) during the paw shake cycle. The mean and SD values for pre- and post-reinnervation conditions (left and right panels, respectively) were computed across all studied paw shake cycles (at least 5 per cat) and cats.

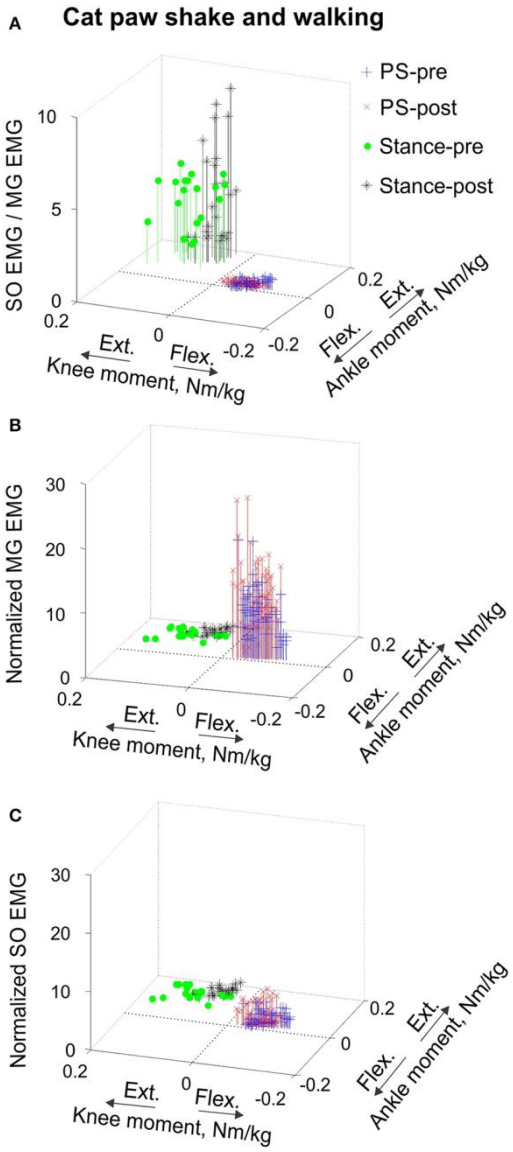

Figure 3.7. Mean SO EMG / MG EMG ratio (A), mean normalized MG EMG activity (B) and mean normalized SO EMG activity (C) as functions of the mean normalized ankle and knee resultant muscle moments during paw shake responses and stance of walking in the cat. Each symbol corresponds to the mean normalized EMG activity plotted versus the respective mean normalized ankle and knee moment in a given movement cycle. During paw shake responses, SO and MG EMG activity bursts occurred at the ankle extension–knee flexion joint moment combination (purple and red crosses designate paw shake cycles recorded pre- and post- SO-GA self-reinnervation; n = 62 and n = 62, respectively). During the stance phase of walking, SO and MG EMG bursts occurred at the ankle extension–knee extension joint moment combination (green circles and black stars correspond to stance phases recorded pre- and post- SO-GA self-reinnervation; n = 20 and n = 25, respectively).

Reinnervation of SO-LG or MG-LG muscle combinations did not cause apparent changes in patterns of joint moments, EMG activity or MTU velocities. Peak EMG bursts of SO and MG after self-reinnervation also occurred in the vicinity of the ankle extension and knee flexion moment peaks, which approximately coincided with muscle lengthening (Fig. 3.6). As in intact cats, the mean SO EMG burst magnitude was low in comparison with the mean MG EMG magnitude. The mean magnitude of MG EMG burst increased after self-reinnervation ($F_{1,119}$ = 6.75, P=0.011; Fig. 3.12A), although the SO EMG / MG EMG ratio did not change significantly ($F_{1,122}$ = 0.51, P=0.476, Figs. 3.7A, 3.11 A,B).

3.3.1.2 Level walking

EMG activity bursts of SO and MG muscles in intact cats occurred mostly during the stance phase, when the moments at the ankle and knee joints were extension, and peaks of MTU lengthening and shortening velocities of SO and MG were much lower than during the swing phase (Fig. 3.2B) or paw shake responses (Figs. 3.1 and 3.6, Table 3.1). The mean normalized EMG magnitude of SO was 0.77±0.12 and that of MG was 0.30±0.17 during the stance phase of walking (Figs. 3.7 B,C and 3.12 A,B). The SO EMG / MG EMG ratio (3.23±1.34) was several times higher during stance phase of walking than during paw shake response ($F_{1,79}$ = 334.75, P<0.001) and exceeded 1 (one-sample t-test; n = 20, P<0.001; Figs. 3.7A and 3.11 A,B).

Self-reinnervation of SO and GA muscles did not cause changes in the normalized mean activity of SO and MG during stance of walking ($F_{1,40}$ = 2.57, P=0.117 and $F_{1,39}$ = 0.142, P=0.707, respectively; Fig. 3.12 A,B). The SO EMG / MG EMG ratio on average did not change either ($F_{1,39}$ = 1.64, P=0.208; Fig. 3.11B), although in two cats with MG-LG self-reinnervation the ratio significantly increased ($F_{1,28}$ = 192.44, P<0.001; Fig.

3.11A). Overall, self-reinnervation of SO and GA did not change the SO EMG / MG EMG ratio, which was still several times greater during stance of walking than paw shake response (Figs. 3.7A and 3.11B).

3.3.2 Human experiments

3.3.2.1 Back load lifting

During back load lifting, ankle extension and knee flexion moments were produced simultaneously, MG EMG activity was sharply modulated in parallel with the magnitudes of ankle and knee moments while the SO EMG magnitude increased initially and then decreased earlier than MG EMG (Fig. 3.8). Peaks of MTU lengthening and shortening velocities of SO (11.3±2.7 mm/s and -12.9±4.4 mm/s, respectively) and MG (13.2±3.9 mm/s and -15.3±6.6 mm/s, respectively) were very low compared to the corresponding MTU velocity peaks during human walking (300 mm/s and 350 mm/s, respectively (Cronin et al., 2013); Figs. 3.3 and 3.8). Patterns of ankle and knee joint moments, SO and MG EMG activity and MTU velocities were generally similar between 5%- and 15%-loads (Fig. 3.8) with slightly greater magnitudes of joint moments and EMG activity reaching statistically significant differences only for the mean MG EMG ($F_{1,47}$ = 47.10, P=0.015; Fig. 3.12C). The SO EMG / MG EMG ratios during back load lifting were 0.85±0.40 and 0.92±0.31 for 5% and 15%, respectively, and they were not statistically different ($F_{1,47}$ = 0.002, P=0.966, Fig. 3.11C). The SO EMG / MG EMG ratios combined together from the two tasks were statistically less than 1 (one-sample t-test; n = 52, P=0.021; Fig. 3.11C).

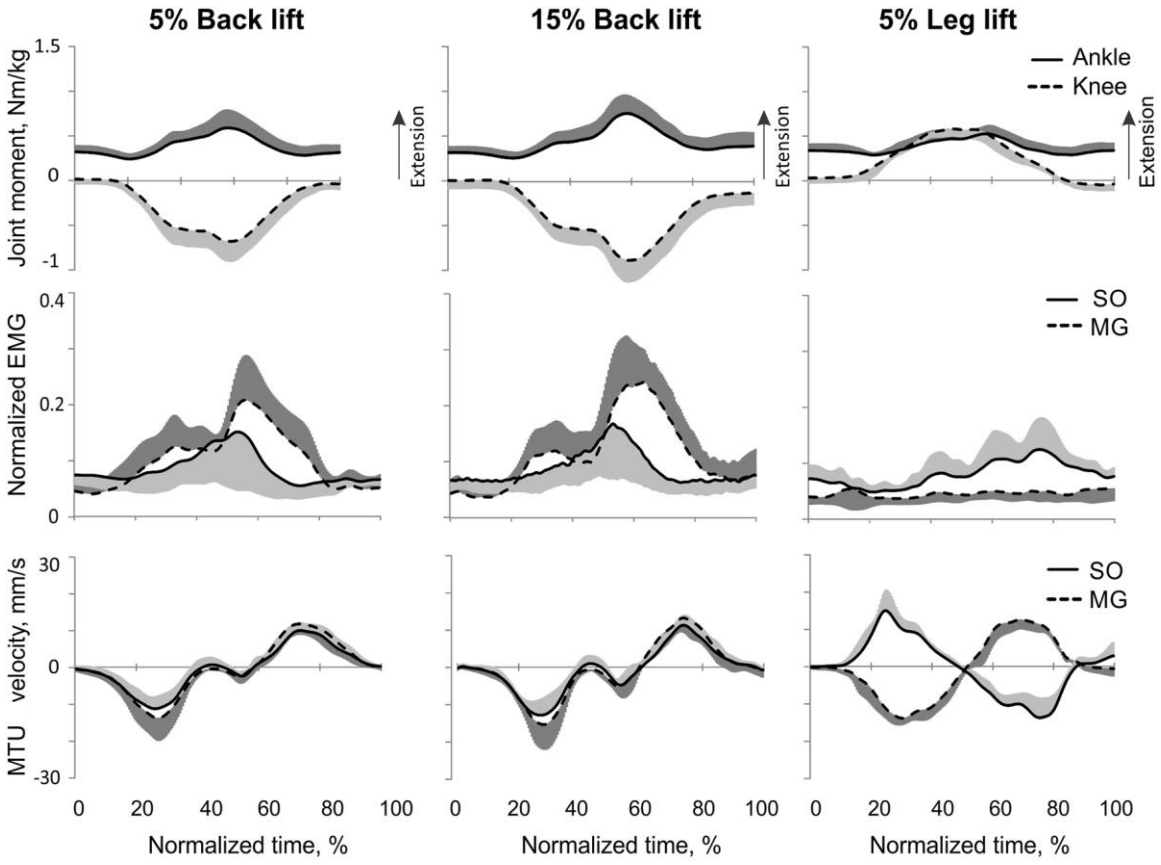

Figure 3.8. Mean (+/– SD) normalized ankle and knee joint moments (top traces), low-pass SO and MG EMG activity (middle traces), and MTU SO and MG velocity (bottom traces) during human back load lifting (left column, load 5% body weight; middle column, load 15% of body weight) and leg load lifting (load 5% body weight). Positive moments and MTU velocity designate joint moment extension and MTU lengthening, respectively.

3.3.2.2 Leg load lifting

During leg load lifting, with the extension muscle moments at the ankle and knee, SO EMG was modulated roughly in parallel with ankle extension moment while MG EMG was relatively constant and low (Figs. 3.4 and 3.8). MTU velocity changes of SO and MG during leg load lifting were opposite; SO MTU was lengthening during the first half of the movement (squatting) and then shortening during load lifting in the next half (extending legs), whereas MG MTU was shortening first (due to much larger knee flexion than ankle flexion) and then lengthening (Figs. 3.4 and 3.8). The mean

normalized EMG activity of SO (0.080±0.017) and MG (0.047±0.014) was lower ($F_{1,48}$ = 9.60, P=0.003 and $F_{1,48}$ = 258.23, P<0.001, respectively) compared to the back lift values for the 5% load (Fig. 3.12 C,D). The SO EMG / MG EMG ratio (1.88±0.64) was almost 2 times higher during leg lift than back lift ($F_{1,48}$ = 163.41, P<0.001, Fig. 3.11C) and was significantly greater than 1 (one-sample t-test, n = 29, P<0.001).

3.3.2.3 Counter-movement vertical jumping

The resultant joint moments at the ankle and knee were both extension during the counter-movement phase (from ~0% to 60% of the jump period) and push-off phase (from ~60% to 80%) of jumping until the lift-off at ~80% of the jump period (Figs. 3.5 and 3.9). During the counter-movement phase, SO MTU velocity was positive, indicating muscle lengthening, while MG MTU was shortening with a low negative velocity due to a greater flexion at the knee than at the ankle. Both muscles showed high peaks of shortening velocities during the push-off phase with a lower velocity peak in MG (Fig. 3.9, Table 3.1) due to opposite MTU length changes caused by ankle and knee extensions. EMG activity of SO and MG started to rise in the middle of the counter-movement and reached very high values in both muscles during the push-off phase (Figs. 3.5 and 3.9). The normalized mean EMG activity of SO (0.482±0.100) and MG (0.412±0.079) during the push-off phase was significantly greater than during the three load lifting tasks ($F_{3,121}$ = 298.2, P<0.001 and $F_{3,121}$ = 290.7, P<0.001, respectively; Figs. 3.10 B,C and 3.12 C,D). The SO EMG / MG EMG ratio during jumping (1.18±0.17) was significantly greater than for the 5% and 15% back load lifting tasks ($F_{3,121}$ = 39.5; P=0.008 and P=0.044, respectively). In contrast, the ratio was significantly lower in jumping compared to leg load lifting ($F_{3,121}$ = 39.5, P<0.001; Figs. 3.10A and 3.11C). The

SO EMG / MG EMG ratio for jumping was significantly greater than 1 (one-sample t-test, n = 43, P<0.001).

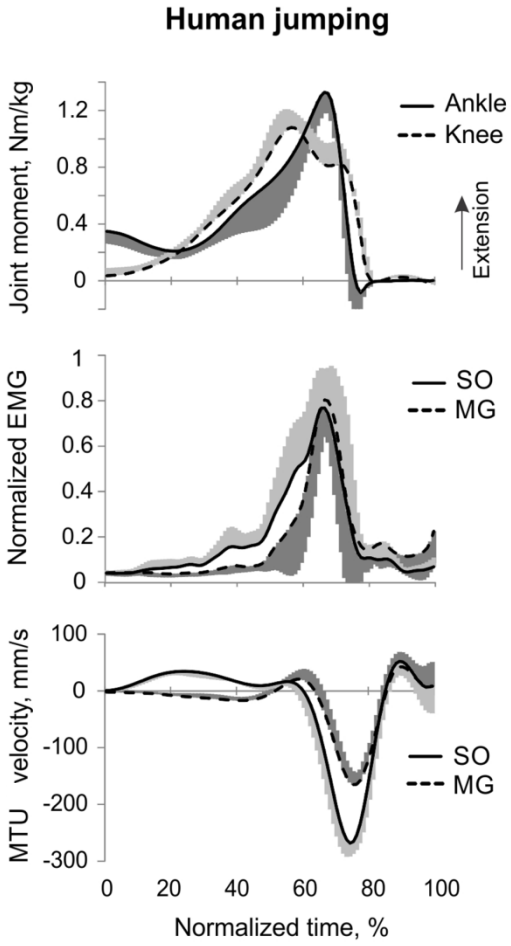

Figure 3.9. Mean (+/– SD) normalized ankle and knee joint moments (top traces), low-pass SO and MG EMG activity (middle traces), and MTU SO and MG velocity (bottom traces) during human jumping across all subjects (n = 5). Positive moments and MTU velocity designate joint moment extension and MTU lengthening, respectively.

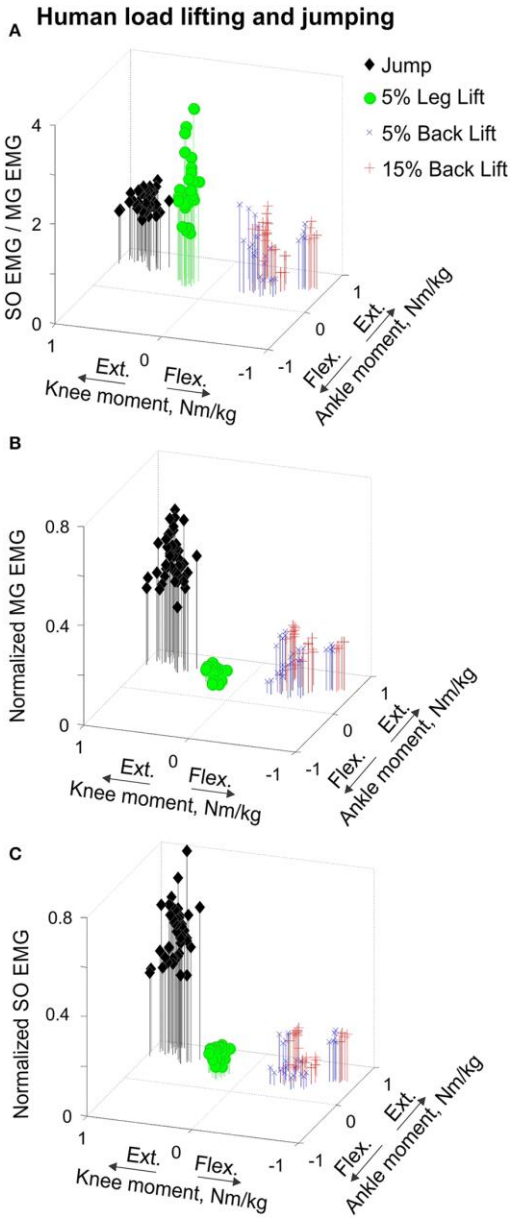

Figure 3.10. Mean SO EMG / MG EMG ratio (A), normalized mean MG EMG activity (B) and normalized mean SO EMG activity (C) as functions of the mean ankle and knee resultant muscle moments during human load lifting and jumping. Each symbol corresponds to the mean EMG activity plotted versus the respective mean ankle and knee moment obtained for a single load lifting or jumping trial. During back load lifting, SO and MG EMG activity occurred at the ankle extension–knee flexion joint moment combination (blue and red symbols designating lifting 5% and 15% body weight loads, n = 25 and n = 28, respectively). During leg load lifting and jumping, SO and MG EMG activity occurred at the ankle extension–knee extension joint moment combination (green circles, n = 29 and black diamonds, n = 40, respectively).

3.4 Discussion

3.4.1 Comparison with previous studies

Results obtained in this study on mechanics and muscle activity of paw shake responses and walking in intact cats, as well as load lifting and vertical jumping in humans, are in good agreement with the literature. Several reports described a relative inhibition of SO EMG or force with respect to MG EMG or force during paw shake responses (Smith et al., 1980, Abraham and Loeb, 1985, Smith et al., 1985, Fowler et al., 1988, Hodson-Tole et al., 2012). During steady-state paw shakes, triceps surae EMG activity occurred during MTU stretch, as in this study (Figs. 3.1 and 3.5), in phase with the extremely high activity of muscle length-velocity sensitive group Ia afferents (Prochazka et al., 1977, Prochazka et al., 1989). Although previous kinetic analysis of paw shake responses focused primarily on the interactive motion-dependent moments at the joints (Hoy et al., 1985, Hoy and Zernicke, 1986, Smith and Zernicke, 1987), selected illustrations of the resultant muscle moments at the ankle and knee in those studies did indicate the ankle extension–knee flexion muscle moment combination during one half of the paw shake cycle (see Fig. 7, muscle moments in Hoy and Zernicke (1986)).

SO and MG EMG activity, resultant muscle moments at the ankle and knee, and MTU length changes during cat level walking have been well documented in the literature (Goslow et al., 1973, Fowler et al., 1993, Gregor et al., 2006, Prilutsky et al., 2011) and are in good agreement with my results. Reinnervated ankle extensors in the cat have been reported to recover their EMG activity patterns and magnitude 12-13 weeks after nerve cut and surgical repair (O'Donovan et al., 1985, Gregor et al., 2003, Pantall et al., 2012), as also shown in this study (Figs. 3.6 and 3.12 A,B).

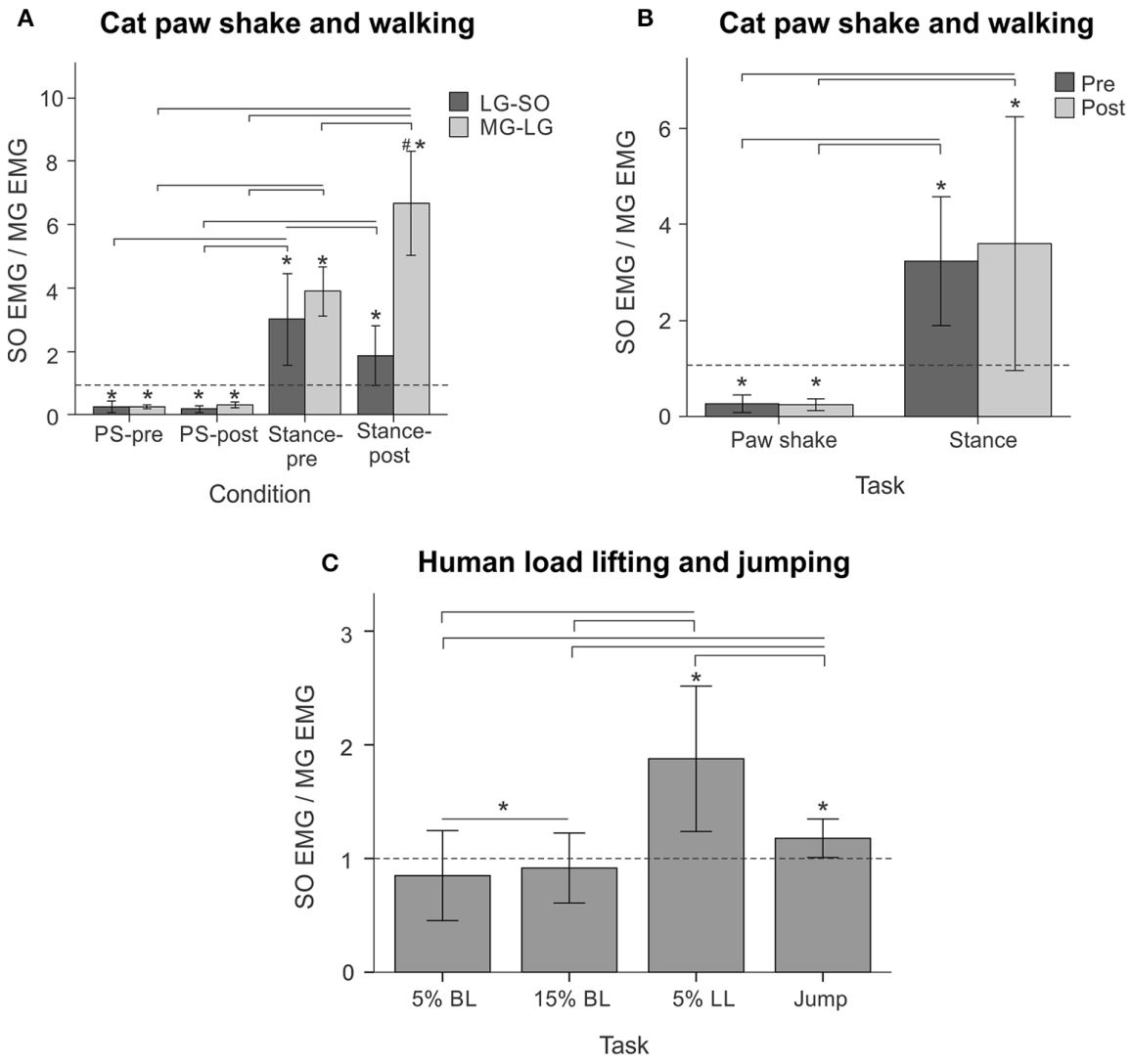

Figure 3.11. SO EMG / MG EMG ratio (mean±SD) during different motor behaviors performed by cats and humans. Horizontal dashed lines indicate the ratio value of 1. (A-B) SO EMG / MG EMG ratio during cat paw shake responses and stance of walking pre- and post- self-reinnervation of SO-LG (in 4 cats) and MG-LG (in 2 cats) muscles. Horizontal bars with brackets indicate statistical significance ($p<0.05$) between experimental conditions (motor tasks), symbol # indicates a significant difference between pre- and post- self-reinnervation, asterisks indicate statistically significant difference of the ratio from 1. (C) SO EMG / MG EMG ratio during human back load lifting (5% and 15% body weight), leg load lifting (5% body weight) and vertical jumping. Horizontal bars with brackets indicate statistical significance ($p<0.05$) between experimental conditions (motor tasks), asterisks indicate statistically significant difference of the ratio from 1.

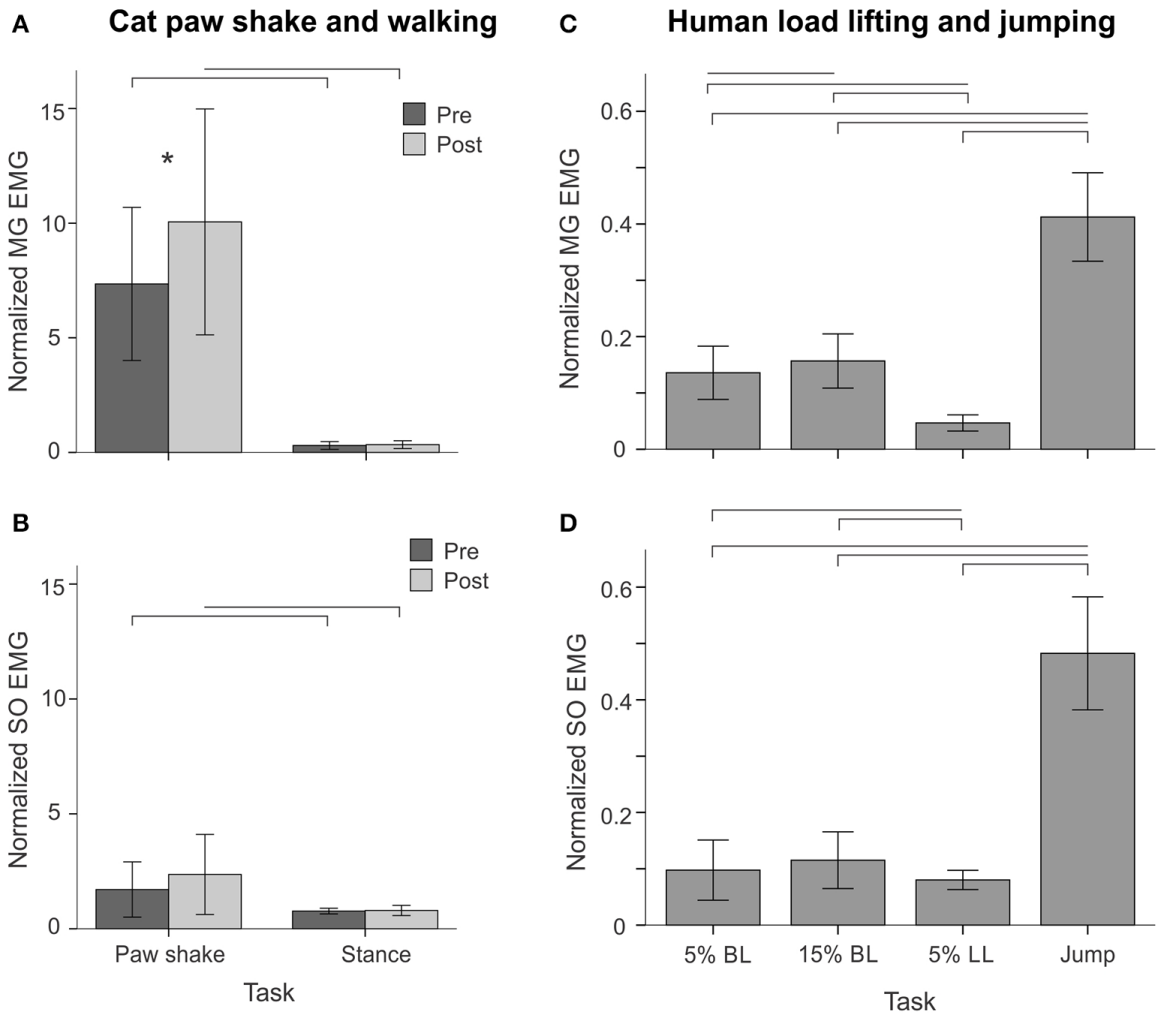

Figure 3.12. Normalized MG and SO EMG activity (mean±SD) during different motor behaviors performed by cats and humans. (A-B): MG and SO EMG during paw shake responses and stance of walking pre- and post- self-reinnervation of SO-LG muscles in 4 cats and MG-LG muscles in 2 cats. Horizontal bars show statistical significance ($p<0.05$) between experimental conditions (motor tasks), asterisk indicates a significant difference between pre- and post- self-reinnervation. (C-D): Normalized MG and SO EMG during human back load lifting (5% and 15% body weight), leg load lifting (5% body weight) and vertical jumping. Horizontal bars indicate statistically significant difference ($p<0.05$) between experimental conditions (motor tasks).

Patterns and peak values of the resultant muscle moments at the ankle and knee during back and leg load lifting and the corresponding MG EMG activity patterns obtained in this study (Figs. 3.3, 3.4 and 3.8) are in good agreement with other studies (de Looze et al., 1993, Prilutsky et al., 1998b). For example, the ankle extension–knee flexion and ankle extension–knee extension moment combinations occurred during back

and leg load lifting, respectively, with much reduced MG EMG during leg load lifting compared with back load lifting. No studies were found in which SO EMG was measured and compared with MG EMG during load lifting.

Ankle and knee resultant muscle moments, MTU velocities and EMG activity patterns of SO and MG obtained in this study for jumping (Figs. 3.5 and 3.9) are generally similar to those reported in other studies. For example, the ankle and knee moments are extension and reach their peak values during the push-off phase of jumping; the SO MTU peak shortening velocity is higher than that of MG MTU; and SO and MG are highly active during vertical jumping (Bobbert et al., 1986, Bobbert and van Ingen Schenau, 1988).

3.4.2 Study hypotheses

This study tested two major explanations for the relative low activity of the slow-twitch head of triceps surae SO with respect to a fast-twitch head, MG. The explanation that this low activity is related to high movement velocities and mediated by the stretch velocity-sensitive spindle Ia afferents was tested by comparing the SO EMG / MG EMG ratio between fast tasks of cat paw shaking and human vertical jumping and slow tasks of cat walking and human load lifting (Table 3.1). In addition, the SO EMG / MG EMG ratio was determined during paw shaking and stance of walking in intact cats and cats without stretch reflex in SO and GA removed by self-reinnervation of these muscles. The second explanation that the relative SO inhibition depends on the ankle-knee combination of joint moments and does not require high muscle velocities was tested by comparing the SO EMG / MG EMG ratio between tasks with the ankle extension–knee flexion combination of joint moments (fast cat paw shaking and slow human back load lifting)

and with the ankle extension–knee extension moment combination (fast human vertical jumping and slow human leg load lifting and cat walking, Table 3.1). Coordination between SO and MG was defined in this study by the SO EMG / MG EMG ratio and whether the ratio was less than or greater than 1.

The obtained results do not support the hypothesis that SO activity would be low compared to GA activity at high movement velocities and would be mediated by length-velocity related sensory feedback. Removal of length-velocity dependent feedback from SO-LG in 4 cats and MG-LG in 2 cats by their self-reinnervation (Cope and Clark, 1993, Cope et al., 1994, Alvarez et al., 2011, Bullinger et al., 2011) did not affect the SO EMG / MG EMG ratio (coordination) (Fig. 3.11B) in relation to the resultant muscle moment requirements at the ankle and knee (Fig. 3.6). Although intact synergists of self-reinnervated SO and MG, such as plantaris, can still supply SO and MG motoneurons with velocity dependent afferent input (Eccles et al., 1957b, Nichols, 1994), this input is expected to be dramatically diminished by self-reinnervation of SO and GA. In addition, the relatively low SO activity (the SO EMG / MG EMG ratio was below 1) was observed in the nearly isometric task of back load lifting (Figs. 3.8 and 3.11C), in which velocity dependent afferent input is expected to be very low. Furthermore, high SO activity with respect to MG (the SO EMG / MG EMG ratio above 1, Fig. 3.11C) and a very high mean SO activity (Fig. 3.12D) was found during a fast task of human vertical jumping. Thus, the first hypothesis cannot explain the relative low activity of SO during paw shake responses in cats with self-reinnervated SO and GA and during slow back load lifting tasks in humans, neither can it explain the high SO EMG during fast vertical jumping.

The second hypothesis that SO activity would be low compared to GA activity for tasks requiring an ankle extension–knee flexion joint moment combination and does not require high movement velocities or length-velocity related sensory feedback received strong support in this study. The SO EMG / MG EMG ratio (coordination) was lower than 1 for tasks which required an ankle extension–knee flexion moment combination (fast cat paw shaking and slow human back load lifting), whereas the ratio was greater than 1 (i.e., no SO inhibition) for tasks which required an ankle extension–knee extension moment combination (fast human jumping, slow cat walking, and slow human leg load lifting; Fig. 3.11), irrespective of MTU velocities (Figs. 3.6, 3.8 and with Fig. 3.9; Table 3.1).

The rejection of hypothesis 1 and support for hypothesis 2 are based on comparisons of SO and MG EMG activities and functions across two different species: cats and humans. Although morphology, architecture and size of SO and MG muscles may differ substantially from one species to another, e.g. dogs do not have SO (Spoor and Badoux, 1989) and SO in horses is very small to contribute significantly to ankle extension (Meyers and Hermanson, 2006), there are similarities in properties of SO and MG muscles between cats and humans that justify our comparisons. Specifically, muscle volumes of SO and MG, determined as the product of the mean muscle fiber length and physiological cross-sectional area, constitute 10% and 21% of total volume of all ankle extensors, respectively, in cats (Sacks and Roy, 1982) and 45% and 21% in humans (Ward et al., 2009). The SO is a slow-twitch muscle in cats and humans – the percentage of slow-twitch muscle fibers is 100% in cats (Ariano et al., 1973) and 88% in humans

(Johnson et al., 1973), whereas the MG is a predominantly fast-twitch muscle in cats (25% of slow-twitch fibers) and a mixed muscle in humans, 51%.

3.4.3 Potential mechanisms and functional significance

Differential activity of individual heads of triceps surae has been first observed during paw shake responses in the cat (Smith et al., 1980). It is characterized by an increased EMG activity of GA and a relatively low SO EMG. The relative inhibition of SO activity during slow human movements is shown for the first time in the present study. Note that in the current study, the mean SO EMG during fast cat paw shake responses and slow human back load lifting was higher than during cat stance of walking (Fig. 3.12B) and human leg load lifting (Fig. 3.12D), respectively, although the SO EMG / MG EMG ratio was much lower during paw shake responses (Fig. 3.11 A,B) and back load lifting (Fig. 3.11C). The differences in movement speed cannot consistently explain this behavior, as discussed above. Although it may seem counterintuitive, activating slow-twitch muscles like SO during high-speed movements may be mechanically advantageous for achieving high movement velocities (Holt et al., 2014).

The fact that (1) biomechanical task requirements for paw shake responses and back load lifting require the simultaneous production of ankle extension and knee flexion moments and that (2) the mean MG EMG activity in these tasks is much higher than during cat stance of walking and human leg lifting (the latter two tasks require ankle extension and knee extension moments) (Fig. 3.12 A,C) is consistent with the idea that increasing the relative contribution of the two-joint MG to production of ankle extension and knee flexion moments simultaneously is mechanically advantageous. The task-specific increase in MG activity could involve excitatory inputs from extensor and flexor

half-centers of the CPG (Perret and Cabelguen, 1980, Prilutsky, 2000a) and possibly proprioceptive feedback other than velocity dependent ones (Klishko et al., 2011). The simultaneous excitatory inputs to the MG motoneuron pool from extensor and flexor spinal centers, explaining higher MG activity, is also consistent with the relatively lower activity of SO, whose motoneurons presumably receive central excitatory input only from the extensor center.

During vertical jumps, both SO and MG demonstrated the highest mean EMG magnitude among all human tasks (Fig. 3.12 C,D) and the ratio SO EMG / MG EMG exceeding 1 (Fig. 3.11C). These results likewise can be explained by a strong excitatory input to motoneuronal pools of both muscles from an extensor center, whereas the relatively lower MG activity with respect to SO could be caused by inhibitory influences on MG motoneurons. A spinal pathway that could provide such inhibition is the force-dependent inhibitory pathway from the quadriceps, knee extensor muscles that are highly active during jumping (Bobbert and van Ingen Schenau, 1988), to MG (Wilmink and Nichols, 2003). This inhibition along with the length-dependent excitation from the vastus intermedius (VI), one-joint knee extensor, to SO (Wilmink and Nichols, 2003) appear to be functionally appropriate during motor tasks with ankle extension–knee extension moment combinations, as in vertical jumping and leg load lifting, because they act to reduce the MG antagonistic action at the knee joint and the MG contribution to the ankle extension moment. Another potential mechanism for low MG activity could be muscle length related – MG activity has been shown to decrease and SO activity to increase during production of ankle extension moments while the knee joint is flexing, causing shortening of MG fascicles (Lauber et al., 2014). The latter mechanism does not

seem to influence substantially MG activity in this study, as similar maximum knee flexion angles during leg lifting and vertical jumping (82±14° and 89±8°, respectively) produced dramatically different MG and SO EMG activities (Fig. 3.12 C,D).

Although there was no evidence of a decrease in the mean SO activity during paw shake responses or back load lifting compared to walking or leg load lifting (Fig. 3.12 B and D, respectively), inhibitory influences on SO motoneurons from central or peripheral sources cannot be excluded. First, ankle extension moments during the back load lifting in humans were much higher than during leg load lifting (Fig. 3.8), suggesting that perhaps central excitatory input from an extensor center to SO motoneurons was higher in former task, which could explain in part the higher mean SO EMG during back load lifting as opposed to leg lifting (Fig. 3.12D). No significant increase in mean SO EMG activity from 5%- to 15%-back lifting was found, even though the latter task required a greater ankle extension moment and MG EMG activity (Fig. 3.8). Assuming there would be increased input to all ankle extensor motoneurons with 15% load versus 5% load, this may suggest a net cancellation effect on SO due to additional inhibitory inputs.

There may be at least two neural mechanisms responsible for potential inhibition of slow-twitch motor units during fast tasks that require high power output. Eccles et al. (1961) and Friedman et al. (1981) have found evidence in experiments on cats that the average size of recurrent inhibition via Renshaw cells measured at resting motoneuron membrane potential was greater in slow-twitch motor units than in fast-twitch ones, and suggested that this mechanism could contribute to selective inhibition of slow-twitch motor units during fast movements. However, when recurrent inhibitory post-synaptic potentials were measured at the membrane potential corresponding to the motoneuron

firing threshold, no difference in recurrent inhibition between slow and fast motor unit types could be detected (Hultborn et al., 1988a, Hultborn et al., 1988b, Lindsay and Binder, 1991). Thus, recurrent inhibition via Renshaw cells does not seem a probable mechanism for potential inhibition of SO motor units.

Another possible mechanism responsible for potential inhibition of SO motoneurons could be the force-dependent inhibition of SO from MG mediated by the Golgi tendon organ afferents (Nichols, 1994, Nichols, 1999). This mechanism is consistent with the idea that in order to increase the mechanically advantageous contribution of MG to the combination of ankle extension and knee flexion moments, the contribution of one-joint SO to the ankle extension moment should be reduced (Prilutsky, 2000a).

CHAPTER IV

SPECIFIC AIM 3

EFFECTS OF LENGTH-VELOCITY DEPENDENT SENSORY FEEDBACK AND KNEE AND HIP JOINT MOMENT COMBINATIONS ON RELATIVE ACTIVITY OF CAT VASTII AND RECTUS FEMORIS DURING WALKING AND PAW SHAKE

4.1 Introduction

Individual muscles within synergist groups can exhibit differential activity that is highly task-dependent (Conway et al., 1987, Chanaud and Macpherson, 1991, Brown et al., 2007). In the previous chapter, it was shown that the distinct activity of distal medial gastrocnemius (MG) and soleus (SO) muscles depends on moment requirements at the ankle and knee joints and does not depend on movement speed or length-velocity dependent sensory feedback. Stereotypical activation of proximal quadriceps and hamstring muscles also show task-dependent activations, which has been suggested to be consistent with an efficient motor control strategy that minimizes muscle fatigue and stress or maximizes muscular output (Jacobs et al., 1996, Prilutsky et al., 1998b, Prilutsky, 2000a, Prilutsky and Zatsiorsky, 2002, Wakeling et al., 2010, Blake et al., 2012). As discussed previously, muscles that cross two joints have a mechanical advantage in tasks where they can contribute agonistic actions at each joint and are known to show the greatest activity under these conditions (Wells and Evans, 1987,

Prilutsky, 2000a, Mehta and Prilutsky, 2014). For example, if a knee extension and hip flexion moment was required for a given task, a greater contribution of the two-joint RF muscle (knee extensor and hip flexor) to these actions would be mechanically more advantageous than utilizing one-joint hip flexor iliopsoas (IP) and one-joint knee extensor vastii (VA) instead.

However, the extent to which proximal hindlimb muscles rely on joint moment requirements and the length-velocity related afferent feedback in order to execute the stereotypical activations is not clear. Findings by Markin et al. (2012b) that activity patterns of two-joint RF are different, while those of its one-joint synergists VA are similar, between cat fictive locomotion lacking motion-dependent feedback and real walking, suggest that RF activity relies more on motion-dependent feedback than on central input from CPG, whereas the opposite is true for VA. The similar activity patterns of SO and GA in fictive and real walking reported in the same study suggests that activities of these muscles might have a lesser dependence on motion-dependent feedback, which is consistent with the results of Chapter 3.

Additional work is needed in order to understand the role of motion-dependent sensory feedback in coordination between proximal one- and two-joint muscles. Therefore, the goals of these experiments were to (1) investigate the coordination between RF and VA, (2) determine whether length-velocity dependent afferent feedback from quadriceps and sartorius (Q-Sart) contributes to the coordination between RF and VA, and (3) investigate whether there is a differing contribution of this feedback to the activity of RF and VA. These goals were addressed by comparing coordination between RF and VA muscles during tasks with different combinations of joint moments before

and after removal of length-velocity dependent sensory feedback from Q-Sart. It was hypothesized that: (1) coordination between VA and RF would depend on the combination of joint moment requirements at the hip and knee and would be altered by removal of length-velocity dependent feedback from Q-Sart; and (2) removal of this feedback would have a greater effect on activity of RF compared to VA. Findings from this study will help to better understand the mechanisms which underlie coordination between proximal one- and two-joint muscles. Preliminary results have been published in abstract form (Mehta et al., 2014).

4.2 Material and Methods

4.2.1 Animals and surgical procedures

The surgical and experimental procedures employed in these experiments corresponded to the "Principles of Laboratory Animal Care" (NIH Publication No. 86-23, Revised 1985) and were approved by the Institutional Animal Care and Use Committee of the Georgia Institute of Technology.

Seven female, adult cats (*felis domesticus,* mass = 3.5±0.4 kg) were used in this study. Prior to all surgeries, cats were trained using food reward to walk on a Plexiglas enclosed walkway (3.0 x 0.4 m^2) with up to three embedded force plates (16 x 11 cm^2 and 11 x 7 cm^2; Bertec Corporation, Columbus, OH, USA) for several hours a day, 5 days a week, for 3-4 weeks; for additional details see Prilutsky et al. (2005) and Gregor et al. (2006). Surgical procedures will briefly be described here since they have been described in detail previously (Gregor et al., 2006, Prilutsky et al., 2011, Hodson-Tole et

al., 2012). Two survival surgeries were performed under aseptic conditions using general isoflurane anesthesia.

4.2.1.1 Implantation surgery

Animal anesthesia, monitoring during surgery and after surgery pain medication were the same as described in Chapters 2 and 3. Teflon-insulated multi-stranded stainless steel fine wires (CW5402; Cooner Wire, Chatsworth, CA, USA) attached to two multi-pin Amphenol connectors were passed subcutaneously from skin incision on the skull along the back toward the right hindlimb. The connector was attached to the skull using four stainless steel or titanium screws and dental cement. A small strip of insulation (~1 mm) was removed near the distal end of each wire and a pair of wires was implanted in the mid belly of RF, VA, biceps femoris posterior (BFP), biceps femoris anterior (BFA), iliopsoas (IP), tibialis anterior (TA), MG and SO muscles of the right hindlimb (the distance between wires in each muscle was approximately 5-10 mm). Skin incisions were closed using Vicryl 4-0 suture for the deep fascia and Vicryl 5-0 suture for subcuticular closure. The animal recovered after surgery for 14 days.

4.2.1.2 Nerve transection and repair surgery

Anesthesia during the surgery and pain medication following the surgery were the same as those for the implantation surgery. A longitudinal incision in the femoral triangle region of the right hindlimb was made in order to identify and isolate the branches of the femoral nerve which innervate single heads of quadriceps (RF and VA) and sartorius (SA) muscles. After dissecting surrounding tissue, the quadriceps and SA nerves were transected before the branching point using sharp scissors, carefully aligned together, secured in the aligned position with one or two stiches of Vicryl 5-0 suture, and then

fixed in place using fibrin glue (equal parts of thrombin and a 1:1 mixture of fibrin and fibronectin; Sigma-Aldrich, St. Louis, MO, USA (English, 2005)). The animal recovered for at least 3-5 days before experiments were resumed.

4.2.2 Data collection

Animal kinematics and electromyographic (EMG) activity were recorded during upslope (27^{o}), downslope (-27^{o}), level walking and paw shake responses before and at least 12 weeks after nerve transection and repair (12 weeks for five cats and 16 weeks for two cats). The period of 12 weeks allowed sufficient time for the injured muscles to be reinnervated and regain the pre-nerve transection EMG activity level (Gordon and Stein, 1982, O'Donovan et al., 1985, Gregor et al., 2003, Pantall et al., 2016).

Kinematics of walking and paw shake responses were recorded using light reflective markers (as described in Chapters 2 and 3). Ground reaction forces during walking were collected using embedded force plates (Bertec Corporation, Columbus, OH, USA) at 360 Hz. A 16-conductor, shielded flexible cable was connected to the Amphenol connector on the cat's head to record EMG activity. EMG and mechanics data collection was synchronized by an electronic trigger pulse from the Vicon system. EMG signals were recorded at 3000 Hz, band-pass filtered (30-1000 Hz, 3 dB), amplified (100x), and saved on a computer for further analysis.

Two motor behaviors were studied. The first was overground walking, a slow task, in which two combinations of knee and hip joint moments are developed within the stance phase. The initial part of stance consists mostly of knee extension–hip extension moments (KE-HE), whereas a second phase is a knee extension–hip flexion moment (KE-HF) combination (Gregor et al., 2006, Prilutsky et al., 2011). The second task was a

paw shake response, a fast task, in which knee extension and hip flexion moments (KE-HF) are produced simultaneously during one half of the paw shake cycle (Hoy et al., 1985, Prilutsky et al., 2004). Paw shake responses (PSRs) were elicited by placement of a small piece of adhesive tape on paw pad of the right hindlimb (for details see Chapter 3). PSR and locomotion experiments were performed both before and at least 12 weeks after RF-VA-SA nerve transection and repair.

4.2.3 Data analysis and statistics

EMG activity and hindlimb mechanics during PSR episodes (Fig. 4.1) and walking cycles (Fig. 4.2) were analyzed using custom software (Prilutsky et al., 2005, Gregor et al., 2006). Walking and PSR cycles were identified using vertical ground reaction forces produced by the right hindlimb or computed joint moments, respectively. Joint angles were calculated after filtering recorded marker coordinates using a fourth order, zero lag Butterworth filter (10 and 15 Hz cut-off frequencies for walking and paw shakes, respectively). Resultant muscle moments of the right hindlimb joints were computed in the sagittal plane using a standard inverse dynamics analysis, described in detail elsewhere (Prilutsky et al., 2005, Gregor et al., 2006, Prilutsky et al., 2011). Inertial properties of cat hindlimb segments necessary for calculations were obtained using the regression equations from Hoy and Zernicke (1985). The computed moments were normalized by cat mass. The numbers of cycles analyzed for joint kinetics are shown in Table 4.1.

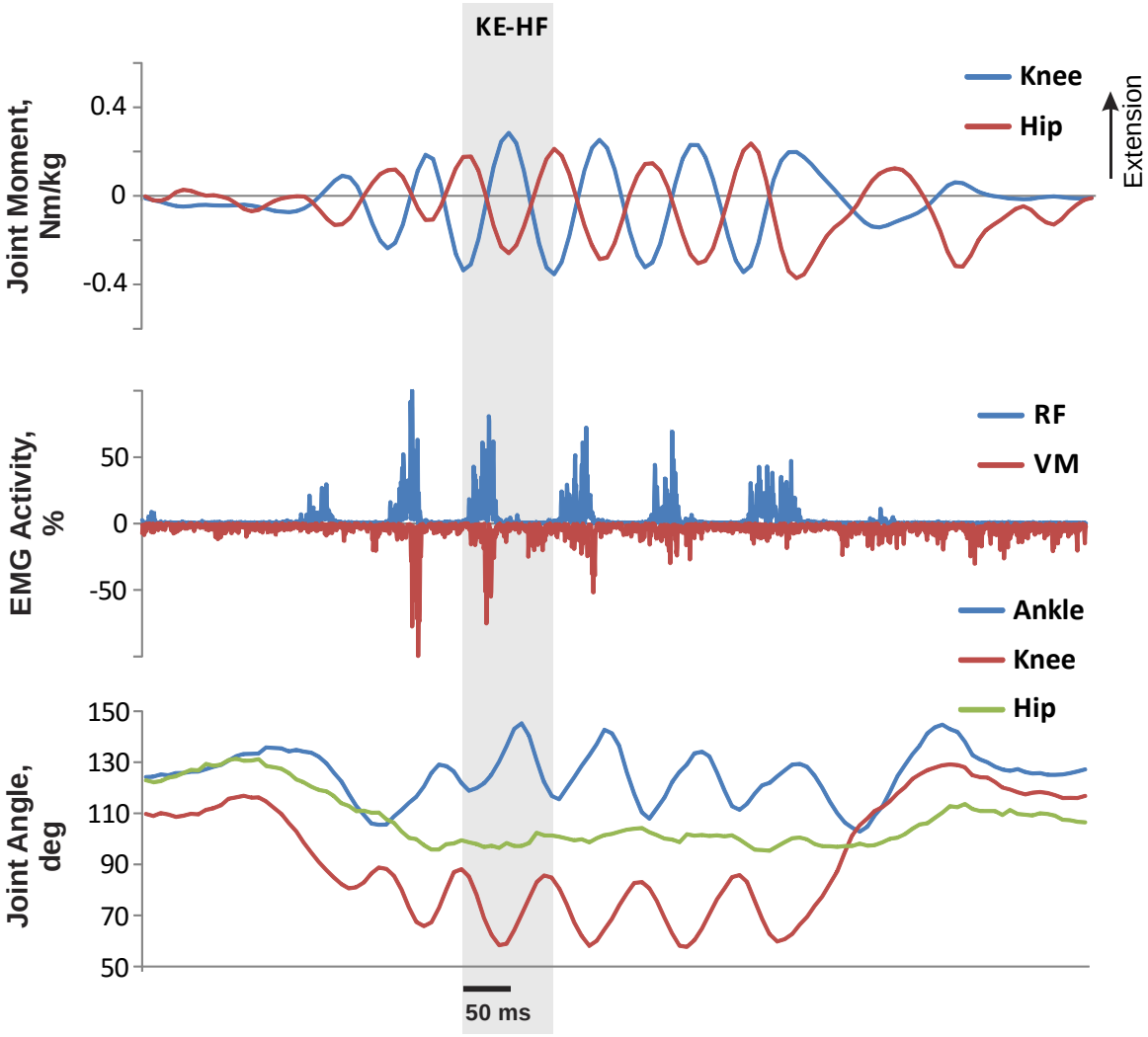

Figure 4.1. A representative paw shake response (PSR) episode. From top to bottom: normalized resultant muscle moments at the knee and hip joints (positive values correspond to extension); normalized raw, full-wave rectified EMG activity of RF (positive values) and VM (negative values); and intersegment joint angles for the ankle, knee and hip joint. Grey shaded region represents a single steady-state cycle within the PSR determined using the peak knee flexion joint moment**.**

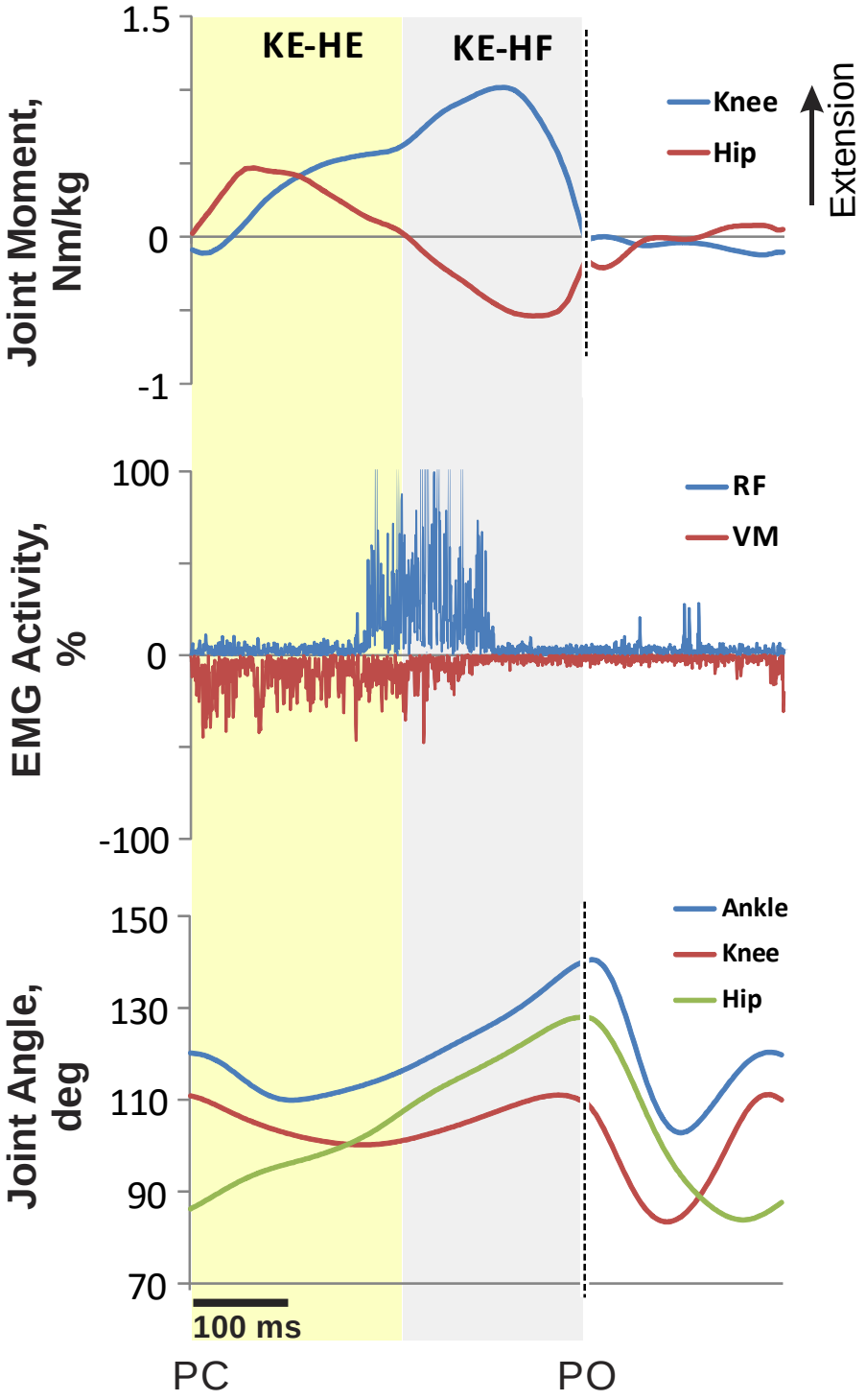

Figure 4.2. A representative level walking cycle. From top to bottom: normalized resultant muscle moments at the knee and hip joints (positive values correspond to extension); normalized raw, full-wave rectified EMG activity of RF (positive values) and VM (negative values); and intersegment joint angles for the ankle, knee and hip joint. Yellow shaded region represents knee extension–hip extension (KE-HE) phase of stance. Grey shaded region represents knee extension–hip flexion (KE-HF) phase of stance**.** PC, paw contact; PO, paw off

Table 4.1. Number of analyzed cycles from each cat and task, before (Pre) and after (Post) self-reinnervation. Cycles for joint mechanics used in general analysis for average plots of joint moments, joint angles, joint yield and stance/cycle duration (Figs. 4.4 – 4.7). Cycles used in all VA-RF coordination analyses and average VA / RF plots (Figs. 4.4, 4.5, 4.8). Coordination walking cycles are per phase (one each for KE-HE and KE-HF).

		AM		BO		BR		CL		ES		JU		VE		Total	
		Pre	Post	Pre	Post	Pre	Post	Pre	Post	Pre	Post	Pre	Post	Pre	Post	Pre	Post
Joint Mechanics Walking	Down	10	15	13	11	7	6	11	14	10	13	15	12	8	8	74	79
	Level	14	14	10	9	7	9	13	11	16	15	17	13	15	11	92	82
	Up	8	10	14	14	7	7	13	13	11	13	14	15	9	10	76	82
Coordination Walking (per phase)	Down	5	14	-	-	-	-	7	4	-	-	6	10	-	-	18	28
	Level	14	7	-	-	-	-	7	2	-	-	14	10	-	-	35	19
	Up	4	9	-	-	-	-	6	6	-	-	13	14	-	-	23	29
Joint Mechanics Paw shake	PS	6	4	7	7	-		-		-		7	12	-		20	23
Coordination Paw shake	PS	6	4	-		-		-		-		7	12	-		13	16

For walking conditions, recorded and band-pass filtered EMG signals (see above) were full-wave rectified and EMG burst onset and offset times determined either visually or by a computer program using a 2-SD threshold above the EMG baseline observed during the swing or stance phase of walking (Gregor et al., 2006). The mean burst EMG activity and burst duration (offset minus onset time) for VA and RF was computed for each cycle (number of cycles shown in Table 4.2). The mean EMG burst values were normalized to the maximum peak EMG magnitude found across all walking conditions before nerve cut and repair for each cat and muscle. For analyses of muscle coordination in walking and PSR, full-wave rectified signals were also low-pass filtered (fourth order, zero lag Butterworth filter, cut-off frequency of 30 Hz and 75 Hz for walking and paw shake, respectively) to obtain EMG linear envelopes. The linear EMG envelope values

were normalized to the maximum burst EMG magnitude found across all walking conditions before nerve cut and repair for each cat and muscle.

Table 4.2. Number of analyzed EMG bursts from each cat for locomotion tasks, before (Pre) and after (Post) self-reinnervation. Cycles analyzed here used for EMG burst analyses (Fig. 9).

		AM		BO		BR		CL		ES		JU		VE		Total	
		Pre	Post	Pre	Post	Pre	Post	Pre	Post	Pre	Post	Pre	Post	Pre	Post	Pre	Post
RF	Down	8	15	-	-	-	-	3	5	-	-	14	7	-	-	25	27
	Level	12	14	-	-	-	-	8	9	-	-	10	11	-	-	30	34
	Up	7	10	-	-	-	-	7	9	-	-	9	14	-	-	23	33
VA	Down	8	15	13	-	7	5	3	8	-	-	4	11	7	-	42	39
	Level	14	8	10	-	7	8	12	11	13	15	11	10	14	-	81	52
	Up	9	10	14	7	7	7	7	6	10	13	5	15	8	10	60	68

Joint moment, joint angle and EMG data obtained for walking were time-normalized to the duration of the stance and swing phase separately. For each walking cycle, joint yield was calculated as the angle at toe contact minus the minimum angle during stance. Joint moments, joint angles and EMG traces for PSR were time normalized to the duration of individual steady-state cycles in the middle of PSRs, which were manually identified using consecutive peaks of the knee flexion moment considered as the start and end of the paw shake cycle (grey shaded region in Fig. 4.1). The peak knee and hip joint moments and peak VA and RF EMG activity were identified within the two phases of stance for each cycle and walking condition (Fig. 4.2: yellow shaded region, knee extension–hip extension moment combination, KE-HE; grey shaded region, knee extension–hip flexion moment combination, KE-HF). In order to quantify muscle coordination, the difference between normalized EMG peaks (peak VA EMG – peak RF EMG) was calculated for each phase of stance during walking, described above. For PSR, the coordination between VA and RF was also calculated as the difference between normalized EMG peaks (peak VA EMG – peak RF EMG). A positive value in this

difference meant a greater normalized activity of VA versus RF, whereas a negative value indicated a greater normalized activity of RF. The number of cycles used for analysis of coordination between VA and RF are shown in Table 4.1. Additionally, the peak knee extension and peak hip extension and flexion moment were determined within each phase in walking and paw shake cycles. Stance time and cycle time were also determined for each walking and paw shake cycle, respectively.

All statistical tests were performed using IBM SPSS Statistics v20 software (IBM SPSS, Chicago, IL, USA). A linear mixed model analysis was used to test for significant differences between control (Pre) and post self-reinnervation (Post) conditions. The task, time (pre- or post- self-reinnervation), joint moment combination, joint, and muscle were used as fixed factors. Cats and individual PSR or walking cycles were considered random factors. Stance duration and cycle time were used as covariates for walking and PSR comparisons, respectively. The Bonferroni post-hoc test was used for pairwise comparisons. A Pearson's two-tailed partial correlation analysis (stance duration or cycle time used as covariates) was performed between the difference (peak VA EMG – peak RF EMG) and the difference (peak knee moment – peak hip moment) for all conditions and phases combined, before and after self-reinnervation. Finally, t-tests were used to compare the values of difference (peak VA EMG – peak RF EMG) to 0 for each condition, phase, and time period. Significance level for all tests was set at an alpha level of 0.05.

4.3 Results

In this study, the coordination between two-joint RF and one-joint VA was characterized during cat level locomotion, sloped locomotion, and PSR before and after

removal of length-velocity dependent afferent feedback from RF, VA and SA using self-reinnervation (Cope and Clark, 1993, Cope et al., 1994). Success of the surgery was validated by the absence of EMG activity in RF, vastus lateralis (VL) or vastus medialis (VM) within several weeks after surgery, and recovery of EMG activity to pre surgery levels in 10-12 weeks (see example in Fig. 4.3). A clear limp (rapid flexion of the knee joint during stance) was also observed immediately following the surgery, which disappeared in 12 weeks after the surgery; the absence of limping was another quantitative measure of recovery. All cats showed recovered EMG bursts in RF and/or VA and no observable limp three months following the self-reinnervation procedure. Details of findings will be presented in the following sections.

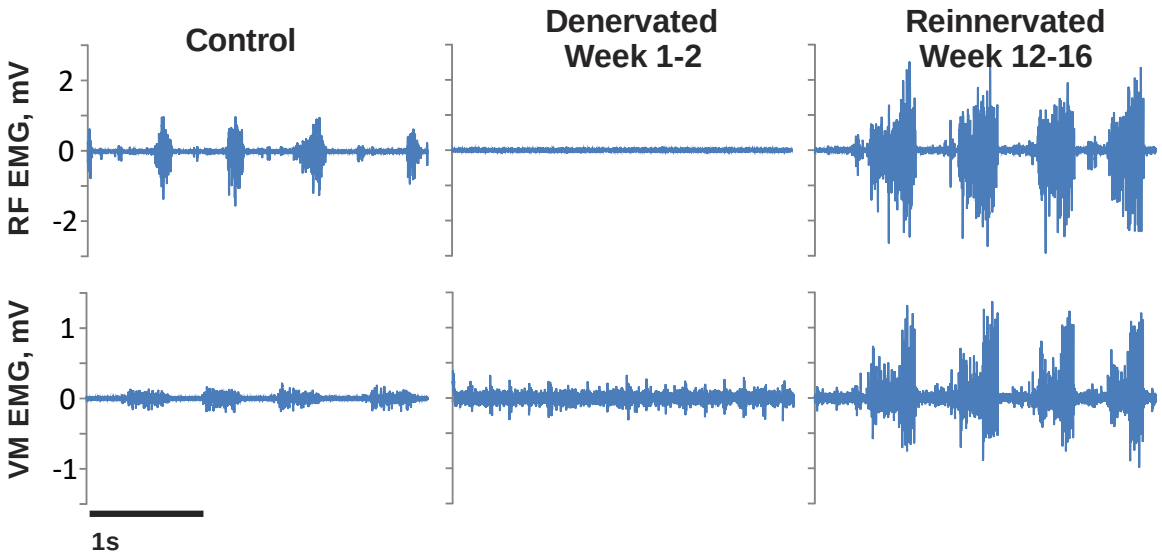

Figure 4.3. Representative EMG burst activity for RF and VM during level locomotion for three time periods.

4.3.1 Paw shake response characteristics

Average knee and hip joint moments, vastus medialis (VM) and RF EMG activity, and joint angles for all paw shake cycles before and after self-reinnervation are shown in Fig. 4.4. Frequency of rapid oscillations in the intact cat ranged from 8 to 12 Hz

where each PSR consisted of about 3 to 7 cycles. Steady-state cycles, which occurred in the middle of a typical PSR episode, showed approximate time synchronization between the occurrence of peak hip flexion and knee extension moments, RF and VA EMG bursts, and decreasing knee angle, increasing hip angle (Fig. 4.1, grey shaded region) and thus lengthening of RF and VA muscle-tendon unit. Peaks of EMG bursts occurred approximately 10 to 20 ms earlier than the peaks of joint moments. Therefore, the low-pass filtered EMG was shifted forward to align with peaks of knee and hip joint moments.

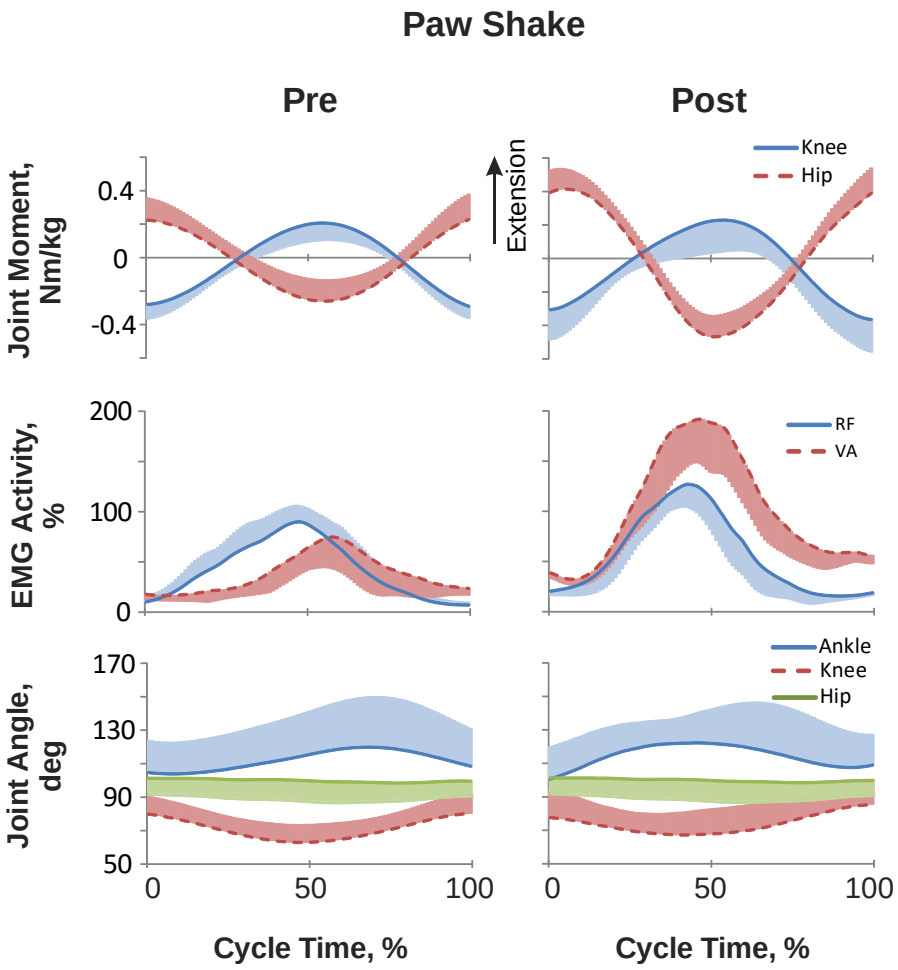

Figure 4.4. Average (+/- SD) data for paw shake cycle. From top to bottom: normalized resultant muscle moments at the knee and hip joints (positive values correspond to extension); normalized low-pass filtered EMG activity of RF (solid line) and VA (dashed line); and intersegment joint angles for the ankle, knee and hip joint. Left panels show control data (Pre) while right panels show data after self-reinnervation (Post)**.**

After self-reinnervation, cats were still able to consistently produce a PSR. There were no apparent changes in the phasing of knee and hip joint moments, VA and RF EMG burst and knee and hip joint angles after reinnervation. There was also no significant difference in paw shake cycle duration before and after self-reinnervation (mixed model analysis, P=0.153, Fig. 4.6B), and the shift between EMG activity and joint moments remained similar.

4.3.2 Characteristics of level and slope walking

Average knee and hip joint moments, VA and RF EMG activity, and joint angles for all walking conditions before and after reinnervation are shown in Fig. 4.5. In intact cats, the knee moment during stance phase of walking in all slope conditions remained an extension moment for the majority of the stance phase. In contrast, the hip moment showed an extension moment during the beginning of stance while changing to a flexion moment later in stance. This reversal of moment direction occurred in downslope, level, and upslope after about 25%, 50% and 75% of the stance phase, respectively. This allowed for the separation of stance into a KE-HE phase (Fig. 4.2, yellow shaded region) and a KE-HF phase (Fig. 4.2, grey shaded region). The majority of VA and RF EMG activity occurred within the stance phase. The onset of the VA EMG burst typically occurred just prior to PC while the offset occurred just before PO. The onset of RF burst, on the other hand, was dependent on the slope.

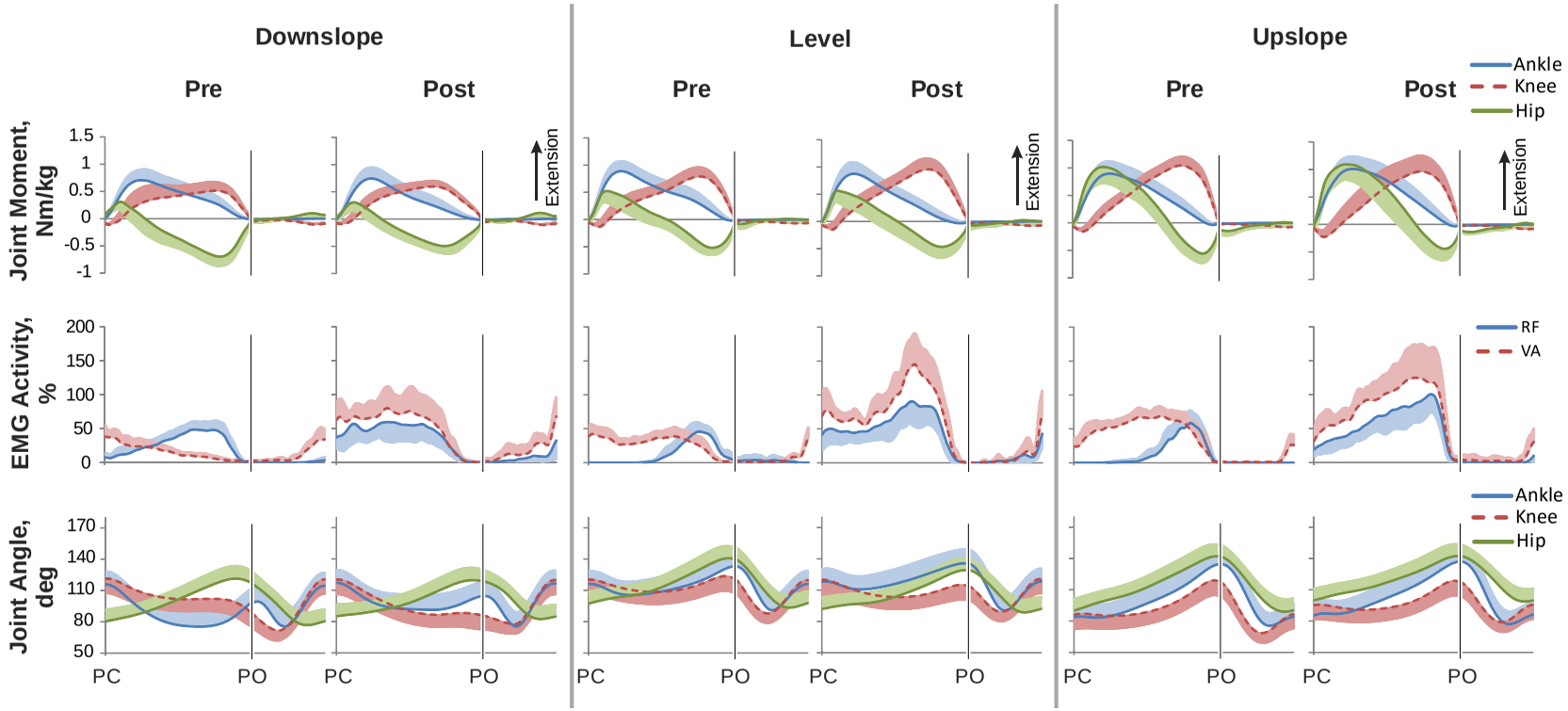

Figure 4.5. Average (+/- SD) cycle data for all three walking conditions. From top to bottom: normalized resultant muscle moments at the ankle, knee and hip joints (positive values correspond to extension); normalized low-pass filtered EMG activity of RF (solid line) and VA (dashed line); and intersegment joint angles for the ankle, knee and hip joint. Within a walking condition, left panels show control data (Pre) while right panels show data after self-reinnervation (Post). PC, paw contact; PO, paw off

Following self-reinnervation, joint moments and joint angles appeared qualitatively similar, however quantitative results are discussed in detail below (see "*Joint angles*"). There was no significant difference in stance duration for upslope walking (mixed model analysis, P=0.09, Fig. 4.6A). There was, however, a significant increase in stance duration for downslope and level walking after self-reinnervation (mixed model analysis, P=0.001 and P=0.003, respectively, Fig. 4.6A). There were considerable changes in VA and RF EMG activity, which will be discussed below (see "*Coordination between RF and VA*" and "*EMG activity*").

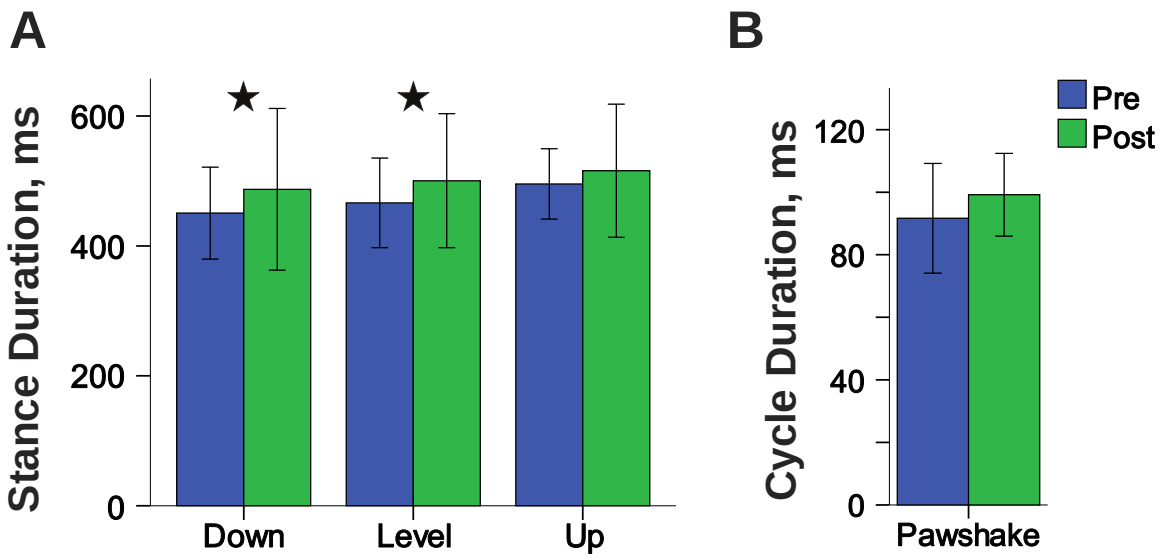

Figure 4.6. Average (±SD) stance and cycle duration time. (A) Stance duration time for all walking conditions. (B) Cycle duration time for paw shake condition. Blue bars show average for control data (Pre) while green bars show data following self-reinnervation (Post). Stars above condition represent significant difference between Pre and Post at an alpha level of 0.05.

4.3.3 Coordination between RF and VA

Correlation between (VA EMG – RF EMG) and (knee moment – hip moment). In order to investigate possible relationships between joint moment requirements and coordination between one-joint VA and two-joint RF, the moment difference (peak knee moment – peak hip moment) and corresponding EMG difference (peak VA EMG – peak RF EMG) for each cycle was plotted for all tasks (KE-HE and KE-HF phases combined), before and after self-reinnervation (Fig. 4.7D). Before reinnervation, a strong negative correlation was found between the moment difference and the EMG difference (partial correlation test, $R = -0.759$, $P<0.001$, Fig. 4.7D, Pre). As the knee – hip joint moment difference decreased, there was a decrease in VA EMG – RF EMG difference, and therefore a greater RF activation relative to VA at the knee extension–hip flexion combination of joint moments. After self-reinnervation, the strong correlation between the VA EMG – RF EMG difference and knee – hip joint moment difference was lost and was no longer significant (partial correlation test, $R = -0.103$, $P=0.416$, Fig. 4.7D, Post).

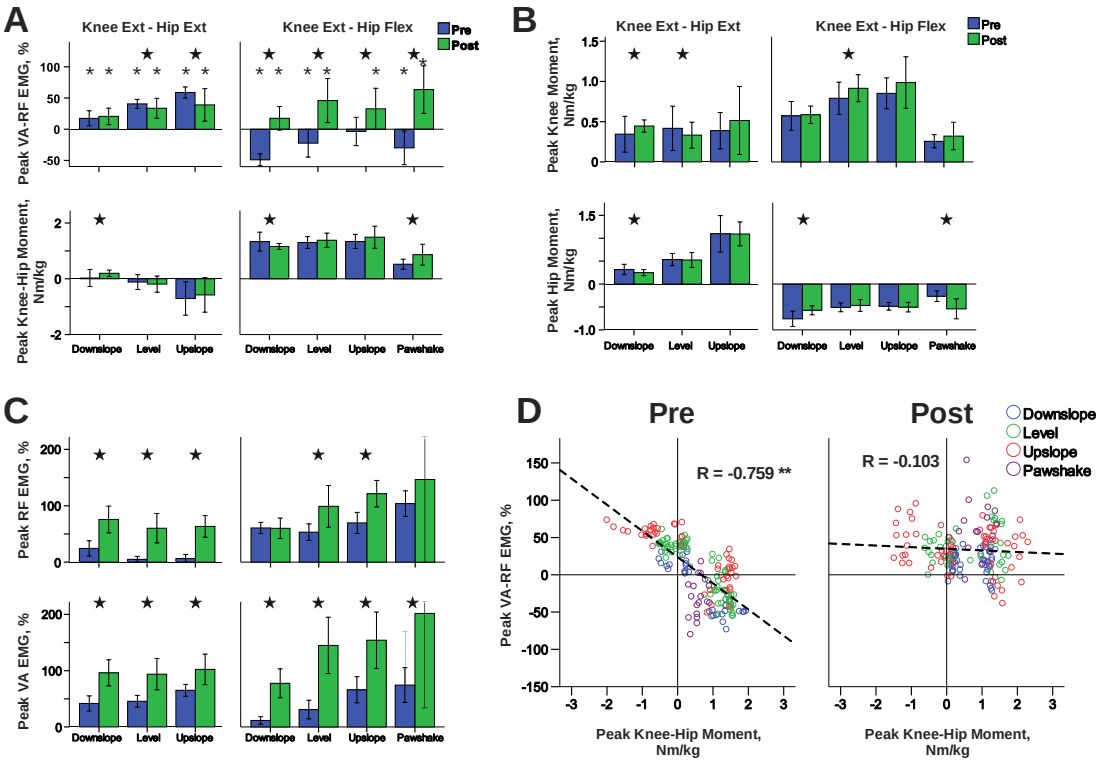

Figure 4.7. Average (+/- SD) coordination data for all three walking conditions and paw shake. (A) normalized peak VA – RF EMG difference and peak knee – hip moment difference for all conditions for KE-HE (left panels) and KE-HF (right panels) phases. (B) normalized peak knee and hip moment for all conditions for KE-HE (left panels) and KE-HF (right panels) phases. (C) normalized peak, low-pass filtered RF and VA EMG for all conditions for KE-HE (left panels) and KE-HF (right panels) phases. (D) plot for peak VA – RF EMG difference and the corresponding peak knee – hip moment difference for each individual cycle, all conditions, and KE-HE and KE-HF phases combined before (Pre, left) and after self-reinnervation (Post, right). For A-C, values are for control (Pre) and after self-reinnervation (Post). Thick stars represent significant difference between Pre and Post ($p<0.05$). For A, thin stars indicate significant difference from 0 ($p<0.05$). For D, partial Pearson's correlation value shown for Pre and Post (two thin stars indicates significant correlation ($p<0.001$)).

Knee extension–hip extension (KE-HE) moment combination. The (peak VA EMG – peak RF EMG) difference for the knee extension–hip extension (KE-HE) joint moment combination was significantly greater than 0 for all walking tasks before and after reinnervation (Fig. 4.7A, $P<0.05$, one-sample t-test). For the KE-HE joint moment combination, there was a significant decrease in the peak VA EMG – RF EMG difference before and after reinnervation for level and upslope walking (mixed model, $P=0.029$ and $P=0.001$, respectively). After reinnervation, there was a significant increase in peak knee

– hip joint moment (Fig. 4.7A) for downslope walking (mixed model, P=0.001), however there was no change for the level and upslope walking (mixed model, P=0.218 and P=0.364, respectively).

Both the peak VA and peak RF EMG activity significantly increased following self-reinnervation for all walking conditions (mixed model, P<0.001 for all tasks, Fig. 4.7C). After self-reinnervation, during downslope walking, there was an increase in peak knee moment (mixed model, P<0.001, Fig. 4.7B), while the hip moment decreased (mixed model, P=0.024). There was a decrease in peak knee moment for level walking after self-reinnervation (mixed model, P=0.017), while there was no change in the peak hip extension moment (mixed model, P=0.813). For upslope walking after reinnervation, there was no change in peak knee and hip moment (mixed model, P=0.251 and P=0.587, respectively).

Knee extension–hip flexion (KE-HF) moment combination. For the KE-HF moment combination, the VA – RF EMG difference for downslope walking, level walking, and PSR were significantly less than 0 prior to reinnervation (Fig. 4.7A, P<0.05, one-sample t-test). For upslope walking, the VA – RF EMG difference was not significantly different from 0 (P=0.455, one-sample t-test). Following reinnervation, the VA – RF EMG difference within the KE-HF moment combination significantly increased to values greater than 0 across all tasks (Fig. 4.7A, P<0.05 for all tasks, one-sample t-test). Due to this change, there was also a significant increase in VA – RF EMG difference after reinnervation across all tasks (mixed model analysis, P<0.001 for all tasks, Fig, 4.7A). The peak knee – hip moment difference decreased for downslope walking, whereas it increased in paw shake (mixed model, P=0.011 and P<0.001,

respectively). In contrast, there was no change for level and upslope walking (mixed model, P=0.078 and P=0.174, respectively).

There was an increase in peak RF EMG (Fig. 4.7C) for level and upslope walking (mixed model, P<0.001 for both), whereas there was no change for downslope walking and paw shake (mixed model, P=0.436 and P=0.076, respectively). There was a significant increase in peak VA activity (Fig. 4.7C) across all tasks (mixed model, P<0.001 for all walking tasks, P=0.005 for paw shake). It should be noted that standard deviations for peak VA and RF EMG during paw shake after reinnervation were substantial. After self-reinnervation, cat "AM" showed a four-fold increase in peak VA and RF EMG during paw shake, while cat "JU" showed a large increase in peak VA EMG but a decrease in peak RF EMG. The upper standard deviation bars for this condition were cropped to allow for easier viewing of lower values while maintaining a consistent scale across all tasks. For peak knee moments (Fig. 4.7B), there was a significant increase after reinnervation for level walking (mixed model, P<0.001), whereas there was no change for downslope, upslope and paw shake (mixed model, P = 0.752, 0.136 and 0.115, respectively). For peak hip flexion moments (Fig. 4.7B), there was a decrease after reinnervation in downslope walking, while in contrast, an increase in paw shake task (mixed model, P<0.001 for both tasks). On the other hand, there was no change in peak hip flexion moment in level and upslope walking (mixed model, P = 0.125 and 0.472, respectively).

4.3.4 Joint angle yield

Joint angles during locomotion prior to removal of length-velocity dependent feedback are consistent with previous findings (Maas et al., 2007). Immediately

following the self-reinnervation surgery, all cats showed lack of activity in the targeted muscles (RF and/or VA, Fig. 4.1) and an exaggerated flexion of the knee joint (not shown). Following self-reinnervation, joint angles appeared qualitatively similar to control patterns at each joint except in downslope walking (Fig. 4.5). Analysis of joint yield revealed a significant increase in yield for the knee joint for all slope conditions following self-reinnervation (mixed model, $P<0.001$ for downslope and level walking, $P=0.001$ for upslope, Fig. 4.8). In contrast, the ankle joint yield decreased significantly for all walking conditions (mixed model, $P<0.001$ for all walking tasks, Fig. 4.8). The hip showed a significant increase in yield during stance only for downslope walking (mixed model, $P<0.001$), while showing no change in level and upslope walking (mixed model, $P = 0.074$ and 0.094, respectively). It can be seen, however, that there was often no or minimal yield at the hip joint during stance.

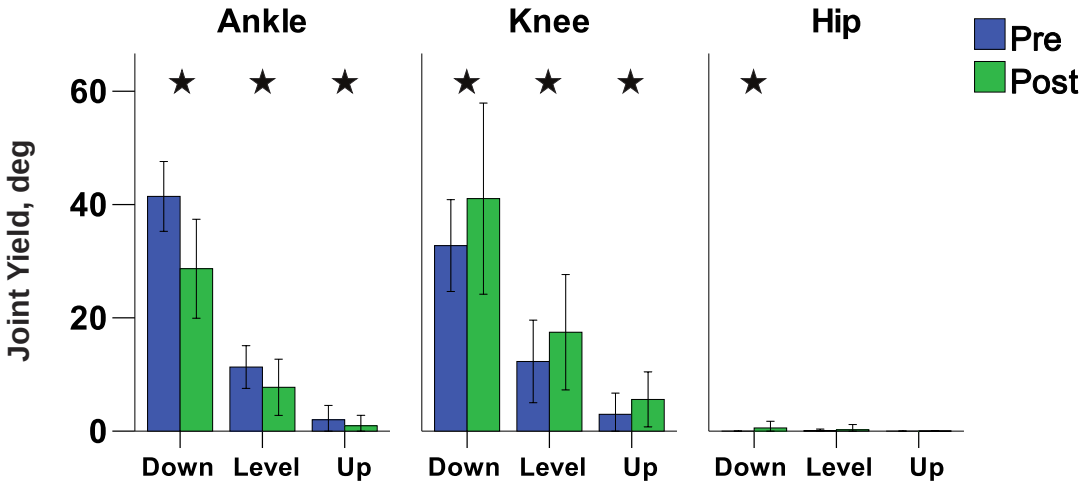

Figure 4.8. Average yield (±SD) for ankle, knee and hip joint for all walking conditions. Calculated by subtracting the minimum angle during stance from the initial angle at PC. Values are for control (Pre) and after self-reinnervation (Post). Thick stars represent significant difference between Pre and Post ($p<0.05$).

4.3.5 Changes in VA and RF EMG burst characteristics

For all walking slopes, average burst activity, burst duration, and pre-contact activation were analyzed before and after self-reinnervation (Fig. 4.9). Both RF and VA had increased average EMG burst activity following self-reinnervation (mixed model, $P<0.001$ for both muscles and all slopes). Burst duration increased in all slopes for RF (mixed model, $P<0.001$ for all slopes), whereas VA burst duration increased, although minimally (~3%), only in upslope (mixed model, $P=0.016$). There was no change in VA EMG burst duration after self-reinnervation for downslope and level walking (mixed model, $P = 0.077$ and 0.620, respectively). Average pre-contact activation EMG was significantly increased after self-reinnervation in level walking for RF (mixed model, $P<0.001$) and downslope and level walking for VA (mixed model, $P<0.001$ for both). After self-reinnervation, there was no change in average pre-contact activation EMG for RF in downslope and upslope walking (mixed model, $P = 0.497$ and 0.0407, respectively) and for VA in upslope walking (mixed model, $P=0.131$). There was, however, a trend towards increased average pre-PC EMG in all walking tasks for RF and VA.

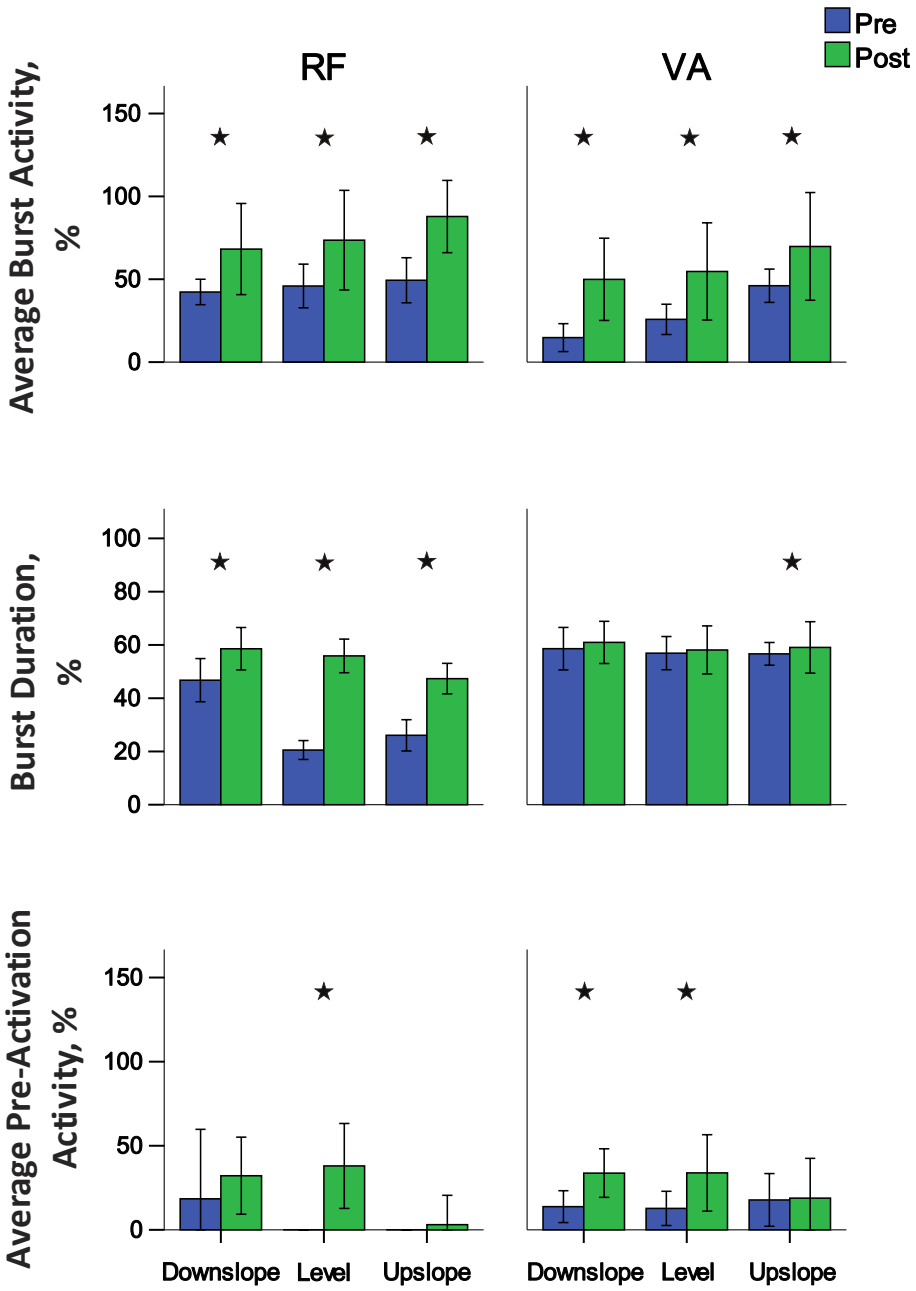

Figure 4.9. Average normalized burst activity, duration and pre-PC activation (±SD) for RF and VA for all walking conditions. Values are for control (Pre) and after self-reinnervation (Post). Thick stars represent significant difference between Pre and Post ($p<0.05$).

4.4 Discussion

This study examined the effects of selective removal of length-velocity dependent sensory feedback from quadriceps (RF and VA) and sartorius on the coordination between RF and VA during locomotion and paw shake responses in freely moving cats. Analysis of stance duration and cycle time revealed no differences after removal of this feedback for upslope walking and paw shake responses. Although there was a significant increase in stance duration for downslope and level walking, these changes appear to be quite small (~25 ms or <5%). Qualitative observations of all motor tasks after removal of length-velocity dependent feedback (through muscle self-reinnervation) indicated no substantial motor deficits. These cats appeared to mostly recover patterns of joint angles and joint moments. However, results of this work provide evidence for a change in coordination between RF and VA, which may impact the energetic cost of performing motor tasks. Results also showed an enhanced knee joint yield during stance, similar to that which occurred at the ankle and elbow after self-reinnervation of ankle (Abelew et al., 2000, Maas et al., 2007) and elbow (Livingston and Nichols, 2014) extensors.

4.4.1 Comparison with previous studies

Resultant joint moments, joint angle changes, and RF and VA EMG activity have been well documented during cat level and sloped locomotion in previous studies (Goslow et al., 1973, Smith et al., 1998, Gregor et al., 2006, Prilutsky et al., 2011, Markin et al., 2012b) and are similar to control results presented here (Fig. 4.5). Net joint moments at the knee, VA EMG, and joint angles during paw shake are well described in the literature (Hoy et al., 1985, Smith and Zernicke, 1987). It is difficult to compare results obtained in this study to that found previously due to the technique used to elicit

paw shake in previous studies which involved holding the cat in a vertical orientation. This technique causes a more extended initial posture of the joints due to effects of gravity and therefore may cause differences in joint kinematics. Overall, however, previously reported knee joint moments and VA EMG are in good agreement with results in this study (Fig. 4.4). To the best of my knowledge, RF EMG and hip moments during paw shake have not been previously investigated.

4.4.2 Changes in VA and RF coordination and joint moment requirements

It was hypothesized that (1) coordination between VA and RF would depend on the combination of joint moment requirements at the hip and knee and would be altered by removal of length-velocity dependent feedback from Q-Sart, and (2) removal of length-velocity dependent feedback from Q-Sart will have a greater effect on activity of RF compared to VA. The obtained results strongly support the first hypothesis for the following reasons: (1) for the KE-HF moment combination, peak VA – RF EMG was less than 0 for paw shake, downslope and level walking, which indicates a greater activation of RF compared to VA (Fig. 4.7B, Pre); (2) during the KE-HE moment combination, peak VA – RF EMG was greater than 0 in all walking conditions, indicating a greater contribution of VA over RF during the KE-HE phase (Fig. 4.7A); (3) there was a strong correlation between VA – RF EMG difference and knee – hip moment difference (Fig. 4.7D, Pre); and (4) after removal of length-velocity dependent feedback from Q-Sart, coordination between VA and RF was changed during the KE-HF phase (Fig. 4.7A, Post) and correlation between the VA – RF EMG difference and knee – hip joint moment difference was lost (Fig. 4.7D, Post). The results also provide support for the second hypothesis based on the finding that following self-reinnervation, RF burst duration

increased significantly in all walking conditions while only increasing (albeit by a much lesser extent) for upslope walking in VA (Figs. 4.5 and 4.9). It should be noted, however, that average and peak activity of RF and VA significantly increased for all tasks.

During upslope walking in the KE-HF phase, the VA – RF EMG difference was not significantly different from zero, therefore indicating an equal contribution of RF and VA EMG. There was, however, a clear increase in RF EMG activity during this phase (Fig. 4.7C), where onset of activity coincided well with the reversal of the hip moment from extension to flexion in all walking conditions (Fig. 4.5). VA tended to remain active throughout stance phase and simultaneously with RF during paw shake. During the KE-HF phase, RF can contribute agonistically to the knee and the hip resultant muscle moments, therefore providing a mechanical advantage over VA, although it appears that VA activity is still required to produce the necessary knee extension moment.

Although it is difficult to assess preferential activation directly in this study, the results show that peak VA activity in the KE-HF phase in all walking conditions does not exceed the corresponding activations in the KE-HE phase (Fig. 4.7C), whereas peak knee moment appears much greater in the KE-HF phase compared to the KE-HE phase (Fig. 4.7B). Peak VA activity also appears lower in the KE-HF phase compared to the KE-HE phase. These results suggest a preferential activation of RF compared to VA within the KE-HF phase.

4.4.3 Potential mechanisms and functional implications

This is the first study to show a coordination strategy between RF and VA in the cat during locomotion and paw shake, which is dependent on the combination of knee and hip joint moments required by the task. It was also found that this coordination

strategy is partly mediated by length-velocity dependent feedback from Q-Sart muscles. The possible functional significance of coordination between one- and two-joint muscles has been described previously in humans within static and dynamic tasks where two-joint muscles have the greatest activation when they can contribute as agonists to the joint moments at both joints simultaneously (Wells and Evans, 1987, Prilutsky and Gregor, 1997, Prilutsky et al., 1998b, Prilutsky, 2000a, Prilutsky and Zatsiorsky, 2002). Here these findings are extended to walking and paw shake tasks in the intact cat where a similar strategy for RF and VA coordination was found. Studies modeling activation of muscles using optimization techniques by minimizing muscle fatigue/stress have been able to predict EMG and force of one- and two-joint muscles with considerable accuracy (Prilutsky et al., 1998b, Prilutsky, 2000a, Prilutsky and Zatsiorsky, 2002). There is also evidence which shows a reduced energy expenditure in tasks with greater contribution of two-joint muscles compared to tasks where only one-joint muscles act (Smith et al., 1998). The preferential use of RF over VA during the KE-HF phase may therefore represent an energy-efficient strategy which has been adopted by the nervous system. This study showed that removal of length-velocity dependent feedback from VA and RF significantly altered the coordination between these muscles in both the KE-HF and KE-HE phases during stance of locomotion. This change in the coordination between RF and VA may cause increases in energy expenditure and metabolic cost of the task.

Major changes in the phasing of RF EMG activity occurred after self-reinnervation during walking tasks (Figs. 4.5 and 4.9). This finding is in agreement with comparisons of RF activity patterns between fictive and real locomotion (Markin et al., 2012b). It should be noted that although phasing of RF was altered after self-

reinnervation in this study, activity was still limited to the stance phase of walking. This is contrary to the finding by Markin et al. (2012) where RF activity occurs in the flexion phase in the absence of motion-dependent feedback. It is possible that feedback from other unaffected sources, such as cutaneous feedback, force-dependent feedback or feedback from antagonist muscles (i.e. hamstrings) could prevent such drastic changes in RF activity. Additionally, there were no major changes in timing of VA EMG, which is in agreement with the finding of similar VA activity patterns in fictive versus real locomotion (Markin et al., 2012b).

RF and VA EMG activity during paw shake appeared qualitatively similar while there were no changes in paw shake cycle duration after self-reinnervation (Fig. 4.6B). One explanation could involve compensation from remaining sources of sensory feedback in non-reinnervated muscles in order to maintain paw shake rhythm and phase of muscle activity. In a study by Koshland and Smith (1989), deafferentation of the entire hindlimb lead to a delay in VA activity onset and an increase in cycle duration during paw shake. Therefore, motion-dependent feedback appears to be important in organization of VA activity in paw shake task, however, the results of this study suggest length-velocity dependent feedback from Q-Sart is not required to mediate this organization. Additionally, fictive paw shake has been previously observed in the cat, indicating a substantial contribution of a CPG drive in paw shake activity. However, RF activity during fictive paw shake was not investigated (Pearson and Rossignol, 1991). Coordination between VA and RF during paw shake, however, appears to rely on length-velocity dependent feedback from Q-Sart, since this coordination was disrupted following self-reinnervation.

VA and RF share many heterogenic feedback pathways from group Ib and Ia afferents (Eccles et al., 1957a, Eccles and Lundberg, 1958, Nichols, 1994, Wilmink and Nichols, 2003, Ross and Nichols, 2009). It is unlikely that these changes are caused by changes in Ib force feedback as these afferents appear to be mostly unaffected by reinnervation (Lyle and Nichols, unpublished results).

Overall, mechanics of all tasks were well preserved and joint moment combinations within each phase did not change after self-reinnervation. On the other hand, significant changes in joint yield were found during stance phase at the knee and ankle joint across all walking conditions (Fig. 4.8). There was an increased yield at the knee joint along with a decreased yield at the ankle for all walking conditions. This effect is consistent with previous work which reveals a compensatory strategy after denervation of ankle extensors that seeks to preserve overall trajectories of limb length, limb orientation, and hip height in order to allow for a more symmetric gait (Maas et al., 2007, Chang et al., 2009). This would be expected if a lack of stretch reflex response from the Q-Sart muscles caused a decrease in activity; however, this is not a likely explanation due to an overall increase in RF and VA EMG activity in all conditions following reinnervation (Figs. 4.5 and 4.9). The total mass of quadriceps muscles before and after reinnervation was not significantly different, therefore a change in force production capability is also unlikely (Lyle and Nichols, unpublished results). There may be some difficulty in interpreting changes in EMG activity as previous studies have shown an increase in motor unit size after reinnervation (for review see Pantall et al., 2016). This may explain the overall increase in RF and VA EMG activity, however this was not directly tested. An alternative explanation could be that without length-velocity

dependent feedback, central drive is increased in order to prevent a drastic flexion of the knee. Indeed, there was a trend to increase average pre-contact activation magnitude in all conditions. However, these were only significant for level walking in RF and downslope and level walking for VA. Effects from other Ia heterogenic pathways onto VA and RF also cannot be discounted.

In this study, a strategy of coordination between RF and VA was revealed that was dependent on length-velocity dependent feedback, and where removal of this feedback lead to changes in joint kinematics. This finding may help to understand deficits which persist in some motor tasks even after recovery of motor function from self-reinnervation. There were also greater changes in burst duration of RF activity compared to VA after self-reinnervation, which provides additional evidence for a greater dependence of RF activity on length-velocity feedback compared to that of VA during walking tasks. Additional work is needed in order to understand the complex neural mechanisms involved in compensatory behavior.

CHAPTER V

SUMMARY

5.1 Characteristics of Coordination between One- and Two-Joint Muscles

In Aim 1, evidence was found, for the first time in freely moving cats, suggesting that the coordination between (relative force developed by) synergist one- and two-joint muscles can be influenced by mechanical interactions via intermuscular myofascial force transmission in pathological conditions leading to enhanced muscle lengths (Mehta et al., 2015). Limited effects of myofascial force transmission have been found previously in cat and rat ankle extensor muscles (Maas and Sandercock, 2008, Tijs et al., 2015), although the range of muscle lengths tested were restricted to those during normal physiological ranges of motion. Integrating effects of epimuscular myofascial force transmission when analyzing muscle function has been previously suggested (Huijing, 2003). This work shows that following selective muscle injuries which can lead to large shifts in relative lengths of synergist muscles, such as muscle paralysis, effects of myofascial force transmission should be taken into consideration when analyzing coordination between one- and two-joint synergist muscles. This mechanical pathway mediating interactions between the SO and GA is shown in Figure 5.1 by the dashed arrow GA and SO muscles. The direction of the arrow indicates the direction of myofascial force transmission which was tested; red crosses indicate interruption of transmission of neural signals to and from motoneurons caused by muscle denervation or self-reinnervation.

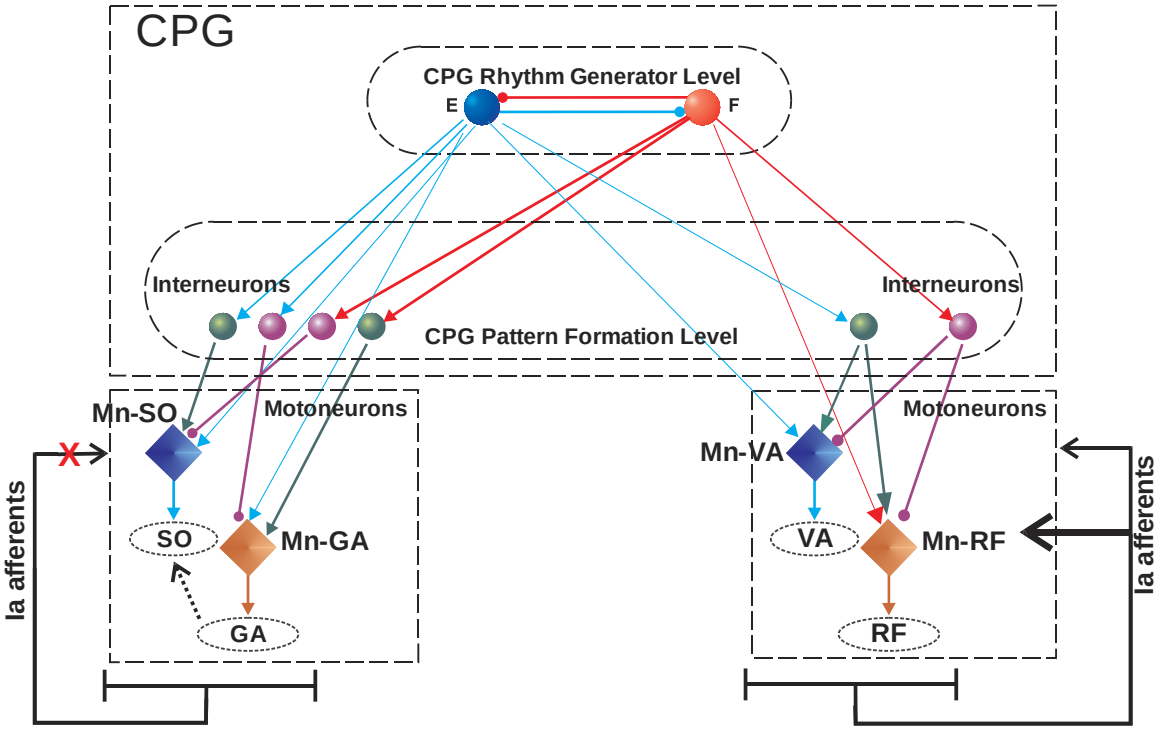

Figure 5.1. Summary of major findings for coordination between distal soleus and gastrocnemius (SO, GA) and proximal vastii and rectus femoris (VA, RF) one- and two-joint muscles. Neuronal populations E and F represent extensor and flexor half-centers of the CPG rhythm generator. The CPG pattern formation network consists of populations of interneurons that receive inputs from the rhythm generator and skin and muscle receptors (only Ia afferent pathways are shown for simplicity). The pattern formation level provides inputs to motoneurons (Mn). The thick solid black lines represent Ia afferent pathways from specific muscles to motoneurons directly or through interneurons of the pattern formation network. The black dotted line connecting GA with SO indicates the possible mechanical intermuscular pathway between SO and GA. Closed circles represent inhibitory connections while filled triangles represent excitatory ones. Red crosses indicate interruption of transmission of neural signals to and from motoneurons caused by muscle denervation or self-reinnervation**.** Note that the circuitry is simplified and is not inclusive of all possible descending and afferent pathways. Modified from Shevtsova et al. (2016). Evidence for intermuscular mechanical interactions was found after denervation of LG-SO and is indicated by the dashed arrow from the GA to SO muscle. Findings also suggest Ia afferents are not required for the coordination between GA and SO, shown by the red cross over this pathway. Finally, coordination between RF and VA does require Ia afferent feedback. This is indicated by solid arrows to the RF and VA box. Furthermore, the thicker arrow illustrates the greater dependence of this feedback for RF compared to VA.

In Aims 2 and 3, it was shown that coordination between one- and two-joint synergist muscles depended on the joint moment requirements of the task and on whether the muscles cross distal or proximal joints. This work is the first to show a consistent coordination strategy for selected one- and two-joint synergist muscle pairs of both the

distal and proximal lower limb segments. In both cases, the results revealed a significantly greater activation of two-joint muscles compared to their one-joint synergist muscle during joint moment combinations in which the two-joint muscle could contribute agonistically to the resultant moments at both joints it crosses (Figs. 3.11 and 4.7A). In contrast, one-joint muscles showed significantly greater activity compared to their two-joint synergist muscle during the joint combination in which the two-joint muscle produces an antagonistic action at one of the joints it crosses (Figs. 3.11 and 4.7A). These findings support and expand on earlier work in one- and two-joint muscle coordination, where activity and force predictions for two-joint muscles such as RF, GA, and hamstrings showed the greatest activity during tasks in which they could contribute agonistically at both joints for static and dynamic tasks (Prilutsky and Gregor, 1997, Prilutsky et al., 1998a, Prilutsky, 2000a, Prilutsky and Gregor, 2000). Therefore, this work supports the suggestion that the nervous system selects this coordination strategy in order to minimize muscle force/stress, perceived effort, mechanical and metabolic energy expenditure, as well as effort dependent neural noise (Anderson and Pandy, 2001, Prilutsky and Zatsiorsky, 2002, Haruno and Wolpert, 2005). Details on the possible mechanisms involved in this coordination are discussed in the next section.

5.2 Length-Velocity Dependent Feedback Contribution in Coordination between One- and Two-Joint Muscles

Aims 2 and 3 tested the effects of self-reinnervation and removal of length-velocity dependent feedback from distal (SO, GA) and proximal (VA, RF) muscles. This provided a unique opportunity to investigate whether there is a difference in contribution of this type of sensory feedback to coordination between proximal and distal, one- and

two-joint synergist muscle pairs. Changes in coordination between SO and GA (Aim 2) were determined by whether the EMG ratio was altered after muscle self-reinnervation or if the ratio was changed from below 1 to above 1 or vice versa. Results from Aim 2 suggest that the coordination between one-joint SO and two-joint MG is not determined by high movement speed nor mediated by length-velocity dependent (Ia) sensory feedback (Figs. 3.11 and 5.1). Changes in coordination between VA and RF (Aim 3) were determined by whether the EMG difference was changed from negative to positive or vice versa. In Aim 3, it was found that normal coordination between VA and RF was altered following loss of length-velocity dependent feedback from these muscles to motoneurons in all experimental tasks (Figs. 4.7A and 5.1), where the EMG difference changed from negative (or zero for upslope) to positive in all tasks for the required knee extension–hip flexion moment combination. This indicates that sensory information from length-velocity dependent afferents must be integrated with CPG input to motoneurons in order to achieve this coordination (Fig. 5.1). The combined findings from Aims 2 and 3 provide evidence for the difference in the influence of length-velocity dependent feedback on coordination between one- and two-joint synergist muscles, where coordination between proximal muscles is more influenced by length-velocity dependent feedback than the coordination between distal muscles (Fig. 5.1). Changes in burst duration in RF but not in stance/cycle duration suggest Ia feedback for RF may have access to the pattern formation level but does not directly influence the rhythm generator network of the CPG. It could still be possible, however, that any effects on the rhythm generator network with removal of length-velocity dependent feedback were compensated for by other sources of feedback or changes in descending drive to the CPG

after reinnervation of both proximal and distal muscles. In the coordination between SO and MG muscles, it appears likely that length-velocity dependent afferents do not have a major role in modulating CPG output to produce the coordination strategy found between these two muscles. One possibility is that in coordination between distal SO and MG, CPG input alone is able to produce this coordination without sensory feedback. This, however, does not seem likely as force-dependent feedback has been shown to be important in regulation of ankle extensor activity (Sinkjær et al., 2000, Donelan and Pearson, 2004). Therefore, other sources of feedback, excluding length-velocity dependent ones, are likely involved in organizing coordination between distal SO and MG through modulation of the CPG input. Differences in responses to reinnervation of distal and proximal muscles could also be caused by distribution of inter-joint feedback pathways. For example, there is evidence for inhibitory pathways from quadriceps to MG and excitatory pathways from VI to SO (Wilmink and Nichols, 2003). Finally, in both distal and proximal muscle coordination, it is likely that the CPG must play an integral role, although this was not tested in this work.

Results are in line with previous work which has shown that removal of stretch reflex mediated by Ia afferents in forelimb extensor muscles or hindlimb ankle extensor muscles in cats showed no deficits in locomotion mechanics during level and upslope walking but led to substantially increased yielding during downslope walking (Abelew et al., 2000, Maas et al., 2007, Livingston and Nichols, 2014). It is possible that a change in coordination between SO and MG may have been observed if downslope walking was analyzed, however analysis for Aim 2 was limited to stance phase of level walking only. It has also been found that removal of Ia feedback from ankle extensor muscles through

ischemic block caused no change in SO activity during mechanical unloading of ankle extensors (Sinkjær et al., 2000). The relatively modest effect of removal of length-velocity dependent sensory feedback from ankle extensors on movement mechanics and muscle activity is consistent with findings that the patterns of muscle nerve recordings from MG and SO during cat fictive locomotion (no motion-dependent feedback) were qualitatively similar to muscle activity patterns during normal overground locomotion (Markin et al., 2012b), suggesting a greater contribution of central CPG drive to regulating activity of these muscles during walking.

The difference found in the influence of length-velocity dependent feedback between the distal and proximal muscles (Aims 2 and 3) seems consistent with the hindlimb anatomy and design of distal and proximal muscles and their locations with respect to the joints. Proximal two-joint muscles tend to have longer muscle fascicle lengths with shorter tendons compared to distal muscles (Sacks and Roy, 1982, Ward et al., 2009). As a result, a larger portion of MTU length changes is taken up by muscle fascicles of the proximal muscles and, thus, by the muscle spindles embedded in parallel. Since distal muscles, like ankle extensors, have relatively shorter muscle fascicles and longer compliant tendons, the muscle spindles of these muscles might "see" less muscle fascicle length changes because their tendons take up more of the MTU length changes (Rack and Ross, 1984, Hoffer et al., 1989, Prilutsky et al., 1996b, Maas et al., 2009). In addition, proximal muscles as a rule have larger moment arms with respect to the joints as opposed to distal muscles (Goslow et al., 1973, MacFadden and Brown, 2010). This causes greater length changes in proximal muscles compared to distal ones at similar joint angular displacements. The above design features of limb muscles apparently

contribute to a greater proprioceptive sensitivity in proximal joints than in distal ones (Hall and McCloskey, 1983). Furthermore, length changes in muscles crossing the hip joint trigger phase transitions and entrain locomotor rhythm of CPG presumably via length-velocity dependent afferent pathways (Andersson and Grillner, 1983, Kriellaars et al., 1994, Lam and Pearson, 2001, McVea et al., 2005, Frigon et al., 2010).

It should be noted, however, that although length-velocity dependent sensory feedback from ankle extensors demonstrated a limited contribution to regulation of muscle activity during walking and paw shake responses, it must play a vital role in postural control during quiet standing (Eng and Hoffer, 1997) or in recovery of balance after postural perturbations (Torres-Oviedo et al., 2006). In this work, responses to perturbations were not investigated before and after reinnervation. Therefore, spindle receptors of distal muscles may require more rapid changes in length in order to elicit a motor response, especially during locomotion. This work does not imply that velocity-length dependent feedback is not important for distal muscles, as local regulation of muscle stiffness and joint coupling is an important result of this feedback pathway (Nichols, 1999). Additionally, the density of muscle spindles in distal SO (22.5 per gram of muscle mass) is much higher than in proximal RF (12.5/g) (Kokkorogiannis, 2004), suggesting a potentially greater role of SO in sensing muscle fascicle length. On the other hand, although the density of muscle spindles may be a functionally important characteristic of muscle sensory function, Banks (2006) has argued that a better measure of relative spindle abundance in muscles is the residual value in the relationship: natural logarithm of spindle number versus natural logarithm of muscle mass, which is independent of muscle mass. According to this measure, distal and proximal muscles in

the hindlimb have the same spindle abundance, whereas axial muscles and especially those concerned with head position have significantly greater residual values.

Others have proposed a gradient of feedback dependence throughout the leg where proximal muscles are driven primarily by feed-forward control while distal muscles are regulated through proprioceptive feedback (Daley et al., 2007). Although this control strategy may be useful in order to make rapid responses to perturbations, it is unclear whether the same strategy applies to unperturbed voluntary tasks or steady-state locomotion. Daley et al. (2007) attributed this strategy to an increased gain of proprioceptive feedback in load-sensitive receptors of distal muscles and therefore the effect of length-velocity dependent afferents was not explored by them. In fact, it has been shown in humans that reflex gains of Ia afferent pathways in distal ankle extensors are decreased when transitioning from standing to walking, and walking to running (Capaday and Stein, 1986, 1987, Stein and Capaday, 1988); see also the discussion above about possible role of length-velocity dependent afferent input to CPG. It should be noted that although H-reflex does not test the stretch reflex, relative changes in H-reflex can still provide information about the changes in excitability of the motoneuron pool. Testing stretch reflex during human walking by sudden dorsiflexion of the ankle in stance demonstrates independence of stretch reflex on speed of walking from 3 to 4 km/h, however soleus fascicle stretch velocity decreased with increasing speed (Cronin et al., 2009). When the same group conducted these experiments with sudden ankle unloading, they concluded that their “results are consistent with the idea that force-related afferent feedback contributes both to the background locomotor activity and to the medium latency stretch reflex. In contrast, length-related afferent feedback may contribute to only

the medium latency stretch reflex" (af Klint et al., 2010, p. 2747). Since self-reinnervation removes the short-latency stretch reflex, the latter results seem consistent with the finding in Aim 2 of limited effects of stretch reflex to level walking and paw shake response.

Computational models of neuromechanical systems can provide additional insight into functions of the neural circuitries in the spinal cord. Recently, neuromechanical control models of the cat hindlimbs have shown to reproduce hindlimb mechanics and muscle activity of fictive and real cat locomotion (McCrea and Rybak, 2008, Markin et al., 2016, Shevtsova et al., 2016). These models incorporate a CPG contained within the spinal cord, consisting of two half-center neuron oscillators for each limb, which generates flexor and extensor phases of activity (first suggested by Brown (1911)). Although the CPG allows an animal to produce locomotor-like activity without input from the brain and sensory feedback (Brown, 1911, Grillner, 2006, McCrea and Rybak, 2008), the models incorporate both of these inputs to modulate motoneuron activity. In agreement with experimental findings, simulations using this model have shown that removal of input from Ia afferents of ankle extensor muscles does not affect stable locomotion (Markin et al., 2016). However, the role of sensory input from proximal muscles has not been fully explored.

5.3 Clinical Implications

As has been suggested in previous studies and in Aim 1, intermuscular mechanical interactions between synergist muscles may act as a safety net following injury (Maas and Sandercock, 2010). Specifically, during muscle paralysis, the affected

muscle is much more prone to atrophy (Edgerton et al., 2002, Bodine, 2013). Although additional studies would be needed, it may be possible to take advantage of myofascial force transmission between intact and injured muscle in order to treat this type of injury. It has been shown that repetitive stretch-shortening cycles of the muscle can significantly reduce the extent of atrophy (Roy et al., 1998, Martineau and Gardiner, 2001, Bassel-Duby and Olson, 2006, Agata et al., 2009); thus during recovery of paralyzed muscles, patients may be encouraged to perform specific tasks which activate intact synergist muscles and enhance length changes in the paralyzed synergist.

Based on results of Aims 2 and 3, it is clear that coordination between one- and two-joint muscles depends on the joint moment requirements. This finding may also be beneficial when there is a need to preferentially activate a specific muscle. Additionally, if there is a need to limit the activity of an individual muscle, one can again take advantage of the fact that coordination between one- and two-joint muscles depends on a combination of moments at the specific joint.

Muscle length-velocity dependent feedback had a differential effect on coordination strategy for the distal and proximal muscle pairs explored in this work (Fig. 3.11 versus Fig. 4.7 A,D). Since there was a limited effect of length-velocity dependent feedback on coordination between one- and two-joint distal ankle extensor muscles, rehabilitation strategies following ankle extensor nerve injury may be able to concentrate on the recovery of motor function rather than on the recovery of stretch reflex, although it is needed for postural control. On the other hand, an injury affecting sensory feedback of the quadriceps should call for a rehabilitation strategy and treatment which focuses on both motor and sensory function. Furthermore, injuries affecting proximal two-joint

muscles, such as RF, may require additional attention compared to injuries affecting only one-joint muscles.

Previous studies have found that there were little differences in kinematics 12 weeks after self-reinnervation of cat ankle and elbow extensors except for downslope walking (Abelew et al., 2000, Maas et al., 2007, Livingston and Nichols, 2014, Pantall et al., 2016). After 12-16 weeks following reinnervation of quadriceps and sartorius, however, this study found that even though motor activity was restored, an increased knee flexion (or yield) for all walking conditions remained (Fig. 4.9). Therefore, findings from this work can help predict the extent of deficits, if any, one would expect after specific levels of injury.

5.4 Future Directions

Many aspects of this work warrants further investigation. All analyses were performed for sagittal joint mechanics and muscles, which primarily cause movement in the sagittal plane. It would be of interest to investigate whether muscles that have their primary action in the frontal plane and contribute to lateral stability, follow the same strategy of coordination between one- and two-joint synergist muscles and demonstrate similar differences in length-velocity dependent feedback actions between distal and proximal muscles. Furthermore, investigation of additional pairs of proximal and distal synergists that function primarily in the sagittal plane can increase the robustness of the proposed differences in feedback actions.

For this dissertation, the role of Ib force-dependent feedback could not be investigated and therefore can be addressed in future work. The Ib afferent pathways are

also widely distributed within the lower limb (Eccles et al., 1957a, Nichols, 1994, Nichols, 1999, Wilmink and Nichols, 2003) and are likely to play a role in coordination between one- and two-joint muscles. Force-dependent feedback has also been shown to be important in regulation of hindlimb extensor activity in cats (Conway et al., 1987, Gossard et al., 1994, Donelan and Pearson, 2004, Ross and Nichols, 2009) and humans (af Klint et al., 2010). It would therefore be of interest to assess whether there are differing influences of Ia length-velocity and Ib force-feedback on coordination between proximal and distal muscle pairs.

5.5 Conclusion

In this dissertation I present evidence for the difference in the length-velocity dependent feedback influences on the coordination between one- and two-joint muscles during unperturbed tasks in humans and cats. The main findings of this work are summarized in Figure 5.1. Under normal conditions, coordination between one- and two-joint muscles depended on the task requirements, quantified by the combination of resultant muscle moments at adjacent joints. This coordination is likely achieved by an integration of sensory feedback and CPG feedforward input through interneurons (Fig. 5.1). Specifically, motoneurons of each two-joint muscle receive input from both extensor and flexor half-centers of the CPG rhythm generator. This ensures that activation of two-joint muscles is higher than that of their one-joint synergists when the motor task requires the resultant moments at the adjacent joints to which the two-joint muscle can contribute as an agonist. Further investigation revealed that coordination between proximal one- and two-joint VA and RF is partly mediated by length-velocity

dependent feedback, while in distal SO and MG, coordination did not rely on movement speed and was not affected by removal of length-velocity dependent feedback to motoneurons. Additionally, under pathological conditions, it may be necessary to consider mechanical intermuscular interactions on one- and two-joint muscle coordination.

Findings presented in this work expand on understanding the role of mechanical interactions, sensory feedback and CPG control in the coordination between one- and two-joint muscles. These findings have potential implications for developing targeted rehabilitation strategies/treatment and implementation of new control paradigms for robotics and prosthetics to improve movement efficiency.

REFERENCES

Abelew TA, Miller MD, Cope TC, Nichols TR (2000) Local loss of proprioception results in disruption of interjoint coordination during locomotion in the cat. Journal of neurophysiology 84:2709-2714.

Abraham LD, Loeb GE (1985) The distal hindlimb musculature of the cat. Patterns of normal use. Exp Brain Res 58:583-593.

af Klint R, Mazzaro N, Nielsen JB, Sinkjaer T, Grey MJ (2010) Load rather than length sensitive feedback contributes to soleus muscle activity during human treadmill walking. J Neurophysiol 103:2747-2756.

Agata N, Sasai N, Inoue-Miyazu M, Kawakami K, Hayakawa K, Kobayashi K, Sokabe M (2009) Repetitive stretch suppresses denervation-induced atrophy of soleus muscle in rats. Muscle & nerve 39:456-462.

Alvarez FJ, Titus-Mitchell HE, Bullinger KL, Kraszpulski M, Nardelli P, Cope TC (2011) Permanent central synaptic disconnection of proprioceptors after nerve injury and regeneration. I. Loss of VGLUT1/IA synapses on motoneurons. J Neurophysiol 106:2450-2470.

Anderson FC, Pandy MG (2001) Static and dynamic optimization solutions for gait are practically equivalent. J Biomech 34:153-161.

Andersson O, Grillner S (1983) Peripheral control of the cat's step cycle. Acta physiologica Scandinavica 118:229-239.

Andrews JG, Hay JG (1983) Biomechanical considerations in the modeling of muscle function. Acta Morphol Neerl Scand 21:199-223.

Ariano MA, Armstrong RB, Edgerton VR (1973) Hindlimb muscle fiber populations of five mammals. J Histochem Cytochem 21:51-55.

Ballantyne B, Kukulka C, Soderberg G (1993) Motor unit recruitment in human medial gastrocnemius muscle during combined knee flexion and plantarflexion isometric contractions. Experimental brain research 93:492-498.

Banks RW (2006) An allometric analysis of the number of muscle spindles in mammalian skeletal muscles. J Anat 208:753-768.

Bassel-Duby R, Olson EN (2006) Signaling pathways in skeletal muscle remodeling. Annu Rev Biochem 75:19-37.

Benjamin M, Kaiser E, Milz S (2008) Structure-function relationships in tendons: a review. J Anat 212:211-228.

Bennell KL, Wrigley TV, Hunt MA, Lim BW, Hinman RS (2013) Update on the role of muscle in the genesis and management of knee osteoarthritis. Rheumatic diseases clinics of North America 39:145-176.

Bernabei M, Dieën J, Maas H (2016) Altered mechanical interaction between rat plantar flexors due to changes in intermuscular connectivity. Scandinavian Journal of Medicine & Science in Sports.

Bernstein N (1967) The Coordination and Regulation of Movements. New York: Pergamon Press.

Biewener AA, Konieczynski DD, Baudinette RV (1998) In vivo muscle force-length behavior during steady-speed hopping in tammar wallabies. J Exp Biol 201:1681-1694.

Blake OM, Champoux Y, Wakeling JM (2012) Muscle coordination patterns for efficient cycling. Med Sci Sports Exerc 44:926-938.

Bobbert MF, Huijing PA, van Ingen Schenau GJ (1986) An estimation of power output and work done by the human triceps surae muscle-tendon complex in jumping. J Biomech 19:899-906.

Bobbert MF, van Ingen Schenau GJ (1988) Coordination in vertical jumping. J Biomech 21:249-262.

Bodine SC (2013) Disuse-induced muscle wasting. The international journal of biochemistry & cell biology 45:2200-2208.

Bottasso CL, Prilutsky BI, Croce A, Imberti E, Sartirana S (2006) A numerical procedure for inferring from experimental data the optimization cost functions using a multibody model of the neuro-musculoskeletal system. Multibody System Dynamics 16:123-154.

Brown J, Wickham J, McAndrew D, Huang X-F (2007) Muscles within muscles: coordination of 19 muscle segments within three shoulder muscles during isometric motor tasks. Journal of Electromyography and Kinesiology 17:57-73.

Brown TG (1911) The intrinsic factors in the act of progression in the mammal. Proceedings of the Royal Society of London Series B, containing papers of a biological character 84:308-319.

Bullinger KL, Nardelli P, Pinter MJ, Alvarez FJ, Cope TC (2011) Permanent central synaptic disconnection of proprioceptors after nerve injury and regeneration. II. Loss of functional connectivity with motoneurons. J Neurophysiol 106:2471-2485.

Capaday C, Stein R (1986) Amplitude modulation of the soleus H-reflex in the human during walking and standing. The Journal of Neuroscience 6:1308-1313.

Capaday C, Stein R (1987) Difference in the amplitude of the human soleus H reflex during walking and running. The Journal of physiology 392:513-522.

Cappellini G, Ivanenko YP, Poppele RE, Lacquaniti F (2006) Motor patterns in human walking and running. J Neurophysiol 95:3426-3437.

Carrasco DI, English AW (1999) Mechanical actions of compartments of the cat hamstring muscle, biceps femoris. Prog Brain Res 123:397-403.

Chanaud CM, Macpherson JM (1991) Functionally complex muscles of the cat hindlimb. III. Differential activation within biceps femoris during postural perturbations. Exp Brain Res 85:271-280.

Chang Y-H, Auyang AG, Scholz JP, Nichols TR (2009) Whole limb kinematics are preferentially conserved over individual joint kinematics after peripheral nerve injury. J Exp Biol 212:3511-3521.

Clark BB, Jaffe D, Henn RF, 3rd, Lovering RM (2011) Evaluation and imaging of an untreated grade III hamstring tear: a case report. Clinical orthopaedics and related research 469:3248-3252.

Conway B, Hultborn H, Kiehn O (1987) Proprioceptive input resets central locomotor rhythm in the spinal cat. Experimental Brain Research 68:643-656.

Cope TC, Bonasera SJ, Nichols TR (1994) Reinnervated muscles fail to produce stretch reflexes. J Neurophysiol 71:817-820.

Cope TC, Clark BD (1993) Motor-unit recruitment in self-reinnervated muscle. J Neurophysiol 70:1787-1796.

Cronin NJ, Ishikawa M, Grey MJ, af Klint R, Komi PV, Avela J, Sinkjaer T, Voigt M (2009) Mechanical and neural stretch responses of the human soleus muscle at different walking speeds. J Physiol 587:3375-3382.

Cronin NJ, Prilutsky BI, Lichtwark GA, Maas H (2013) Does ankle joint power reflect type of muscle action of soleus and gastrocnemius during walking in cats and humans? J Biomech 46:1383-1386.

Crowninshield RD, Brand RA (1981) A physiologically based criterion of muscle force prediction in locomotion. J Biomech 14:793-801.

Cutts A, Alexander RM, Ker RF (1991) Ratios of cross-sectional areas of muscles and their tendons in a healthy human forearm. J Anat 176:133-137.

Daley MA, Felix G, Biewener AA (2007) Running stability is enhanced by a proximo-distal gradient in joint neuromechanical control. Journal of Experimental Biology 210:383-394.

de Looze MP, Toussaint HM, van Dieen JH, Kemper HC (1993) Joint moments and muscle activity in the lower extremities and lower back in lifting and lowering tasks. J Biomech 26:1067-1076.

Donelan JM, Pearson KG (2004) Contribution of force feedback to ankle extensor activity in decerebrate walking cats. Journal of Neurophysiology 92:2093-2104.

Eccles J, Eccles RM, Lundberg A (1957a) Synaptic actions on motoneurones caused by impulses in Golgi tendon organ afferents. The Journal of Physiology 138:227-252.

Eccles JC, Eccles RM, Iggo A, Ito M (1961) Distribution of recurrent inhibition among motoneurones. The Journal of Physiology 159:479-499.

Eccles JC, Eccles RM, Lundberg A (1957b) The convergence of monosynaptic excitatory afferents on to many different species of alpha motoneurones. J Physiol 137:22-50.

Eccles RM, Lundberg A (1958) Integrative pattern of Ia synaptic actions on motoneurones of hip and knee muscles. The Journal of physiology 144:271.

Edgerton VR, Roy RR, Allen DL, Monti RJ (2002) Adaptations in skeletal muscle disuse or decreased-use atrophy. American journal of physical medicine & rehabilitation 81:S127-S147.

Eng JJ, Hoffer J (1997) Regional variability of stretch reflex amplitude in the cat medial gastrocnemius muscle during a postural task. Journal of neurophysiology 78:1150-1154.

English AW (1984) An electromyographic analysis of compartments in cat lateral gastrocnemius muscle during unrestrained locomotion. J Neurophysiol 52:114-125.

English AW (2005) Enhancing axon regeneration in peripheral nerves also increases functionally inappropriate reinnervation of targets. The Journal of comparative neurology 490:427-441.

English AW, Letbetter WD (1982) A histochemical analysis of identified compartments of cat lateral gastrocnemius muscle. Anat Rec 204:123-130.

Fowler EG, Gregor RJ, Hodgson JA, Roy RR (1993) Relationship between ankle muscle and joint kinetics during the stance phase of locomotion in the cat. J Biomech 26:465-483.

Fowler EG, Gregor RJ, Roy RR (1988) Differential kinetics of fast and slow ankle extensors during the paw-shake in the cat. Exp Neurol 99:219-224.

Friedman WA, Sypert GW, Munson JB, Fleshman JW (1981) Recurrent inhibition in type-identified motoneurons. J Neurophysiol 46:1349-1359.

Frigon A, Sirois J, Gossard J-P (2010) Effects of ankle and hip muscle afferent inputs on rhythm generation during fictive locomotion. Journal of neurophysiology 103:1591-1605.

Gans C, Gaunt AS (1991) Muscle architecture in relation to function. J Biomech 24 Suppl 1:53-65.

Garfin SR, Tipton CM, Mubarak SJ, Woo SL, Hargens AR, Akeson WH (1981) Role of fascia in maintenance of muscle tension and pressure. J Appl Physiol 51:317-320.

Gordon T, Stein RB (1982) Time course and extent of recovery in reinnervated motor units of cat triceps surae muscles. The Journal of Physiology 323:307-323.

Goslow GE, Reinking RM, Stuart DG (1973) The cat step cycle: hind limb joint angles and muscle lengths during unrestrained locomotion. Journal of Morphology 141:1-41.

Gossard JP, Brownstone RM, Barajon I, Hultborn H (1994) Transmission in a locomotor-related group Ib pathway from hindlimb extensor muscles in the cat. Experimental Brain Research 98:213-228.

Gregor RJ, Prilutsky BI, Nichols TR, Smith W (2003) EMG output in reinnervated medial gastrocnemius muscle during locomotion in the cat. Program No 493.8. In: 2003 Neuroscience Meeting Planner New Orleans, LA: Society for Neuroscience. Online.

Gregor RJ, Smith DW, Prilutsky BI (2006) Mechanics of slope walking in the cat: quantification of muscle load, length change, and ankle extensor EMG patterns. Journal of neurophysiology 95:1397-1409.

Grillner S (2006) Biological pattern generation: the cellular and computational logic of networks in motion. Neuron 52:751-766.

Haftel VK, Prather JF, Heckman CJ, Cope TC (2001) Recruitment of cat motoneurons in the absence of homonymous afferent feedback. J Neurophysiol 86:616-628.

Hall LA, McCloskey D (1983) Detections of movements imposed on finger, elbow and shoulder joints. The journal of physiology 335:519.

Harris CM, Wolpert DM (1998) Signal-dependent noise determines motor planning. Nature 394:780-784.

Haruno M, Wolpert DM (2005) Optimal control of redundant muscles in step-tracking wrist movements. Journal of Neurophysiology 94:4244-4255.

Herbert RD, Heroux ME, Diong J, Bilston LE, Gandevia SC, Lichtwark GA (2015) Changes in the length and three-dimensional orientation of muscle fascicles and aponeuroses with passive length changes in human gastrocnemius muscles. J Physiol 593:441-455.

Herzog W, Leonard TR, Renaud JM, Wallace J, Chaki G, Bornemisza S (1992) Force-length properties and functional demands of cat gastrocnemius, soleus and plantaris muscles. J Biomech 25:1329-1335.

Hodson-Tole EF, Pantall AL, Maas H, Farrell BJ, Gregor RJ, Prilutsky BI (2012) Task dependent activity of motor unit populations in feline ankle extensor muscles. J Exp Biol 215:3711-3722.

Hoffer J, Caputi A, Pose I, Griffiths R (1989) Roles of muscle activity and load on the relationship between muscle spindle length and whole muscle length in the freely walking cat. Progress in brain research 80:75-85.

Holt NC, Wakeling JM, Biewener AA (2014) The effect of fast and slow motor unit activation on whole-muscle mechanical performance: the size principle may not pose a mechanical paradox. Proceedings Biological sciences / The Royal Society 281:20140002.

Hoy M, Zernicke R, Smith J (1985) Contrasting roles of inertial and muscle moments at knee and ankle during paw-shake response. Journal of neurophysiology 54:1282-1294.

Hoy MG, Zernicke RF (1985) Modulation of limb dynamics in the swing phase of locomotion. J Biomech 18:49-60.

Hoy MG, Zernicke RF (1986) The role of intersegmental dynamics during rapid limb oscillations. J Biomech 19:867-877.

Huijing PA (2003) Muscular force transmission necessitates a multilevel integrative approach to the analysis of function of skeletal muscle. Exercise and sport sciences reviews 31:167-175.

Huijing PA (2009) Epimuscular myofascial force transmission: a historical review and implications for new research. International Society of Biomechanics Muybridge Award Lecture, Taipei, 2007. J Biomech 42:9-21.

Huijing PA, Baan GC (2003) Myofascial force transmission: muscle relative position and length determine agonist and synergist muscle force. Journal of Applied Physiology 94:1092-1107.

Huijing PA, Yaman A, Ozturk C, Yucesoy CA (2011) Effects of knee joint angle on global and local strains within human triceps surae muscle: MRI analysis indicating in vivo myofascial force transmission between synergistic muscles. Surgical and radiologic anatomy 33:869-879.

Hultborn H, Katz R, Mackel R (1988a) Distribution of recurrent inhibition within a motor nucleus. II. Amount of recurrent inhibition in motoneurones to fast and slow units. Acta Physiol Scand 134:363-374.

Hultborn H, Lipski J, Mackel R, Wigstrom H (1988b) Distribution of recurrent inhibition within a motor nucleus. I. Contribution from slow and fast motor units to the excitation of Renshaw cells. Acta Physiol Scand 134:347-361.

Jacobs R, Bobbert MF, van Ingen Schenau GJ (1996) Mechanical output from individual muscles during explosive leg extensions: the role of biarticular muscles. J Biomech 29:513-523.

Jacobs R, Macpherson JM (1996) Two functional muscle groupings during postural equilibrium tasks in standing cats. J Neurophysiol 76:2402-2411.

Jacobs R, van Ingen Schenau GJ (1992) Control of an external force in leg extensions in humans. J Physiol 457:611-626.

Johnson MA, Polgar J, Weightman D, Appleton D (1973) Data on the distribution of fibre types in thirty-six human muscles. An autopsy study. Journal of the neurological sciences 18:111-129.

Kaya M, Leonard T, Herzog W (2003) Coordination of medial gastrocnemius and soleus forces during cat locomotion. J Exp Biol 206:3645-3655.

Klishko AN, Cofer D, Cymbalyuk G, Gregor RJ, Edwards DH, Prilutsky BI (2011) Contributions of proprioceptive feedback and CPG to coordination of two-joint muscles during a paw shake response: A computer simulation study. In: Program No 92010 Society for Neuroscience Washington, DC: Society for Neuroscience, 2011. Online.

Kokkorogiannis T (2004) Somatic and intramuscular distribution of muscle spindles and their relation to muscular angiotypes. J Theor Biol 229:263-280.

Koshland G, Smith J (1989) Mutable and immutable features of paw-shake responses after hindlimb deafferentation in the cat. Journal of neurophysiology 62:162-173.

Kriellaars DJ, Brownstone RM, Noga BR, Jordan LM (1994) Mechanical entrainment of fictive locomotion in the decerebrate cat. Journal of Neurophysiology 71:2074-2086.

Kurokawa S, Fukunaga T, Fukashiro S (2001) Behavior of fascicles and tendinous structures of human gastrocnemius during vertical jumping. Journal of Applied Physiology 90:1349-1358.

LaBella LA, Kehler JP, McCrea DA (1989) A differential synaptic input to the motor nuclei of triceps surae from the caudal and lateral cutaneous sural nerves. J Neurophysiol 61:291-301.

Lam T, Pearson KG (2001) Proprioceptive modulation of hip flexor activity during the swing phase of locomotion in decerebrate cats. Journal of Neurophysiology 86:1321-1332.

Lam T, Pearson KG (2002) The role of proprioceptive feedback in the regulation and adaptation of locomotor activity. In: Sensorimotor Control of Movement and Posture, pp 343-355: Springer.

Lauber B, Lichtwark GA, Cresswell AG (2014) Reciprocal activation of gastrocnemius and soleus motor units is associated with fascicle length change during knee flexion. Physiological reports 2.

Lawrence JH, 3rd, Nichols TR, English AW (1993) Cat hindlimb muscles exert substantial torques outside the sagittal plane. J Neurophysiol 69:282-285.

Lindsay AD, Binder MD (1991) Distribution of effective synaptic currents underlying recurrent inhibition in cat triceps surae motoneurons. J Neurophysiol 65:168-177.

Livingston BP, Nichols TR (2014) Effects of Reinnervation of the Biarticular Shoulder-Elbow Muscles on Joint Kinematics and Electromyographic Patterns of the Feline Forelimb during Downslope Walking. Cells Tissues Organs 199:423-440.

Loeb GE (1985) Motoneurone task groups: coping with kinematic heterogeneity. J Exp Biol 115:137-146.

Loeb GE (1999) Asymmetry of hindlimb muscle activity and cutaneous reflexes after tendon transfers in kittens. J Neurophysiol 82:3392-3405.

Loeb GE, Pratt CA, Chanaud CM, Richmond FJR (1987) Distribution and Innervation of Short, Interdigitated Muscle Fibers in Parallel-Fibered Muscles of the Cat Hindlimb. Journal of Morphology 191:1-15.

Maas H, Baan GC, Huijing PA (2004) Muscle force is determined also by muscle relative position: isolated effects. J Biomech 37:99-110.

Maas H, Gregor RJ, Hodson-Tole EF, Farrell BJ, English AW, Prilutsky BI (2010) Locomotor changes in length and EMG activity of feline medial gastrocnemius muscle following paralysis of two synergists. Experimental brain research 203:681-692.

Maas H, Gregor RJ, Hodson-Tole EF, Farrell BJ, Prilutsky BI (2009) Distinct muscle fascicle length changes in feline medial gastrocnemius and soleus muscles during slope walking. Journal of Applied Physiology 106:1169-1180.

Maas H, Lyle MA, Kajtaz E, Nichols TR (2015) Preservation of reflex pathways following muscle adaptations accompanying tendon transfer. In: Annual Meeting of Society for Neuroscience Program # 15709 Chicago, IL.

Maas H, Prilutsky BI, Nichols TR, Gregor RJ (2007) The effects of self-reinnervation of cat medial and lateral gastrocnemius muscles on hindlimb kinematics in slope walking. Experimental brain research 181:377-393.

Maas H, Sandercock TG (2008) Are skeletal muscles independent actuators? Force transmission from soleus muscle in the cat. Journal of Applied Physiology 104:1557-1567.

Maas H, Sandercock TG (2010) Force Transmission between Synergistic Skeletal Muscles through Connective Tissue Linkages. Journal of Biomedicine and Biotechnology 2010.

MacFadden LN, Brown NA (2010) The influence of modeling separate neuromuscular compartments on the force and moment generating capacities of muscles of the feline hindlimb. Journal of biomechanical engineering 132:081003.

Markin SN, Klishko AN, Shevtsova NA, Lemay MA, Prilutsky BI, Rybak IA (2012a) A neuromechanical computational model of spinal control of locomotion. In: Twenty First Annual Computational Neuroscience Meeting: CNS 2012, vol. 13(Suppl 1), p 48 Atlanta/Decatur, GA: BioMed Central Ltd.

Markin SN, Klishko AN, Shevtsova NA, Lemay MA, Prilutsky BI, Rybak IA (2016) A neuromechanical model of spinal control of locomotion. In: Neuromechanical Modeling of Posture and Locomotion, pp 21-65: Springer.

Markin SN, Lemay MA, Prilutsky BI, Rybak IA (2012b) Motoneuronal and muscle synergies involved in cat hindlimb control during fictive and real locomotion: a comparison study. Journal of neurophysiology 107:2057-2071.

Martineau LC, Gardiner PF (2001) Insight into skeletal muscle mechanotransduction: MAPK activation is quantitatively related to tension. Journal of Applied Physiology 91:693-702.

McCrea DA, Rybak IA (2008) Organization of mammalian locomotor rhythm and pattern generation. Brain research reviews 57:134-146.

McVea DA, Donelan JM, Tachibana A, Pearson KG (2005) A role for hip position in initiating the swing-to-stance transition in walking cats. Journal of neurophysiology 94:3497-3508.

Mehta R, Kajtaz E, Gregor RJ, Prilutsky BI (2014) Effects of stretch-reflex removal by self-reinnervation of one-joint vastii and two-joint rectus femoris on hindlimb muscle activity and mechanics during walking in the cat. In: Society for Neuroscience Washington, DC.

Mehta R, Maas H, Gregor RJ, Prilutsky BI (2015) Unexpected Fascicle Length Changes In Denervated Feline Soleus Muscle During Stance Phase Of Walking. Scientific Reports 5:17619.

Mehta R, Prilutsky BI (2012) Coordination of activity between one-joint, slow soleus and two-joint, fast gastrocnemius muscles. In: Annual Meeting of the Biomedical Engineering Society Atlanta, GA.

Mehta R, Prilutsky BI (2014) Task-dependent inhibition of slow-twitch soleus and excitation of fast-twitch gastrocnemius do not require high movement speed and velocity-dependent sensory feedback. Frontiers in Physiology 5:410.

Meyers RA, Hermanson JW (2006) Horse soleus muscle: postural sensor or vestigial structure? The anatomical record Part A, Discoveries in molecular, cellular, and evolutionary biology 288:1068-1076.

Muraoka T, Muramatsu T, Takeshita D, Kawakami Y, Fukunaga T (2002) Length change of human gastrocnemius aponeurosis and tendon during passive joint motion. Cells Tissues Organs 171:260-268.

Neptune RR, Sasaki K (2005) Ankle plantar flexor force production is an important determinant of the preferred walk-to-run transition speed. J Exp Biol 208:799-808.

Nichols TR (1994) A Biomechanical Perspective on Spinal Mechanisms of Coordinated Muscular Action: An Architecture Principle. Cells Tissues Organs 151:1-1.

Nichols TR (1999) Receptor Mechanisms Underlying Heterogenic Reflexes Among the Triceps Surae Muscles of the Cat. J Neurophysiol 81:467-478.

O'Donovan MJ, Pinter MJ, Dum RP, Burke RE (1985) Kinesiological studies of self- and cross-reinnervated FDL and soleus muscles in freely moving cats. J Neurophysiol 54:852-866.

Otten E (1988) Concepts and models of functional architecture in skeletal muscle. Exercise and sport sciences reviews 16:89-137.

Pandy MG, Zajac FE (1991) Optimal muscular coordination strategies for jumping. J Biomech 24:1-10.

Pantall A, Hodson-Tole EF, Gregor RJ, Prilutsky BI (2012) Changes in relative activity of faster and slower motor unit populations in feline ankle extensors during locomotion following self-reinnervation. Program No. 478.20 In: 2012 Neuroscience Meeting Planner New Orleans, LA Society for Neuroscience. Online.

Pantall A, Hodson-Tole EF, Gregor RJ, Prilutsky BI (2016) Increased intensity and reduced frequency of EMG signals from feline self-reinnervated ankle extensors during walking do not normalize excessive lengthening. J Neurophysiol in press.

Pearson KG, Fouad K, Misiaszek J (1999) Adaptive changes in motor activity associated with functional recovery following muscle denervation in walking cats. Journal of neurophysiology 82:370-381.

Pearson KG (1995) Proprioceptive regulation of locomotion. Current Opinion in Neurobiology 5:786-791.

Pearson KG, Misiaszek JE (2000) Use-dependent gain change in the reflex contribution to extensor activity in walking cats. Brain Res 883:131-134.

Pearson KG, Rossignol S (1991) Fictive motor patterns in chronic spinal cats. Journal of neurophysiology 66:1874-1887.

Perret C, Cabelguen J-M (1980) Main characteristics of the hindlimb locomotor cycle in the decorticate cat with special reference to bifunctional muscles. Brain Research 187:333-352.

Prilutsky BI (2000a) Coordination of two- and one-joint muscles: functional consequences and implications for motor control. Motor Control 4:1-44.

Prilutsky BI (2000b) Muscle coordination: the discussion continues. Motor Control 4:97-116.

Prilutsky BI, Gregor RJ (1997) Strategy of coordination of two- and one-joint leg muscles in controlling an external force. Motor Control 1:92-116.

Prilutsky BI, Gregor RJ (2000) Analysis of muscle coordination strategies in cycling. IEEE transactions on rehabilitation engineering : a publication of the IEEE Engineering in Medicine and Biology Society 8:362-370.

Prilutsky BI, Gregor RJ (2001) Swing- and support-related muscle actions differentially trigger human walk-run and run-walk transitions. J Exp Biol 204:2277-2287.

Prilutsky BI, Gregor RJ, Nichols TR (2004) Coordination of cat ankle extensors during the paw-shake before and after self-reinnervation of medial and lateral gastrocnemius muscles. Program No. 69.12. In: 2004 Neuroscience Meeting Planner San Diego, CA: Society for Neuroscience. Online.

Prilutsky BI, Gregor RJ, Ryan MM (1998a) Coordination of two-joint rectus femoris and hamstrings during the swing phase of human walking and running. Experimental Brain Research 120:479-486.

Prilutsky BI, Herzog W, Allinger TL (1996a) Mechanical power and work of cat soleus, gastrocnemius and plantaris muscles during locomotion: possible functional significance of muscle design and force patterns. Journal of Experimental Biology 199 (Pt 4):801-814.

Prilutsky BI, Herzog Wl, Leonard TR, Allinger TL (1996b) Role of the muscle belly and tendon of soleus, gastrocnemius, and plantaris in mechanical energy absorption and generation during cat locomotion. J Biomech 29:417-434.

Prilutsky BI, Isaka T, Albrecht AM, Gregor RJ (1998b) Is coordination of two-joint leg muscles during load lifting consistent with the strategy of minimum fatigue? J Biomech 31:1025-1034.

Prilutsky BI, Maas H, Bulgakova M, Hodson-Tole EF, Gregor RJ (2011) Short-term motor compensations to denervation of feline soleus and lateral gastrocnemius result in preservation of ankle mechanical output during locomotion. Cells Tissues Organs 193:310-324.

Prilutsky BI, Sirota MG, Gregor RJ, Beloozerova IN (2005) Quantification of motor cortex activity and full-body biomechanics during unconstrained locomotion. J Neurophysiol 94:2959-2969.

Prilutsky BI, Zatsiorsky VM (2002) Optimization-based models of muscle coordination. Exercise and sport sciences reviews 30:32.

Prochazka A, Hulliger M, Trend P, Llewellyn M, Durmuller N (1989) Muscle afferent contribution to control of paw shakes in normal cats. J Neurophysiol 61:550-562.

Prochazka A, Westerman RA, Ziccone SP (1977) Ia afferent activity during a variety of voluntary movements in the cat. J Physiol 268:423-448.

Rack PM, Ross H (1984) The tendon of flexor pollicis longus: its effects on the muscular control of force and position at the human thumb. The Journal of physiology 351:99.

Rack PM, Westbury DR (1969) The effects of length and stimulus rate on tension in the isometric cat soleus muscle. J Physiol 204:443-460.

Rack PM, Westbury DR (1984) Elastic properties of the cat soleus tendon and their functional importance. J Physiol 347:479-495.

Raikova RT, Prilutsky BI (2001) Sensitivity of predicted muscle forces to parameters of the optimization-based human leg model revealed by analytical and numerical analyses. J Biomech 34:1243-1255.

Richmond FJ, Liinamaa TA, Keane J, Thomson DB (1999) Morphometry, histochemistry, and innervation of cervical shoulder muscles in the cat. J Morphol 239:255-269.

Roden-Reynolds DC, Walker MH, Wasserman CR, Dean JC (2015) Hip proprioceptive feedback influences the control of mediolateral stability during human walking. Journal of neurophysiology 114:2220-2229.

Roos EM, Herzog W, Block JA, Bennell KL (2011) Muscle weakness, afferent sensory dysfunction and exercise in knee osteoarthritis. Nature reviews Rheumatology 7:57-63.

Ross KT, Nichols TR (2009) Heterogenic feedback between hindlimb extensors in the spontaneously locomoting premammillary cat. Journal of neurophysiology 101:184-197.

Roy RR, Pierotti DJ, Baldwin KM, Zhong H, Hodgson JA, Edgerton VR (1998) Cyclical passive stretch influences the mechanical properties of the inactive cat soleus. Exp Physiol 83:377-385.

Ryan MM, Gregor RJ (1992) EMG profiles of lower extremity muscles during cycling at constant workload and cadence. J Electromyogr Kinesiol 2:69-80.

Sacks RD, Roy RR (1982) Architecture of the hind limb muscles of cats: functional significance. Journal of Morphology 173:185-195.

Sakakima H, Yoshida Y (2003) Effects of short duration static stretching on the denervated and reinnervated soleus muscle morphology in the rat. Arch Phys Med Rehabil 84:1339-1342.

Schenau GJVI (1989) On the action of bi-articular muscles, a review. Netherlands journal of zoology 40:521-543.

Scott SH, Brown IE, Loeb GE (1996) Mechanics of feline soleus: I. Effect of fascicle length and velocity on force output. J Muscle Res Cell Motil 17:207-219.

Scott SH, Loeb GE (1995) Mechanical properties of aponeurosis and tendon of the cat soleus muscle during whole-muscle isometric contractions. J Morphol 224:73-86.

Segal RL, Wolf SL, DeCamp MJ, Chopp MT, English AW (1991) Anatomical partitioning of three multiarticular human muscles. Acta Anat (Basel) 142:261-266.

Seireg A, Arvikar R (1975) The prediction of muscular load sharing and joint forces in the lower extremities during walking. J Biomech 8:89-102.

Sergio LE, Ostry DJ (1994) Coordination of mono- and bi-articular muscles in multi-degree of freedom elbow movements. Exp Brain Res 97:551-555.

Shevtsova NA, Hamade K, Chakrabarty S, Markin SN, Prilutsky BI, Rybak IA (2016) Modeling the Organization of Spinal Cord Neural Circuits Controlling Two-Joint Muscles. In: Neuromechanical Modeling of Posture and Locomotion, pp 121-162: Springer.

Sinkjær T, Andersen J, Ladouceur M, Christensen L, Nielsen JB (2000) Major role for sensory feedback in soleus EMG activity in the stance phase of walking in man. The Journal of physiology 523:817-827.

Sjogaard G, Jensen BR, Hargens AR, Sogaard K (2004) Intramuscular pressure and EMG relate during static contractions but dissociate with movement and fatigue. J Appl Physiol (1985) 96:1522-1529; discussion.

Smith JL, Betts B, Edgerton VR, Zernicke RF (1980) Rapid ankle extension during paw shakes: selective recruitment of fast ankle extensors. Journal of Neurophysiology 43:612-620.

Smith JL, Carlson-Kuhta P, Trank TV (1998) Forms of forward quadrupedal locomotion. III. A comparison of posture, hindlimb kinematics, and motor patterns for downslope and level walking. Journal of Neurophysiology 79:1702-1716.

Smith JL, Hoy MG, Koshland GF, Phillips DM, Zernicke RF (1985) Intralimb coordination of the paw-shake response: a novel mixed synergy. J Neurophysiol 54:1271-1281.

Smith JL, Zernicke RF (1987) Predictions for neural control based on limb dynamics. Trends in neurosciences 10:123-128.

Spector SA, Gardiner PF, Zernicke RF, Roy RR, Edgerton VR (1980) Muscle architecture and force-velocity characteristics of cat soleus and medial gastrocnemius: implications for motor control. Journal of Neurophysiology 44:951-960.

Spoor CF, Badoux DM (1989) The M. soleus in the domestic dog (Canis familiaris). Anatomia, histologia, embryologia 18:27-31.

Stein RB, Capaday C (1988) The modulation of human reflexes during functional motor tasks. Trends in Neurosciences 11:328-332.

Tabary JC, Tabary C, Tardieu C, Tardieu G, Goldspink G (1972) Physiological and structural changes in the cat's soleus muscle due to immobilization at different lengths by plaster casts. J Physiol 224:231-244.

Tian M, Herbert RD, Hoang P, Gandevia SC, Bilston LE (2012) Myofascial force transmission between the human soleus and gastrocnemius muscles during passive knee motion. Journal of applied physiology 113:517-523.

Tijs C, van Dieën JH, Maas H (2015) No functionally relevant mechanical effects of epimuscular myofascial connections between rat ankle plantar flexors. The Journal of experimental biology jeb. 122747.

Torres-Oviedo G, Macpherson JM, Ting LH (2006) Muscle synergy organization is robust across a variety of postural perturbations. Journal of neurophysiology 96:1530-1546.

Vincent KR, Conrad BP, Fregly BJ, Vincent HK (2012) The pathophysiology of osteoarthritis: a mechanical perspective on the knee joint. PM & R : the journal of injury, function, and rehabilitation 4:S3-9.

Wakeling JM, Blake OM, Chan HK (2010) Muscle coordination is key to the power output and mechanical efficiency of limb movements. Journal of Experimental Biology 213:487-492.

Walmsley B, Hodgson JA, Burke RE (1978) Forces produced by medial gastrocnemius and soleus muscles during locomotion in freely moving cats. J Neurophysiol 41:1203-1216.

Ward SR, Davis J, Kaufman KR, Lieber RL (2007) Relationship between muscle stress and intramuscular pressure during dynamic muscle contractions. Muscle & nerve 36:313-319.

Ward SR, Eng CM, Smallwood LH, Lieber RL (2009) Are current measurements of lower extremity muscle architecture accurate? Clinical orthopaedics and related research 467:1074-1082.

Wells R, Evans N (1987) Functions and recruitment patterns of one-and two-joint muscles under isometric and walking conditions. Human movement science 6:349-372.

Wilmink RJ, Nichols TR (2003) Distribution of heterogenic reflexes among the quadriceps and triceps surae muscles of the cat hind limb. Journal of neurophysiology 90:2310-2324.

Windhorst U (2007) Muscle proprioceptive feedback and spinal networks. Brain Research Bulletin 73:155-202.

Wood JE, Meek SG, Jacobsen SC (1989) Quantitation of human shoulder anatomy for prosthetic arm control--I. Surface modelling. J Biomech 22:273-292.

Yaraskavitch M, Leonard T, Herzog W (2008) Botox produces functional weakness in non-injected muscles adjacent to the target muscle. J Biomech 41:897-902.

Yucesoy CA, Turkoglu AN, Umur S, Ates F (2015) Intact muscle compartment exposed to botulinum toxin type A shows compromised intermuscular mechanical interaction. Muscle & nerve 51:106-116.

Zatsiorsky VM (2002) Kinetics of human motion. Champaign, IL: Human Kinetics.

VITA

RICKY MEHTA-DESAI

Ricky was born in Toronto, Ontario, Canada. He attended public schools in Toronto, ON, and Manahawkin, NJ. He later received his Bachelor of Science in Biomedical Engineering from The College of New Jersey (Ewing, NJ) in 2010 before coming to the Georgia Institute of Technology to pursue a doctorate in Applied Physiology. When he is not working on his research, Ricky Mehta-Desai enjoys playing underwater hockey, roller hockey, and participates in various outdoor recreational activities.